HDL-TR-2197

November 1991

The Effects of Electromagnetic Pulse (EMP) on Cardiac Pacemakers

by Vincent J. Ellis

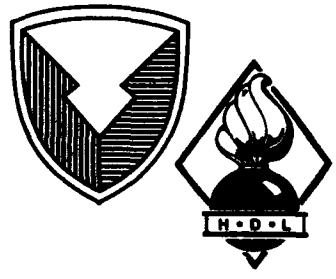

U.S. Army Laboratory Command
Harry Diamond Laboratories
Adelphi, MD 20783-1197

The findings in this report are not to be construed as an official Department of the Army position unless so designated by other authorized documents.

Citation of manufacturer's or trade names does not constitute an official endorsement or approval of the use thereof.

Destroy this report when it is no longer needed. Do not return it to the originator.

A preliminary version of this report was issued as HDL-PRL-91-5 in April 1991.

REPORT DOCUMENTATION PAGE

Form Approved
OMB No. 0704-0188

1. AGENCY USE ONLY *(Leave blank)*	2. REPORT DATE	3. REPORT TYPE AND DATES COVERED
	November 1991	Final, from Nov 88 to Oct 89

4. TITLE AND SUBTITLE
The Effects of Electromagnetic Pulse (EMP) on Cardiac Pacemakers

5. FUNDING NUMBERS
PE: H25

6. AUTHOR(S)
Vincent J. Ellis

7. PERFORMING ORGANIZATION NAME(S) AND ADDRESS(ES)
Harry Diamond Laboratories
2800 Powder Mill Road
Adelphi, MD 20783-1197

8. PERFORMING ORGANIZATION REPORT NUMBER
HDL-TR-2197

9. SPONSORING/MONITORING AGENCY NAME(S) AND ADDRESS(ES)
U.S. Army Laboratory Command
2800 Powder Mill Road
Adelphi, MD 20783-1145

10. SPONSORING/MONITORING AGENCY REPORT NUMBER

11. SUPPLEMENTARY NOTES
AMS code: 612120H250000
HDL PR: R8A9R1

12a. DISTRIBUTION/AVAILABILITY STATEMENT
Approved for public release; distribution unlimited.

12b. DISTRIBUTION CODE

13. ABSTRACT *(Maximum 200 words)*

The U. S. Army Harry Diamond Laboratories' (HDL's) Woodbridge Research Facility (WRF) has conducted an investigation into the effects of electromagnetic pulse (EMP) on medical electronics. This report specifically documents the findings on the effects of WRF's Army EMP Simulator Operations (AESOP) on cardiac pacemakers (CPMs). Empirical data are furnished and compared to the results of two independent analytical studies. The studies support the conclusion that damage to CPMs that might be located near the WRF boundaries is not likely. Furthermore, any upset in a CPM's operation is considered unlikely and inconsequential to the health of the CPM wearer.

14. SUBJECT TERMS
EMP, AESOP, pacemaker, cardiac pacemaker, EMI, simulated EMP, electromagnetic interference, electromagnetic pulse

15. NUMBER OF PAGES
76

16. PRICE CODE

17. SECURITY CLASSIFICATION OF REPORT	18. SECURITY CLASSIFICATION OF THIS PAGE	17. SECURITY CLASSIFICATION OF ABSTRACT	20. LIMITATION OF ABSTRACT
Unclassified	Unclassified	Unclassified	UL

Contents

Contents (cont'd)

page

Appendices

Figures

Figures (cont'd)

page

Tables

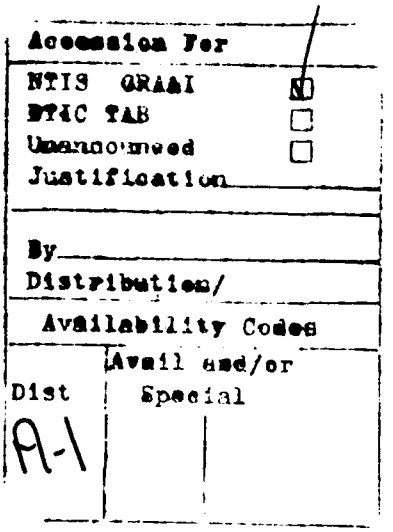

1. Executive Summary

1.1 Introduction

Cardiac pacemakers (CPMs) have experienced significant technological advancements over the last decade, evolving from simple and bulky pulse generators to the small and sophisticated computerized units implanted today.* With the implementation of sensitive digital electronics in modern pacemaker designs, concerns have been expressed for the possibility of an increased sensitivity of CPMs to electromagnetic interference (EMI). To some extent these concerns have abated due to the increased awareness of the EMI problem by the manufacturers, as evident in better pacemaker designs and the decline in reported malfunctions due to EMI.

While the intent of the manufacturer may be to protect the CPM wearer from common and frequent sources of EMI, such as power line fields, microwave oven leakage, security system scanners, etc, there are sources of EMI not foreseen or directly accounted for in CPM designs. One of these sources of EMI is an electromagnetic pulse (EMP) simulator. Although it would be considered unlikely for the average CPM wearer to be subjected to a simulator's EMP,† the effects of EMP on pacemakers must be investigated to ensure the safety of employees at EMP simulator sites, as well as CPM wearers in nearby public areas.

1.2 Purpose

The purpose of this effort was to investigate the effects of the operation of the Army EMP Simulator Operations (AESOP) on cardiac pacemakers that might be located in public areas surrounding the Woodbridge Research Facility (WRF) (the location of AESOP). This investigation was conducted as part of a larger effort to reexamine the WRF's environmental documentation, as prescribed by the National Environmental Policy Act (NEPA).

1.3 Background

An extensive literature search and review was conducted as a precursory effort [1]. The information gathered constitutes a data base of reported EMI effects on pacemakers since their existence. Essentially all the information within the data base is several years old. And as a consequence of the vast changes in pacemaker designs, resulting in a decrease of reported EMI effects on CPMs, more recent subject matter is limited.

**A pacemaker consists of a pulser unit, which houses the electronics and an electrical lead (usually one) that carries signals to and from the heart. The modern pacemaker's pulsers weigh approximately 20 to 40 g and measure approximately 50 × 50 × 7 mm. A modern pacemaker lead is approximately 2 to 4 mm in diameter and 45 cm in length. Some pacemakers have two leads (dual lead) that are used to stimulate/monitor two chambers of the heart.*

† The EMP being simulated is of the type produced by a high-altitude nuclear detonation.

Only a modest number of efforts have addressed the effects of EMP on CPMs; the most recent effort, by T. Bock [2], addressed a small sample (three) of state-of-the-art pacemakers. It is noteworthy, however, to mention that of all EMP testing conducted on cardiac pacemakers, only one permanent damage has been recorded [3]. This failure occurred at peak electric-field (E-field) levels of 500 kV/m, but could not be repeated after the damaged unit was repaired.

1.4 Scope

This report furnishes empirical test data on the effects of EMP on 10 cardiac pacemakers. Most of the test samples (eight) are recent technology designs (1985 to present), with two samples being of older technology types (1950's to early 80's). The empirical data are compared to the independent results of two analytical efforts conducted in parallel with the testing effort.

1.5 Summary of Results

The frequency-domain transfer functions were empirically determined for unipolar, bipolar, and dual-lead pacemaker designs* via continuous-wave (cw) illumination of the pacemakers in electromagnetic "phantom"† bodies. The transfer functions were numerically convolved with selected AESOP E-field and/or magnetic-field (H-field) waveforms to produce EMP-induced CPM lead currents. These currents were obtained in a manner so that they are reasonable upper bounds for the currents that would actually be produced by AESOP on the lead of a pacemaker (for a wearer located just outside the confines of the WRF). These currents also serve as parametric output "models" for current injection testing (CIT). Each pacemaker test sample was injected with a range of currents (there are five selectable current injector output settings) proportional to the upper bound AESOP-induced currents in order to determine what effects AESOP operation might have on CPMs.

The current injection testing was conducted in two phases. Phase I testing was performed with all pacemakers programmed to their default or factory-shipped program settings. Phase II testing, which involved only CPM test samples that are programmable, was performed with the programmable CPMs reprogrammed to their most sensitive setting. No permanent failure or damage to any pacemaker was observed at the upper bound current levels, or at any level, in either phase of the CIT testing. Furthermore, in phase I testing each pacemaker was injected with the CIT level-5 current (at least 235 percent greater in peak amplitude than the upper bound currents, and an energy level at least 1336 percent greater than the upper bound currents) without failure or damage.

** Unipolar pacemaker leads use conductive body tissue as an electrical path from the heart back to the pacemaker's pulser unit. Bipolar leads essentially have two leads, one positive and one negative. Dual-lead pacemakers have two leads that are either bipolar or unipolar (or both, each lead may be different) in design.*

† The "phantom" is a test fixture constructed to represent the physical dimensions and the electrical properties of tissue for the average human body.

During the phase I CIT testing, with all pacemakers programmed to their individual nominal or default program settings, the two "older" technology units experienced upset* at the lowest CIT test level (CIT level 1). One of the pacemakers experienced this CIT level-1 upset at a peak current slightly less than the upper bound peak current but at an energy level slightly higher than the upper bound current energy. The second pacemaker experienced the upset with a peak current and energy level slightly greater than upper bound currents. Three of the "modern" technology units experienced upset during phase I testing, but at levels much larger than the upper bound currents, approximately 200 percent greater in peak amplitude and 1500 percent greater in energy content.

Phase II testing consisted of reprogramming the sensitivity setting of the programmable pacemakers to their most sensitive mode and retesting these units as in phase I. Since they are not programmable, the two older models were not elements of phase II testing. Under phase II conditions, only two of the six programmable pacemakers tested experienced upset. The same two pacemakers had experienced upset in phase I, but here the upset levels were on the order of 150 percent greater (peak amplitude) than the upper bound, as opposed to 200 pecent greater in phase I. The third "modern" pacemaker that had experienced an upset in phase I testing was not tested in phase II because a programmer was unavailable for that model.

For the pacemakers tested and the test conditions imposed, older CPMs experienced upsets at current levels roughly equivalent to the upper bound currents that would be produced by AESOP EMP fields of 8 kV/m (peak E-field). Although AESOP can produce 8 kV/m fields at the WRF fenceline, the currents that created the upsets in the CPMs are upper bound currents. Actual currents induced by 8-kV/m AESOP fields are expected to be on the order of three to five times lower. The modern technology pacemakers did not experience upsets when subjected up to equivalent EMP levels of approximately 20 kV/m (the equivalent peak E-field level required to induce the lowest level phase II upsets due to upper bound currents). No damage to any of the pacemakers was noted during the CIT testing, which attained equivalent EMP peak E-field levels of at least 25 kV/m. Even the upsets noted are, in most instances, inconsequential to the health of the CPM wearer.

Two independent analytical efforts were undertaken in parallel with the testing efforts described here. The results of these efforts were used to reinforce test data and provide additional data to aid in quantifying the upper bound currents. The first effort (referred to as the "Goldstein" analysis, named after the author of the analysis) consisted of a combination of purely analytic

** The upsets were manifested as an inhibition of one CPM output pulse. The CPMs could have misinterpreted the CIT currents as a natural heart pulse or could have interpreted the CIT currents as high-frequency noise. In either case, inhibition due to a heart beat and reversion to an asynchronous fixed rate due to high-frequency noise are expected responses designed into the CPMs. The CIT currents are not damaging the CPMs, but simply fooling them.*

treatments (lower frequencies) and computer-implemented finite-difference time-domain calculations (at higher frequencies) to predict the response of pacemakers to EMP. The second effort (referred to as the transmission line model or T-line model) used a computer code, in which the implanted pacemaker was treated as a transmission line, to calculate EMP-induced currents on pacemaker leads.

The results of the Goldstein analysis are in very good agreement with the test results. Differences in the peak amplitudes were on the order of a factor of 5 to 6 (15 dB), with the Goldstein results being smaller than the test data. These differences are accounted for by the differences between the pacemaker lead configurations used. Throughout the testing, pacemakers with single leads were tested with their leads oriented in a straight run to promote maximum coupling and therefore upper bound responses. The entire Goldstein analysis was performed in a manner to produce results close to actual expected values, e.g., the pacemaker leads were run in a more realistic fashion (partially horizontal and partially vertical). The Goldstein results also contained slightly different responses at the higher frequencies, which may be attributed to the frequency and tissue-type dependent parameters of body tissue that are inclusive to the computer calculations performed but were not accounted for in the test phantom medium. The computer calculations implemented in the Goldstein analysis very specifically accounted for variances in the electrical properties of tissue as a function of tissue type and frequency, whereas the accurate simulation of body tissue was not possible in the test phantoms.

The transmission line model results were 12 times (22 dB) greater than the equivalent experimental results. There are many sources for the discrepancies in the results; these sources are discussed in section 4. The T-line model, which was used to obtain a "quick-look" "worst-case" evaluation of the EMP effects on pacemakers, was primarily focussed on determining energy-related damage to pacemakers. The T-line model, as used, is not capable of handling this application with any accuracy but was performed to simply obtain the absolute theoretical worst-case current that could be produced on a CPM lead by an EMP. The value of the T-line results as a complement to the test data is minimal; however, a particularly significant conclusion can be drawn. Although the T-line model was compounded with unrealistic worst-case conditions, the conclusion by the authors of the efforts [1] was that no damage (energy related) was likely to occur to pacemakers. This result is a significant assertion because under the methodology used, the pacemaker currents determined could not (theoretically) possibly be any greater, yet damage is not likely.

2. Approach

2.1 General

Previous EMP testing of pacemakers consisted of immersing the pacemaker test samples in a saline-filled Plexiglas tank and subjecting the pacemakers to an EMP. A timing circuit is used to fire the EMP pulse within the appropriate pacemaker sense and refractory windows.* The continuous operation of the pacemaker is monitored, and diagnostics are performed on the unit before and following each EMP test pulse. This test procedure is performed in a manner consistent with EMP test methodology and contains elements that have been extracted from the "Pacemaker Standard," published in 1975 by the Association for the Advancement of Medical Instrumentation (AAMI) [4]. The applicable portion of the "Pacemaker Standard" addresses test procedures for testing the electromagnetic compatibility (EMC) of pacemakers (see app A).

At the time of testing, the AESOP was restricted from operation until an Environmental Impact Statement (EIS) was completed for the EMP operations at the WRF. The lack of an equivalent EMP source required an alternate approach to accomplish the program objectives. A combination of cw electromagnetic illumination and Fourier analysis techniques was used to determine the equivalent EMP-induced CPM lead currents. After these currents were determined, a current injector was used to introduce the currents onto the pacemaker leads. Extensive diagnostics were performed to determine if the EMP-equivalent CIT pulse caused an effect in the CPM's operation.

2.2 Pacemaker Test Phantom

The AAMI pacemaker standard specifically calls for a rectangular test cell, or "phantom," that basically represents a typical male torso (app A). This phantom, herein referred to as the AAMI test cell or phantom, is filled with a saline solution of a conductivity which is consistent with the conductivity of human tissue at a defined frequency. A pacemaker is to be immersed in the center of the phantom with the CPM lead in a straight run parallel to the sides of the phantom and parallel to the incident E-field. A constant depth of 1 cm is to be maintained between the CPM lead and the front wall of the phantom. Although these procedures set forth may be consistent with the original objectives of the standard, they are not completely adequate for EMP testing. The test procedures discussed in this report were, for the most part, performed

** A CPM's sense window is a period of time in which the CPM is waiting for a natural heart beat. The refractory window is a period of time in which the CPM is simply waiting between heart beats and is not accepting external input. A CPM is constantly cycling through these windows. If a CPM detects a heart beat in the sense time window, the refractory period starts. If no heart beat is detected in the sense time window, the pacemaker generates a pulse to stimulate the heart, and then the refractory period begins.*

within the AAMI test methodology. Any deviations from the AAMI standard were necessary to provide a more realistic representation of the human body, to promote upper bound results, and/or to fill voids in the AAMI standard test methodology.

2.2.1 *Phantom Construction*

The AAMI phantom specifications do not consider any of the human extremities or surface contours. A better representation of a human may be to model the torso by an ellipsoid or cylindrical shape. In fact, much of the theoretical work in the past has used these and other geometric shapes in comparison to experimental data. However, these shapes are difficult to physically implement. For this effort, two phantoms were constructed that were slight modifications of the AAMI test cell. The phantoms are constructed entirely of a Plexiglas-type material and have a basic torso structure which is the AAMI test cell. One of the phantoms, the "vertical phantom," has been constructed to represent an average male standing vertically upright, with arms outstretched perpendicular to the body. Two 7-in. inner diameter (i.d.) hollow cylindrical "legs" and two 4-in. i.d. hollow cylindrical "arms" were added to the AAMI test cell to produce this vertical phantom (see fig. 1). The other phantom was constructed to represent an average male lying horizontally on his side. This "horizontal phantom" is basically identical to the vertical phantom, with the exception that the horizontal phantom does not have arms (see fig. 2).

Another concern not addressed in the AAMI standard involves the effects of the real earth interaction with the phantom and incident EMP pulse. A human body above the ground will respond with a resonant behavior when subjected to an EM field. At certain frequencies the absorption of EM energy into the body will be greater. This absorption, referred to as the specific absorption rate (SAR), is greatly dependent on the proximity of the body to the earth, as well as the length, size, and mass of the body. Many studies have been performed to describe this frequency-dependent behavior of the human on real earth [5]. These studies have shown the human body to experience a higher SAR when the incident field is oriented with the electric field component parallel to the long or major body axis. For a typical body height of 6 ft, the body will exhibit a resonance at approximately 80 MHz in free space. If the body is very close to the ground, this resonance will shift due to the capacitive coupling to the ground (see fig. 3). The addition of legs to the AAMI test cell not only more accurately represents the body physically, but also facilitates this man-to-ground interaction during testing.

Figure 1. Vertical phantom (Note: all dimensions are in inches).

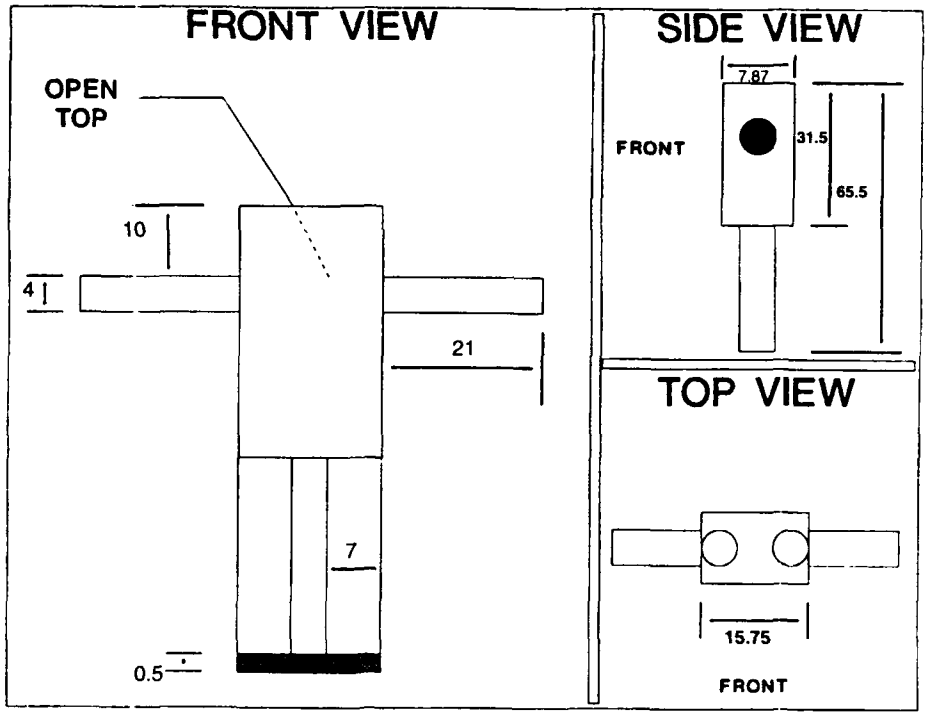

Figure 2. Horizontal phantom (Note: all dimensions are in inches).

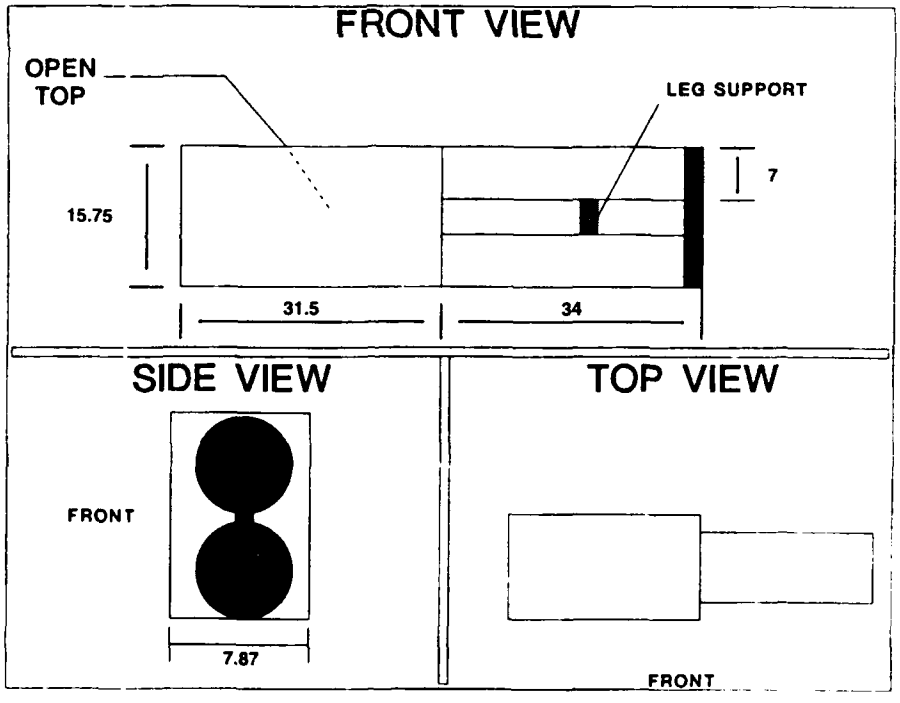

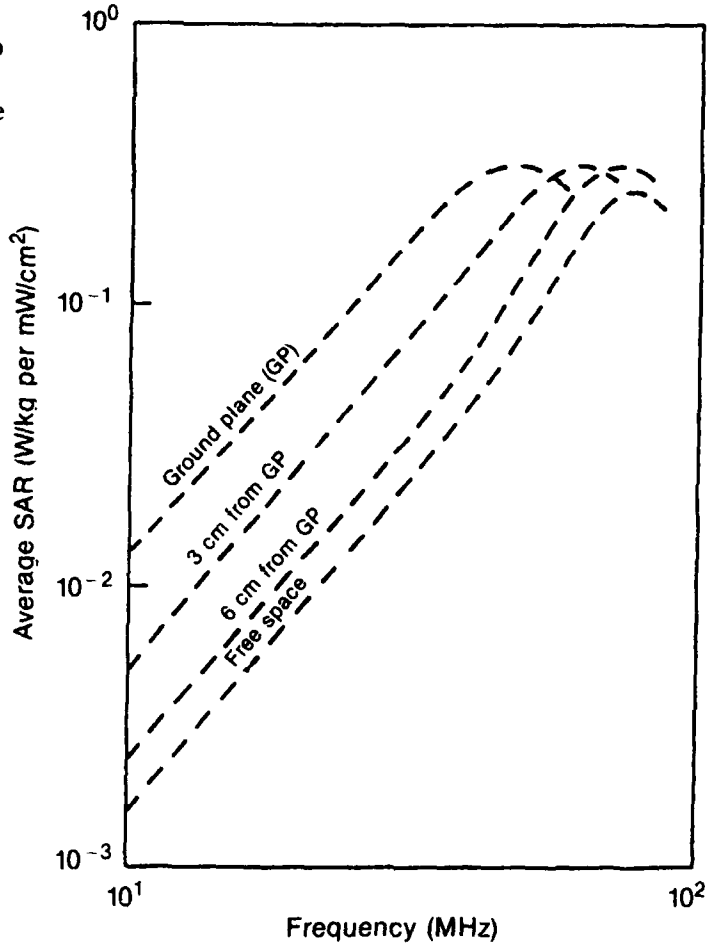

Figure 3. Calculated effect of a capacitive gap between man model and ground plane on average specific absorption rate (SAR). (Extracted from the *Radiofrequency Radiation Dosimetry Handbook, Fourth Edition* [5].)

2.2.2 *Phantom Medium*

The electrical parameters of human tissue vary significantly not only with tissue type but also with frequency [5]. Various compounds have been developed to simulate the electrical properties of specific tissues over limited frequency ranges. For EMP testing we are concerned with the frequency range of approximately 10 kHz to 200 MHz, and, to date, no material has been developed that can accurately simulate body tissues over this wide range of frequencies. A technique has been used quite often which involves using whole body averages (WBAs), inclusive of all tissue types, for values of conductivity and permittivity [5]. Even with this simplified approach, the author is unaware of a material that accurately simulates WBA parameters over the entire frequency range of interest. To facilitate the entire range of experiments in this effort, the approach to resolve this issue was to simplify the phantom medium (filler) by using a saline solution with a conductivity that is an upper bound representation (for EMP testing) of the WBA conductivity for human tissue.

Figure 4 depicts the average conductivity and the average relative permittivity of the human body [5]. Over the frequency range of 10 kHz to 200 MHz, the conductivity varies from 0.08 siemens per meter (S/m) to 0.544 S/m, and the relative permittivity varies from 42×10^3 to 45.9. The body resonances occur between 30 and 80 MHz, dependent on body size and mass and the proximity to the earth. For this resonance frequency range, the conductivity and permittivity are relatively constant. Values for the electrical parameters were chosen in this resonance frequency range to provide reasonable upper bound conditions. Although the "Pacemaker Standard" calls for a saline solution with a conductivity of 0.267 S/m to be used as the test cell filler, the rationale for the use of this value of conductivity is unclear and appears to be an inappropriate choice for EMP testing. From figure 4, in the range of 30 to 80 MHz, the value of 0.45 S/m was chosen to be the conductivity of the saline solution to be used as the phantom medium. The relative permittivity in this range is approximately 55; however, the saline solution will maintain a relative permittivity approximately that of water (70 to 80). The value of 80 is reasonably close to the resonance value when one considers the large excursions of permittivity, as shown in figure 4. Additionally, a permittivity of 80 in this frequency range equates approximately to that of muscle tissue. Therefore, the value of 80 for the relative permittivity is valid, though it may not be an upper bound parameter.

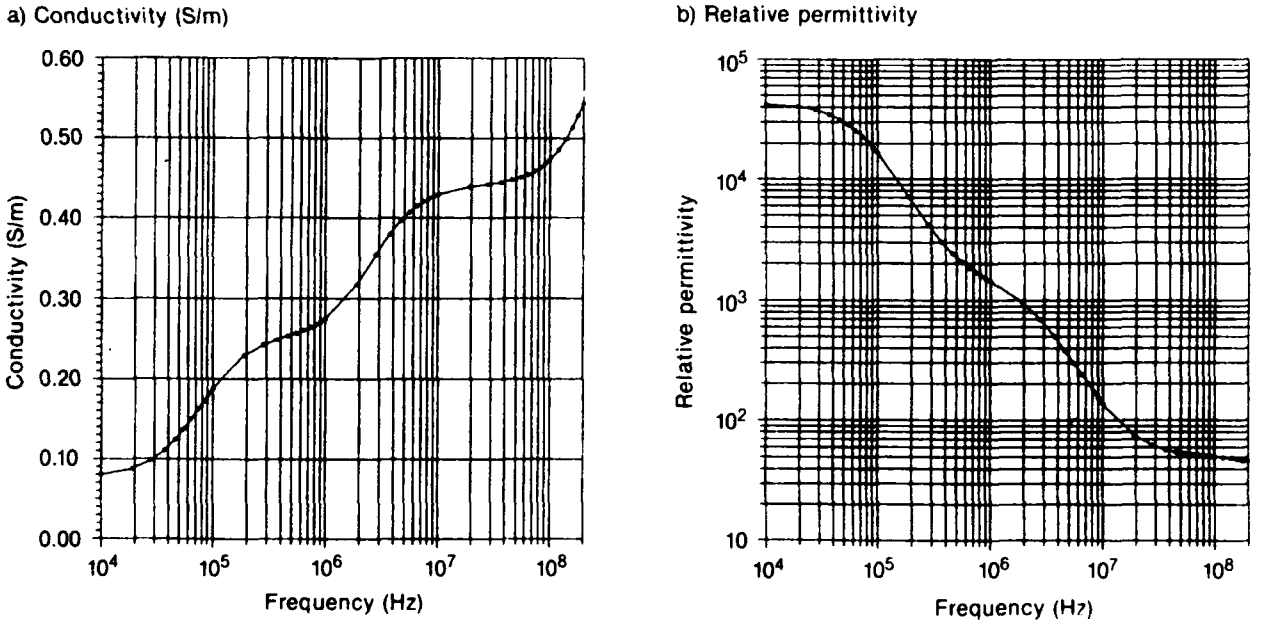

Figure 4. Whole body average (WBA) electrical parameters as a function of frequency. WBA equals two-thirds that of muscle tissue.

2.2.3 *Current Probe Fixture*

To facilitate current measurements on the pacemaker leads (within a phantom) with standard clip-on current probes (EG&G COP-5), an immersible probe fixture was constructed (see fig. 5). This probe fixture, referred to as the "probe submarine" or "probe sub," was designed to prevent moisture from contacting the current probes, be movable within the phantom volume, and be as unobtrusive to EM fields as possible. The probe sub was constructed from a 3-in. i.d. hollow Plexiglas cylinder that is completely sealed at one end with a circular disk. The other end, which is threaded on the inside of the cylinder, accepts a threaded cap that contains an outward nipple with a 7/8-in. opening. At 1 in. from the sealed end of the probe sub, a 1/8-in. Plexiglas tube was inserted through the diameter of the cylinder and sealed where it contacts the cylinder. A pacemaker lead can be passed through this tube and a current probe can be clipped around this tube from inside the cylinder. Several nipples are located on the "back" of the phantoms and protrude into the phantom volume (the front of the phantom is the side on which the source fields are incident). More than one nipple is used to allow some degree of flexibility in the location of the current probe within the phantom. The nipple cap is screwed into the probe sub and attached to one of the phantom nipples via flexible tubing (the unused nipples are plugged), thereby providing an access port to the current probe from outside the phantom (see fig. 6). In this way, when the phantom is filled with the saline medium, the pacemaker is completely immersed yet the current probe is kept dry and is not in direct contact with the pacemaker lead.

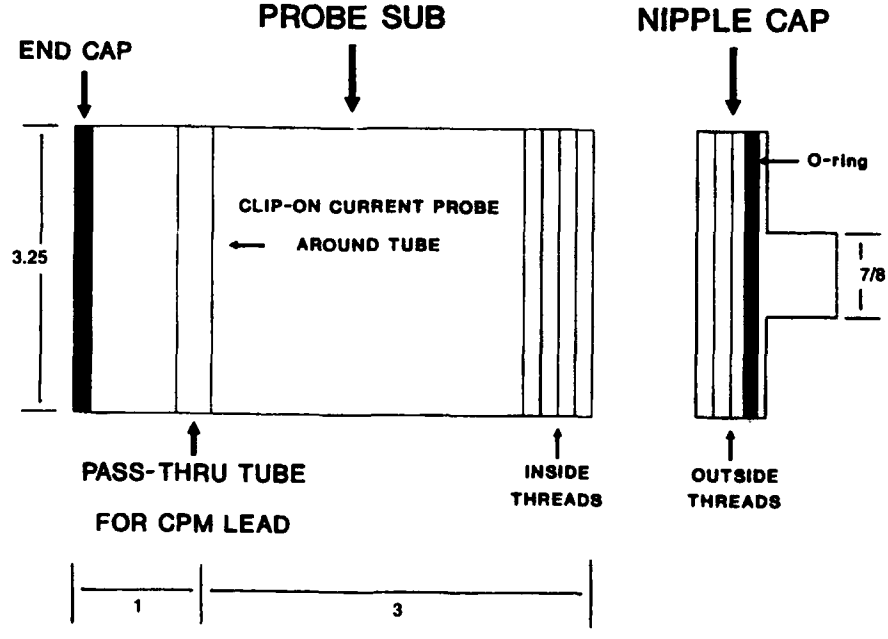

Figure 5. Probe submarine. All dimensions are in inches.

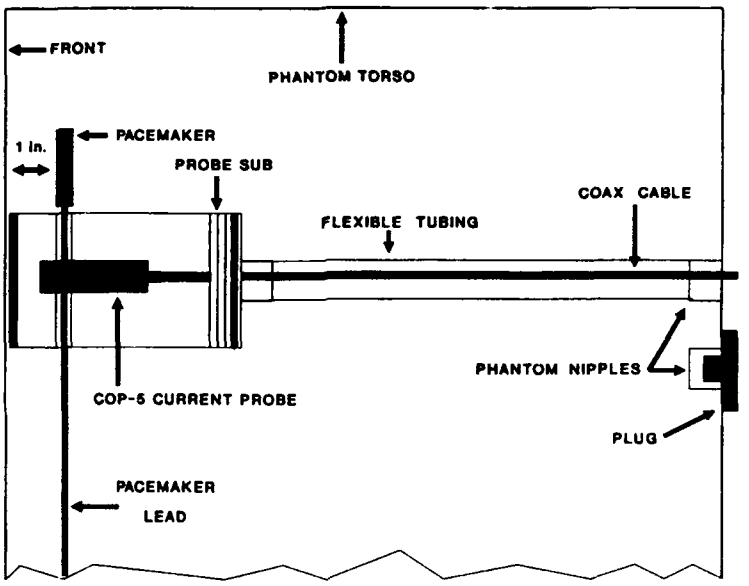

Figure 6. CW test configuration.

2.3 Continuous Wave (CW) Illumination Testing

The WRF currently operates and maintains a Continuous Wave Instrumentation System (CWIS),* which is a useful tool for determining the response of linear systems to electromagnetic fields [6]. With the CWIS, frequency-domain transfer functions can be determined empirically and then analytically convolved with a source function to produce the system response. The objective of the cw tests was to determine the transfer functions of implanted (simulated) pacemakers by normalizing frequency-domain pacemaker lead currents to the source field incident on the phantom.

Two test locations—"V" and "H"—were chosen within the CWIS test volume as shown in figure 7 (location "R" in fig. 7 identifies the location of the magnetic field reference sensor). Although the testing was not actually divided into two phases, the efforts may be described in two parts or phases: a vertical test at location "V" and a horizontal test at location "H." The vertical test consisted of collecting bulk lead current data for three pacemakers embedded in the vertical phantom. The horizontal test was conducted in the same manner as the vertical test with the exception of using the horizontal phantom. The three pacemakers tested were chosen to represent the basic CPM designs in physical construction rather than their operational or technological characteristics. The three CPMs consisted of unipolar, bipolar, and dual-lead designs. The objective was to obtain data that would provide the coupling characteristics of these three CPM lead types. The data collected serve as coupling models for the three pacemaker designs and, when convolved with source fields (AESOP fields) and transformed to the time domain, produce the current models for the current injection testing (to be discussed later).

* *Data taken with the CWIS are transmitted via 1-GHz fiber-optic links.*

Figure 7. CWIS test site—aerial view.

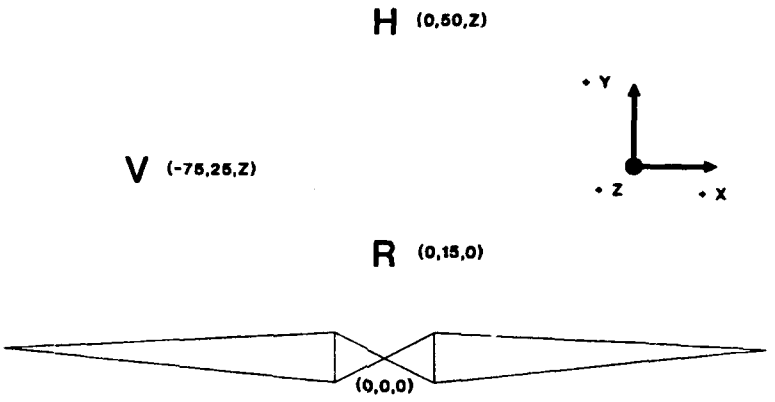

Location "V" was chosen as a test location where the unipolar and the bipolar CPMs (in the vertical phantom) would be excited by vertical E-fields and the dual-lead CPM would be excited by H-fields normal to the loop formed by the two leads. The unipolar and the bipolar pacemaker leads were run in straight paths along the major axis of the phantoms to promote E-field coupling, and the leads of the dual-lead pacemaker were run in a looped configuration to promote magnetic field coupling. The vertical phantom was placed on the ground (equating to a mid-torso height of 1.3 m) at location "V," and each pacemaker was placed in the vertical phantom (in turn) and illuminated with stepped cw fields from 10 kHz to 200 MHz. The vertical phantom was then elevated on a 0.3-m-high wooden platform (1.6 m mid-torso height), and the CPMs were then retested. This same procedure was then performed at location "H" with the horizontal phantom. The ground contact placement of the horizontal phantom equates to a mid-torso height of 0.2 m, and the elevated horizontal phantom, using a 1.1-m wooden table, equates to a 1.3-m mid-torso height. Two configurations (ground contact and elevated) were used to investigate the ground interaction issues (discussed in sect. 2.2.1).

Before testing, a comprehensive mapping of the EM fields within the CWIS test volume was conducted. E- and H-field data for three Cartesian components (frequency domain) were collected at locations corresponding to the future locations of the CPM leads (mid-length), i.e, the appropriate mid-torso position. The primary field component* data were collected daily to continuously monitor any changes in the performance of the CWIS and help minimize the promulgation of any day-to-day measurement error.

All measurements taken at the CWIS are referenced to a common H-field measurement located on the ground, at a distance of 15 m along the CWIS

** The primary field component would be that field, and its orientation, producing the greatest coupling to the CPM leads. The primary field component is therefore configuration dependent.*

electrical centerline. In this way, all data measurements are normalized to the same source, thereby accounting for CWIS output variations. The resultant measurements are actually the combination of several measurements (normalizations) inclusive of the data measure itself, the reference measurement, probe calibration measures, and system calibration measures. The current measurements can be described mathematically as follows:

$$I(jw)_{data} = \frac{I(jw)_{measured}}{H(jw)_{reference}} \quad . \tag{1}$$

The field measurements are described similarly:

$$E(jw)_{data}, H(jw)_{data} = \frac{E(jw)_{measured}, H(jw)_{measured}}{H(jw)_{reference}} \quad . \tag{2}$$

The transfer function, $TF(jw)$, is produced by the ratio of the current response measurement (output) to the primary driving source (input):

$$TF(jw) = \frac{I(jw)_{data}}{E(jw)_{data}, H(jw)_{data}} = \frac{I(jw)_{measured}}{E(jw)_{measured}, H(jw)_{measured}} \quad . \tag{3}$$

2.4 Convolution

The response of a system to any input may be determined through convolution if the impulse response of the system is known. The cw measurements have provided the frequency-domain impulse response (transfer function) for CPMs; therefore, the convolution of an EMP with the transfer function will produce the response of a CPM to EMP. The procedure used in this effort involved the convolution of frequency-domain AESOP field waveforms with the appropriate CPM transfer functions to produce the frequency-domain response. An inverse Fourier transform is then performed on these responses to yield time-domain lead current responses of CPMs to AESOP.

The choice of AESOP source fields to be convolved with the CPM transfer functions is based on several considerations, namely, the output characteristics of AESOP and the geometry of AESOP relative to possible locations of CPM wearers. Figure 8 is an aerial view of the AESOP within the WRF compound. Three primary locations were chosen and are indicated in the figure as A, B, and C. Location C was chosen along the AESOP centerline because the largest E-fields, as a function of distance from AESOP (predominantly horizontal), produced by AESOP lie along the centerline. Location B was chosen because it is the closest point from the WRF boundary to AESOP. Location A was chosen because it is the point at which the projection of AESOP's axis would cross the WRF fenceline and is a candidate for the point at which vertical E-fields are dominant. Three heights were also chosen for

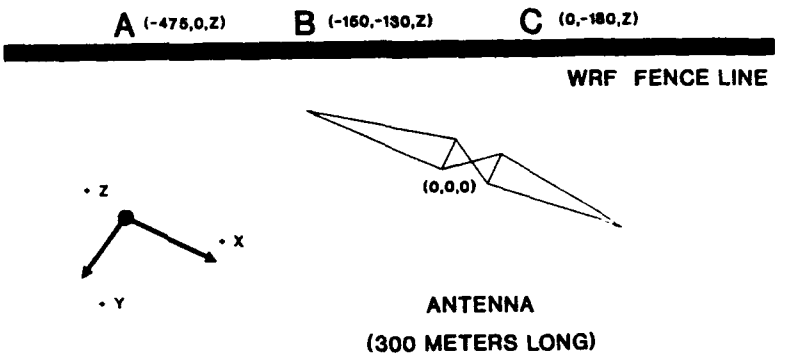

Figure 8. AESOP test site—aerial view.

examination: 0.2, 1.5, and 10 m. A man lying on the ground is represented by the 0.2-m height. The 1.5-m height corresponds to a man standing upright, and the 10-m height is used for a man (either horizontally or vertically oriented) totally isolated from the ground, e.g., a telephone repairman in a cherry-picker. These locations and heights were chosen as a realistic spread of possible CPM wearer locations outside WRF confines that would promote the upper bound coupling of EMP fields from AESOP.

A three-dimensional (3-D) computer code was developed outside this program which predicts the AESOP output at any location relative to AESOP [7]. This computer code was used to predict the electric and magnetic fields produced by AESOP at the three primary locations, for the three heights (nine points in all). At each point, both the E-fields and H-fields in three Cartesian components were obtained (see app B). The computer-predicted AESOP field waveforms were convolved with the appropriate CPM transfer function obtained in the CW experiments, and the results transformed to the time domain via inverse Fourier transforms to determine the actual response of a CPM to EMP. An extensive waveform analysis was performed on these CPM responses in order to determine the scenario which produces the upper bound CPM currents and hence the highest likelihood of AESOP-induced effects on CPMs. For the analysis performed, the upper bound conditions were determined to be for a CPM wearer located at the centerline location (location C) and at a height of 10 m.

2.5 Current Injection Testing (CIT)

The upper bound currents resulting from analysis of the convolved cw data were determined through comparisons of waveform characteristics including maximum slope, peak amplitude, and normalized total energy. These upper bound currents then served as the output design "model"* for CIT. The CIT source used contains five (1 to 5, lowest to highest) output level settings and was modified to nominally produce these upper bound model currents at its

** The term "model," used throughout this document, refers to the upper bound AESOP-induced CPM lead currents (for each type of CPM lead design) for a CPM wearer just outside the WRF confines. These upper bound currents are used as an output model for the CIT pulser.*

second output setting.* In this manner, each pacemaker could be tested at each of the five output settings, starting at a current level less than the upper bound model to a level greater than the model (the objective being to determine the threshold for effects). Although an unrealistic condition, testing to successive levels above the upper bound levels is necessary in order to determine thresholds and obtain safety margins.

The CIT was performed in two phases. The first phase involved testing all 10 pacemakers to the five CIT levels. During this phase, the programmable CPMs were programmed to their individual nominal or factory-shipped settings. The second phase of testing, which included only programmable pacemakers, was performed identical to the phase I testing with the exception that the sensitivity option of the CPMs' programs was programmed to its most sensitive setting.

The CIT procedure consisted of three steps per test pulse (current pulse): prediagnostics, the actual test pulse, and post-diagnostics. In addition to the pre- and post-diagnostics, the performance of each CPM was continuously monitored throughout each test pulse. Before testing, the programmable CPMs were programmed to the desired mode. Prediagnostics were then performed and were composed of recording the CPM program settings and verifying the parameters of the CPM's output pulses (voltage, pulse width, and pulse train period). For the nonprogrammable CPMs and those programmable CPMs for which a programmer was not available, only the output parameters could be recorded as prediagnostics. A CPM was then connected to the CIT source leads and a strip chart recorder, which monitored the voltage output of the CPM just before, during, and following a test pulse (see fig. 9).

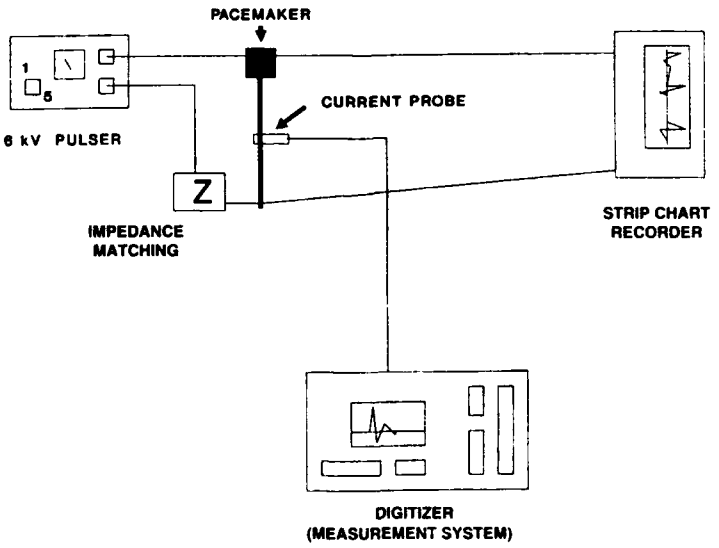

Figure 9. Current injection testing (CIT) test configuration.

**Because of the differences in impedance among the CPMs, it was not always possible to produce the upper bound model currents at level 2.*

The strip chart recorder was turned on before the test pulse to facilitate a physical indication of the CPM's operation. The objective was to determine the timing of the pacemaker's sense and refractory windows and to pulse the CPM in both windows, one at a time. A few cycles of the CPM's output were recorded; then a single CIT level-1 pulse was injected during the CPM's sense window. Following the CIT pulse, several (approximately five) CPM cycles were allowed to lapse and were recorded. Postdiagnostics were then performed, which consisted of checking the pacemaker's program and/or output parameters. If a change in the CPM's function was noted in the postdiagnostics,* it was recorded and the pacemaker was reprogrammed to its pretest mode. The pacemaker was then tested with a CIT level-1 pulse again, this time coincident with the pacemaker's refractory window. Postdiagnostics were then performed again, and the procedure was repeated with the successive CIT output levels 2 to 5. In addition to the hard-copy records provided by the strip chart recorder, any missed or extra CPM output pulses monitored during the test were logged as upsets.

**No change in the program or output pulse characteristics of any pacemaker was noted at any time during the CIT testing.*

3. Results and Analysis

3.1 CW Testing

Before the pacemaker lead data were collected, the electric and magnetic fields at the test locations were measured. These field mapping data not only serve to normalize the CPM lead current data to produce transfer functions, but also describe the field geometry relative to the CWIS antenna and the test setup. Figures 10 to 17 are overlays of the three Cartesian components of the E- and H-fields (magnitude only) for location "V" (heights 1.3 and 1.6 m) and location "H" (heights 0.2 and 1.3 m). In figures 10 to 17 the vertical fields equate to the $+z$ direction shown in figure 7, horizontal fields are in the $+x$ direction, and radial* fields are in the $+y$ direction. Although all data collected at the CWIS were obtained from 10 kHz to 200 MHz, some of the data (particularly H-field and current data) are corrupted by ambient noise below 100 kHz due to low signal-to-noise ratios. The frequency range of 100 kHz to 200 MHz is adequate, however, to cover the EMP spectrum. For the most part, it is not readily apparent from the figures that a particular field component is dominant for all frequencies. However, time-domain waveforms would indicate that vertical E-fields and radial H-fields are dominant at "V," and horizontal E-fields and radial H-fields are dominant at "H." Additionally, the geometry of our test setup is simple enough that the orientation of the CPM leads does not afford significant cross-coupling of the minor field components. Figures 18 to 21 depict the transfer functions (magnitude only), resulting from equation (3) (see sect. 2.3) for the three CPM types.

**The fields oriented in the +y direction are not radially directed by the strict definition. The term "radial" is used to indicate that the fields are directed away from the source antenna and are perpendicular to the antenna (and parallel to the ground), along the length of the antenna.*

Figure 10. Component E-field comparison at location V, 1.3-m height, measured cw data.

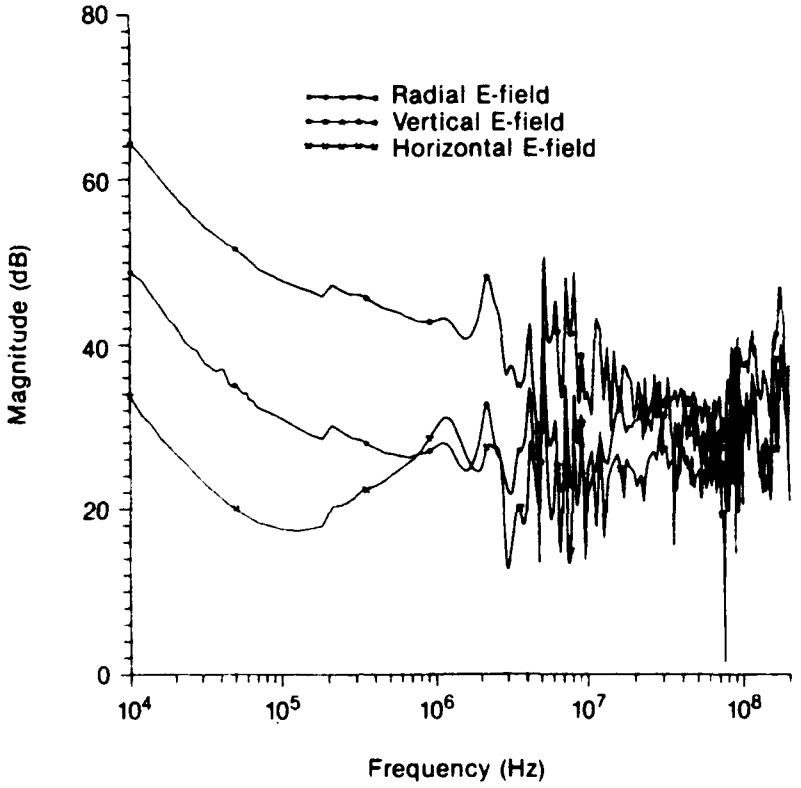

Figure 11. Component H-field comparison at location V, 1.3-m height, measured cw data.

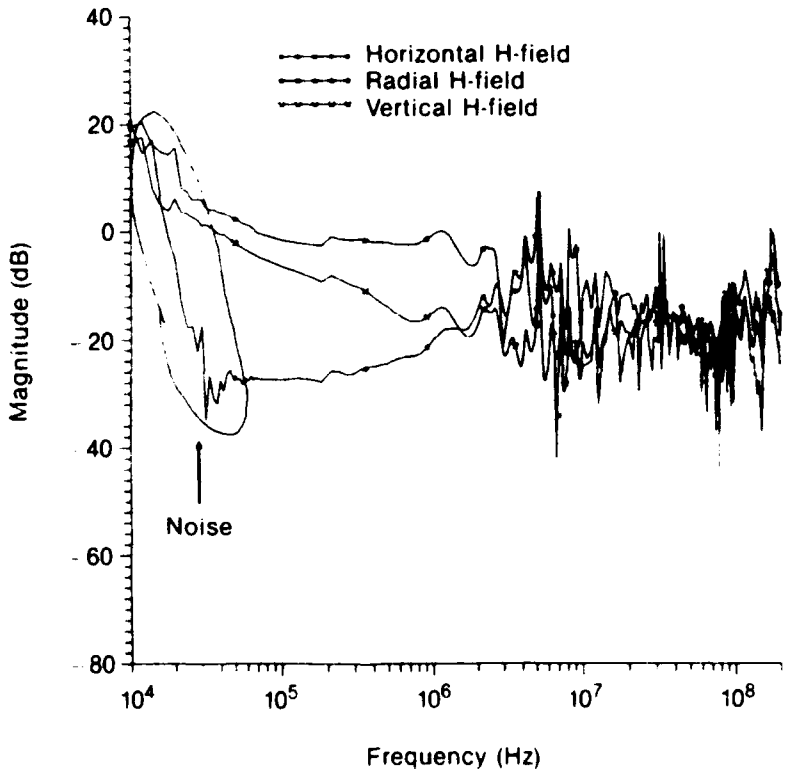

Figure 12. Component E-field comparison at location V, 1.6-m height, measured cw data.

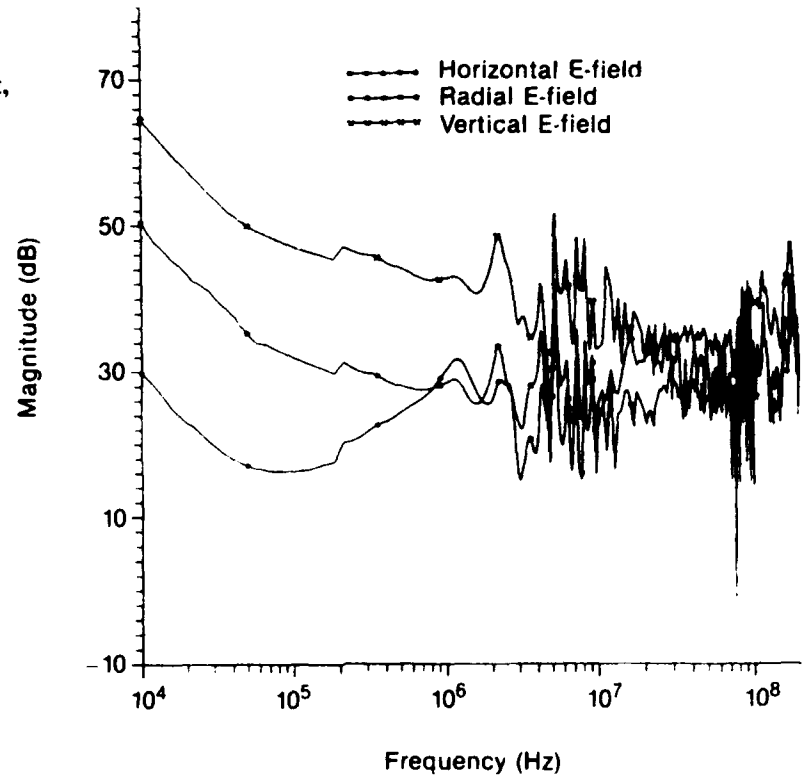

Figure 13. Component H-field comparison at location V, 1.6-m height, measured cw data.

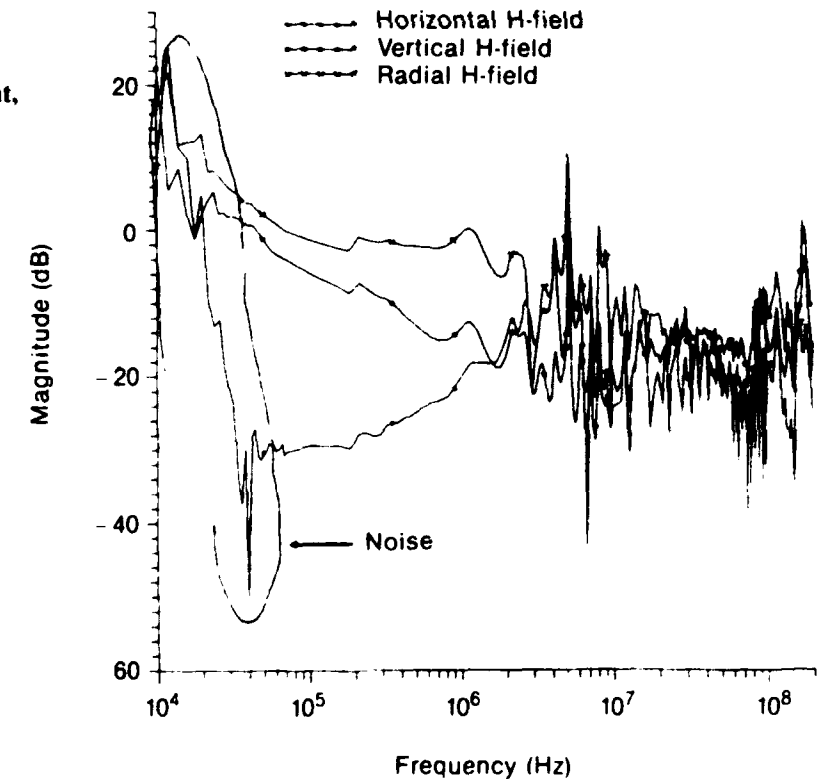

Figure 14. Component E-field comparison at location H, 0.2-m height, measured cw data.

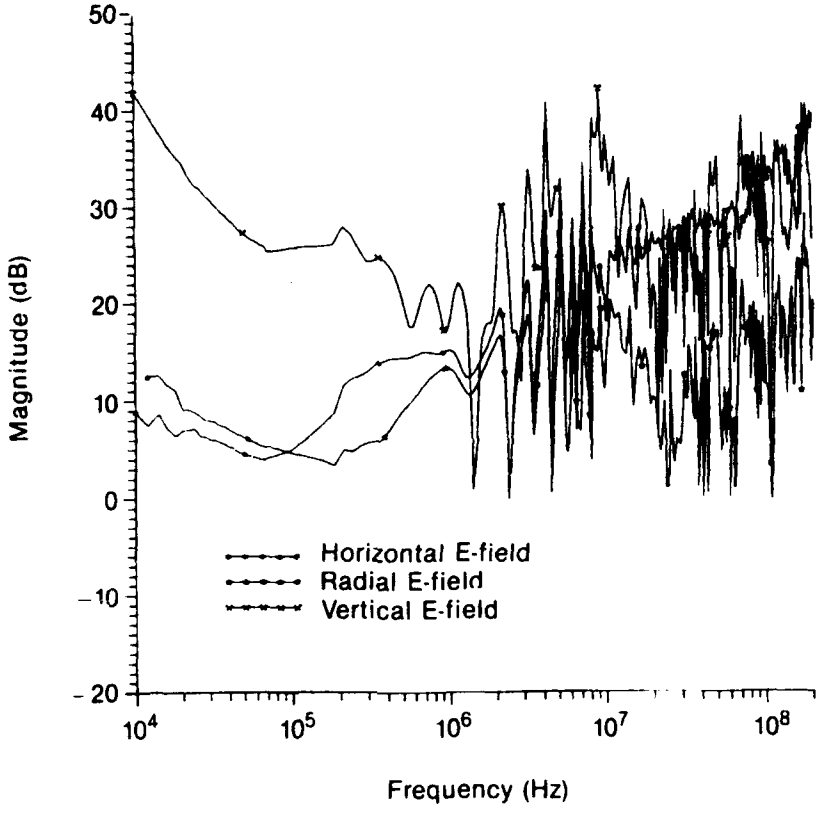

Figure 15. Component H-field comparison at location H, 0.2-m height, measured cw data.

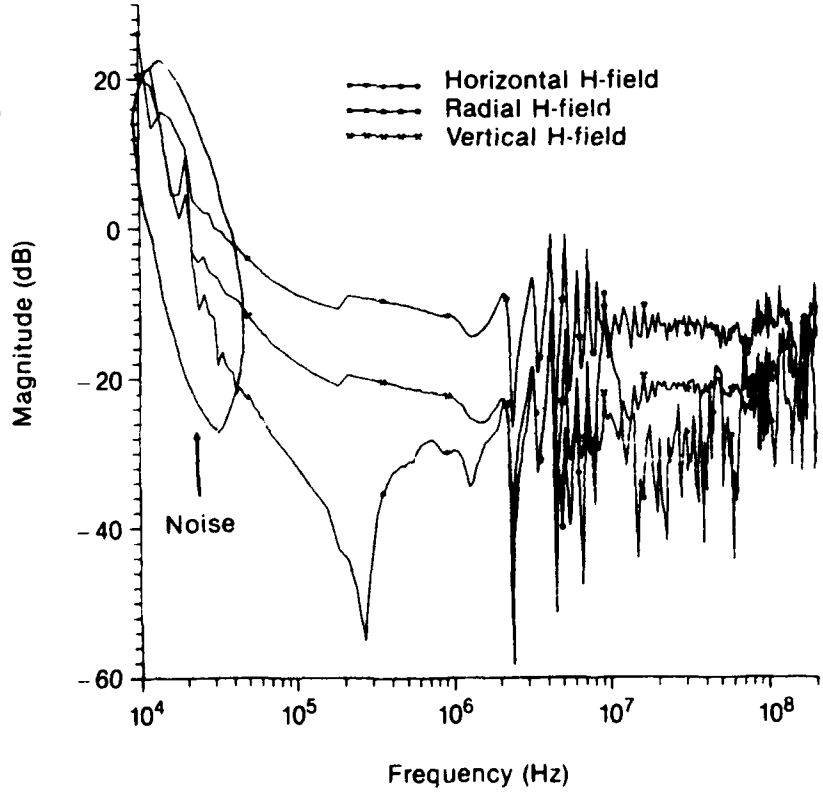

Figure 16. Component E-field comparison at location H, 1.3-m height, measured cw data.

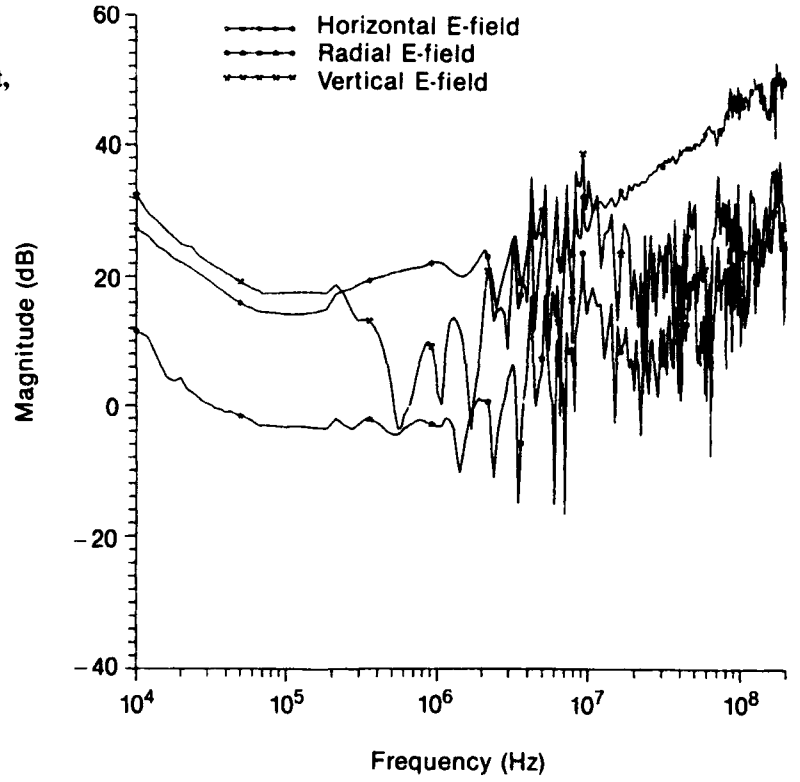

Figure 17. Component H-field comparison at location H, 1.3-m height, measured cw data.

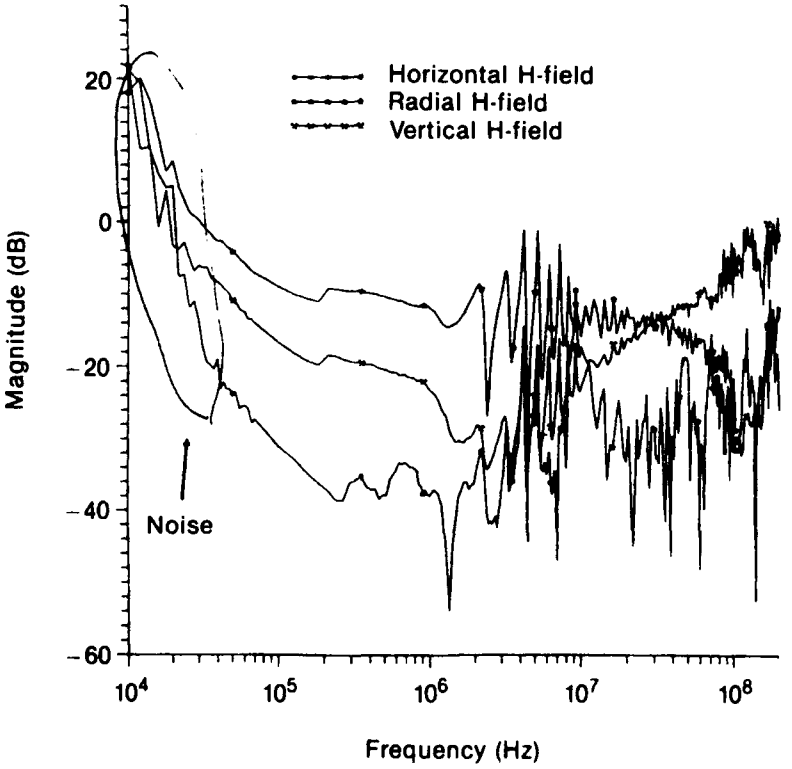

Figure 18. Comparison of transfer functions for three pacemakers in vertical phantom; vertical phantom on ground. Measured cw data.

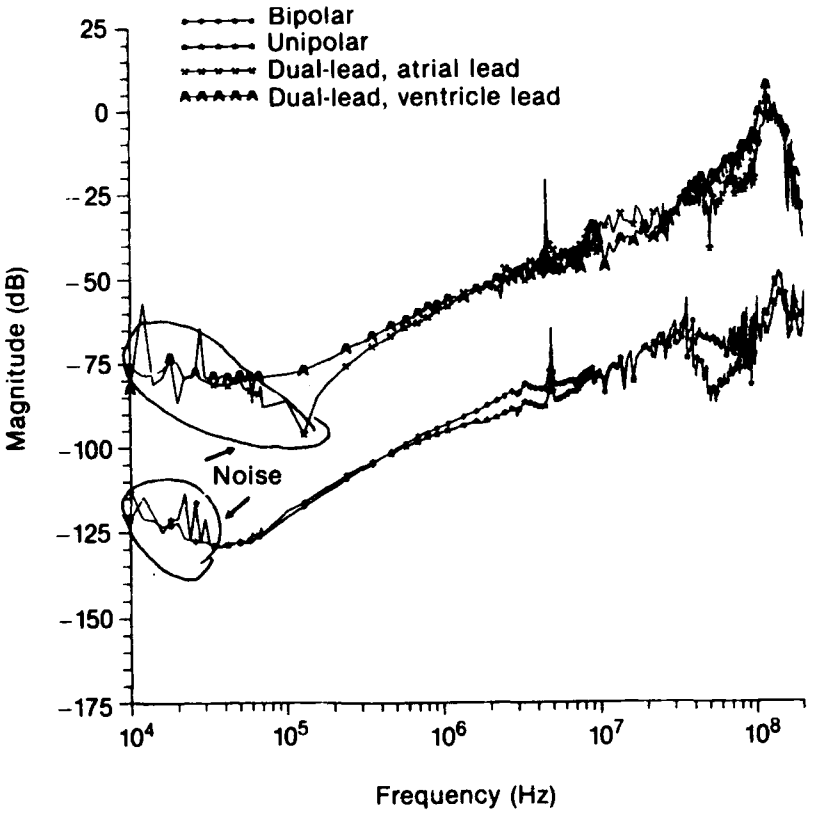

Figure 19. Comparison of transfer functions for three pacemakers in vertical phantom; vertical phantom elevated above ground. Measured cw data.

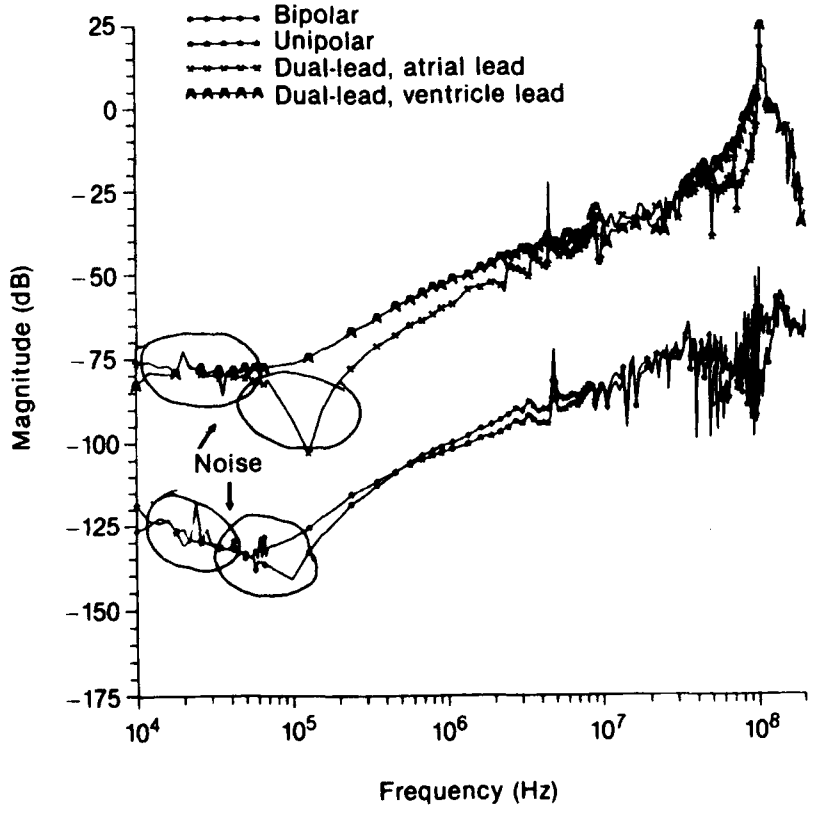

Figure 20. Comparison of transfer functions for three pacemakers in horizontal phantom; horizontal phantom on ground. Measured cw data.

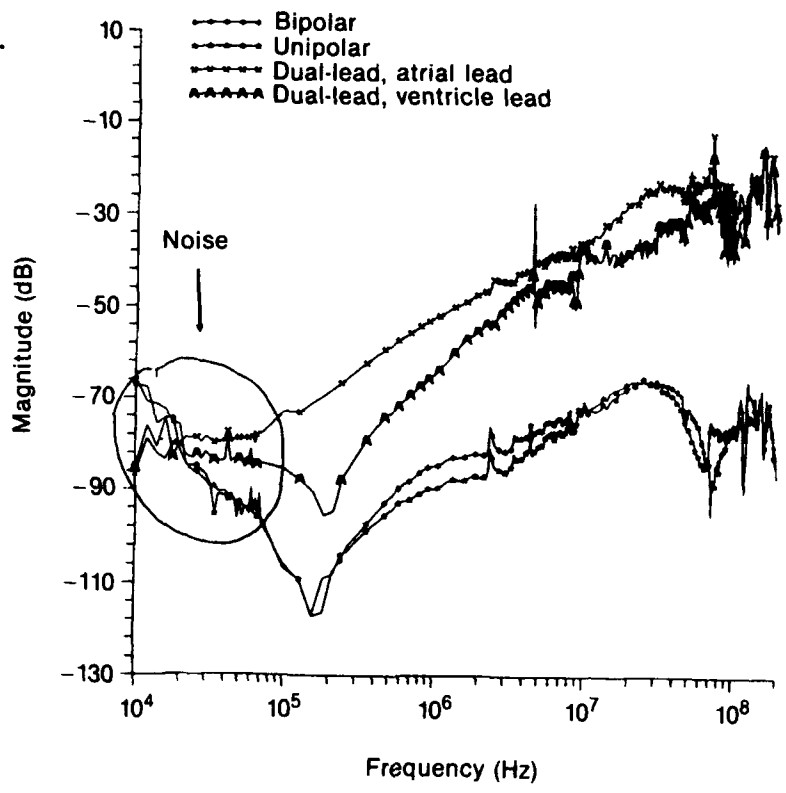

Figure 21. Comparison of transfer functions for three pacemakers in horizontal phantom; horizontal phantom elevated above ground. Measured cw data.

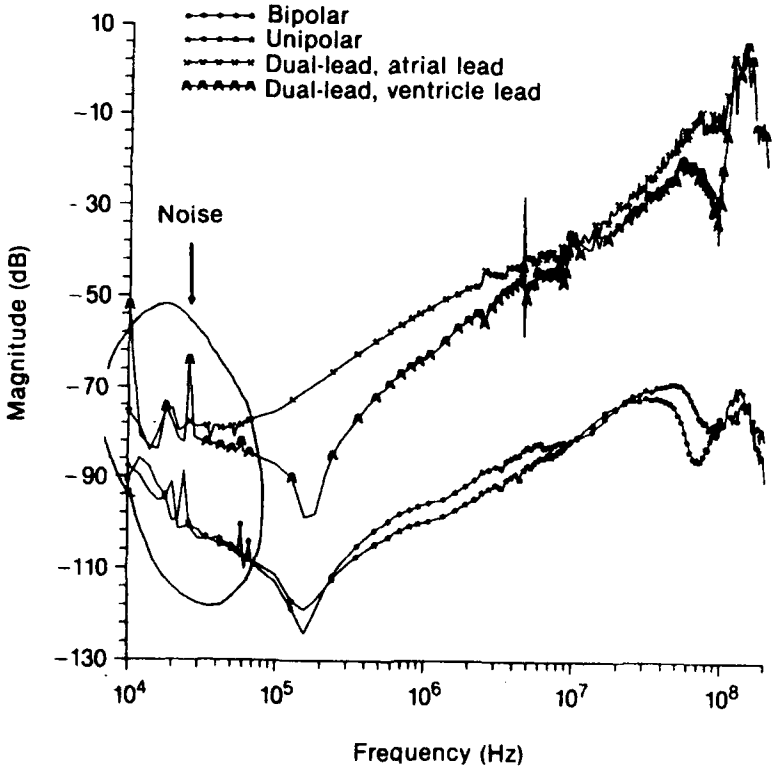

3.2 Convolution and Fourier Transformation

The AESOP fields at the nine locations (see sect. 2.4 and app B) were convolved with the CPM transfer functions to produce the frequency-domain responses of the CPMs to AESOP. Every combination of AESOP field component and CPM transfer function was convolved and inverse Fourier transformed to the time domain. This process, which resulted in over 100 pieces of data, is too extensive to be given here or analyzed piece by piece. A Fortran program was written to analyze this mass of data and statistically report scalar waveform attributes. The statistical data were then screened to determine which scenarios would qualify as the upper bound condition for each pacemaker type (unipolar, bipolar, and dual-lead). The attributes calculated, for which the upper bound determination was based, included time-domain characteristics of peak amplitude (absolute), total energy (normalized into a load impedance of 1 ohm), and maximum slope (peak derivative). In addition to the time-domain attributes, the peak magnitude of each frequency-domain decade was calculated.

Analysis of the time-domain pacemaker lead current data determined that the upper bound condition existed on the centerline of AESOP (location "C") and at the height of 10 m. Every time-domain attribute was greatest at this location, and the highest frequency-domain magnitude was in the 10- to 100-MHz* frequency decade. Other scenarios yielded higher amplitudes in frequency bands other than the 10- to 100-MHz band, but, considering all attributes, the centerline 10-m height location certainly produces upper bound results. Figure 22 contains the time-domain CPM lead responses to the

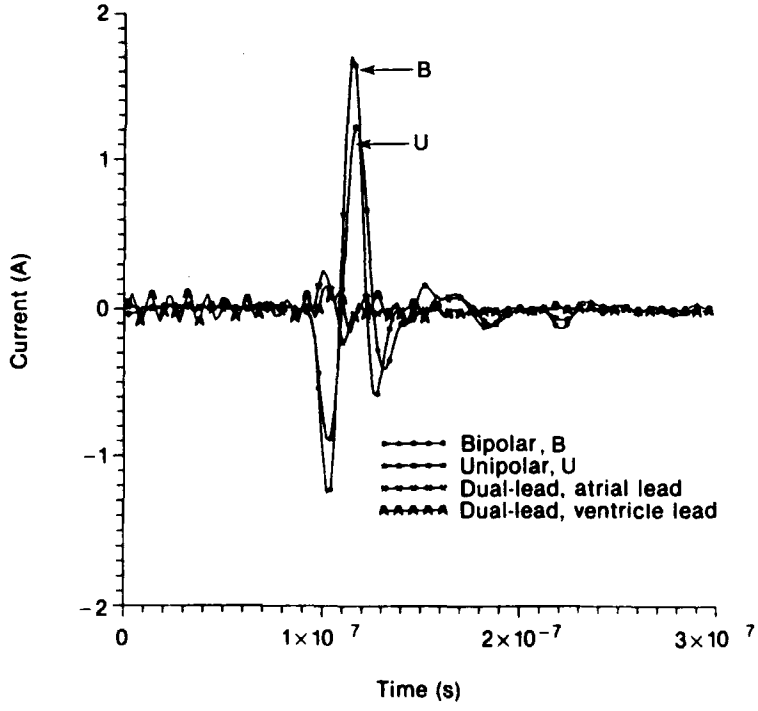

Figure 22. Comparison of model currents for three pacemakers. Upper bound current responses for AESOP fields at centerline location C, 10-m height.

* *The body resonance lies in this decade.*

centerline, 10-m height condition. In every case, the dual-lead CPM responses to H-field excitation were significantly lower than the unipolar and bipolar responses to E-field excitation. Since the dual-lead currents were considerably lower than the unipolar or bipolar responses, the dual-lead responses were discarded and the unipolar and/or bipolar upper bound conditions were imposed on dual-lead pacemakers in the current injection tests. That is, if the leads of a dual-lead CPM are of bipolar construction, the bipolar upper bound conditions apply, and if the leads are of unipolar construction, the unipolar upper bound conditions apply.

3.3 Current Injection

The unipolar and bipolar currents for the upper bound scenario (described above) are used as the control or model currents for the CIT. An effort was made to inject each CPM test sample (10) with currents both less than and greater than the upper bound current in order to determine effects thresholds (see fig. 23). The attributes of the model currents were used to determine the "strength" of the CIT pulse injected into the CPM leads. Table 1 lists the 10 pacemaker test samples by a code identifier and gives the lead type and programmer availability status. Table 1 actually lists 12 pacemakers but, as indicated in the comments column, two units (A and L) were eliminated before testing because of weak internal batteries.

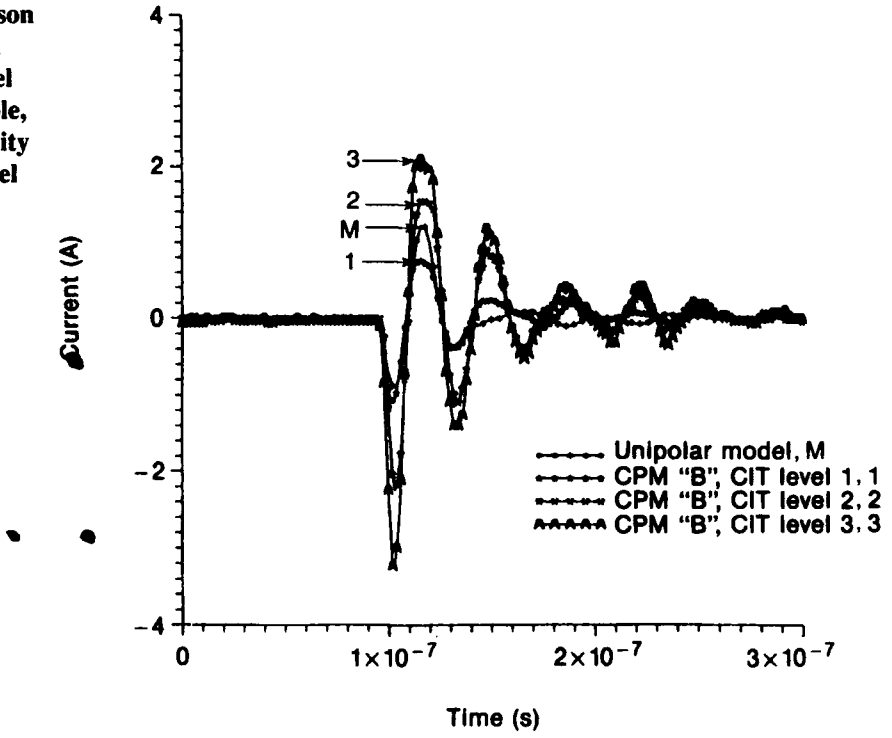

Figure 23. Comparison of CIT currents and corresponding model current. One example, displaying CIT fidelity in reproducing model currents.

Table 1. Description of pacemaker test samples

Code identifier	Description	Programmer availability	Comments
A	Bipolar programmable	Yes	Eliminated before testing—low battery voltage
B	Unipolar programmable	Yes	1986 model
C	Dual-lead programmable	Yes	Pulse unipolar; sense bipolar. 1985 model
D	Bipolar programmable	No	Split-lead design
E	Unipolar programmable	No	
F	Unipolar	N/A	1982 model
G	Unipolar programmable	Yes	
H	Bipolar programmable	Yes	
I	Dual-lead programmable	Yes	Pulse unipolar; sense unipolar
J	Bipolar programmable	Yes	1987 model
K	Bipolar	N/A	1979 model
L	Bipolar	N/A	Eliminated before testing—low battery voltage

Tables 2 to 5 list the results of phase I and phase II current injection tests. Three attributes of the injected currents are given: peak current, normalized energy, and primary frequency.* Next to each of these attributes, a "%AVFM" number is given. This number describes the percentage that the injected currents varied from the model attributes (%AVFM = percentage of absolute variance from model). The %AVFM is an absolute number that indicates the percentage that an injected current's attributes, at a particular level, are less than or greater than the upper bound or model current attributes (negative %AVFM = less than model). For the unipolar model or upper bound current,

**The primary frequency, as used here, is simply the inverse of the period of the first full cycle of the current waveforms. The upper bound currents obtained through convolution are attenuated rapidly and contain only one to two reflections (fig. 22), whereas the CIT currents tended to ring longer (fig. 23). The primary frequency measure was used to evaluate the CIT current's ability to replicate the first full cycle of the upper bound currents. Additional reflections in the CIT currents produce an overtest condition (greater energy).*

the peak current is 1.227 A, the normalized energy is 19.33 nJ, and the primary frequency is 33.33 MHz. The bipolar model or upper bound current has a peak current of 1.712 A, a normalized energy of 32.57 nJ, and a primary frequency of 35.7 MHz. The last column in the tables indicates any upsets or failures* that were noted in the CIT. Upsets are defined as temporary "effects" due to EMP, and failures are defined as permanent "effects" or damage due to EMP. There were no failures noted at any time during the testing, and all upsets that occurred were observed in the CPM's sense window only. Testing on the dual-lead pacemakers was threefold, namely, the atrial lead, the ventricle lead, and both leads, and is annotated as such in tables 2 to 5 as "-A," "-V," and "-B."

During phase I testing, unipolar CPMs B and F experienced type U1 upsets (refer to appropriate tables for a description of this upset). Pacemaker B experienced the upset at CIT level 4, which had a peak current 272 percent greater (272 %AVFM) than the upper bound (the unipolar model current) and an energy level 1539 percent greater (1539 %AVFM) than the upper bound. Pacemaker F experienced its upset at CIT level 1, with a peak current of 1.38 %AVFM and an energy of 3.49 %AVFM. The CIT source could not be adjusted to a lower level; therefore, the effects threshold for CPM F is not certain. Pacemaker F is an older model CPM (1982) and incorporates less sophisticated technology (nonprogrammable) than modern pacemakers.

Three bipolar pacemakers (D, H, and K) experienced upset in phase I testing. Pacemaker H experienced upset type U1 at CIT level 5 with a peak current of 282 %AVFM and an energy level with a 2961%AVFM. Pacemaker D also experienced upset at level 5 but experienced a U2 type upset (see table 3 for a description of this upset), with a 247 %AVFM for the peak current and a value of 1426 %AVFM for energy. Pacemaker K experienced U2 upsets at all 5 CIT levels. The peak CIT current at level 1 for CPM K was 18.6 percent less than the upper bound current peak, but the energy level was 42 percent greater. Similar to unipolar pacemaker F, pacemaker K has an uncertain effects threshold, it is an older model (1979), and it is nonprogrammable.

Phase II testing involved only the pacemakers that are programmable and for which a programmer was available. Unipolar pacemaker B and bipolar pacemaker H were the only samples to experience upset in phase II. Both B and H experienced the same type of upset in phase II as they did in phase I, but at one CIT level lower than in phase I. However, the CIT current attributes in phase II were greater than the upper bound current attributes.

**There were no failures noted at any time in this effort.*

Table 2. Phase I CIT test results for unipolar pacemakers

CPM	CIT level	Peak (A) /%AVFM*	Normalized energy/%AVFM*	Frequency (MHz) /%AVFM*	Observation
B	1	–1.07 / –12.6	1.54 / –20.2	33.36 / 0.0694	
B	2	–2.24 / 82.49	7.24 / 274	33.36 / 0.0694	
B	3	–3.23 / 163.5	14.3 / 642	32.3 / –3.16	
B	4	–4.57 / 272.2	31.7 / 1539	33.36 / 0.0694	U1
B	5	–5.54 / 351.5	45.9 / 2275	33.36 / 0.0694	U1
E	1	–1.17 / –4.7	2.6 / 34.22	35.74 / 7.217	
E	2	–2.144 / 74.7	8.6 / 344.9	33.36 / 0.0694	
E	3	–3.128 / 155	17.6 / 812.1	33.36 / 0.0694	
E	4	–4.418 / 260	33.0 / 1597	33.36 / 0.0694	
E	5	–5.844 / 376	593 / 2967	34.5 / 3.52	
F	1	–1.244 / 1.38	2.58 / 3.49	34.5 / 3.52	U1
F	2	–2.214 / 80.4	8.26 / 327.4	34.5 / 3.52	U1
F	3	–3.128 / 155	18.0 / 855.8	34.5 / 3.52	U1
F	4	–4.488 / 265.7	32.0 / 1573	34.5 / 3.52	U1
F	5	–5.94 / 384	60.0 / 3045	33.36 / 0.0694	U1
G	1	–1.418 / 15.58	3.7 / 91.66	34.5 / 3.52	
G	2	–2.706 / 120.5	12.2 / 530.5	34.5 / 3.52	
G	3	–3.723 / 203.4	23.1 / 1093	33.36 / 0.0694	
G	4	–5.47 / 345.7	47.1 / 2337	33.36 / 0.0694	
G	5	–5.55 / 352	47.2 / 2343	31.27 / –6.185	
I-A	1	–0.9455/–23	1.37 / –29.2	30.3 / –9.03	
I-A	2	–1.652 / 34.6	3.49 / 80.36	27.0 / –18.86	
I-A	3	–2.43 / 98.24	7.59 / 292.7	30.3 / –9.03	
I-A	4	–3.787 / 208.6	16.0 / 730	30.3 / –9.03	
I-A	5	–5.65 / 360	36.4 / 1784	31.3 / –6.185	
I-B	1	–1.57 / 27.74	3.38 / 74.96	35.74 / 7.22	
I-B	2	–2.88 / 134.9	11.3 / 482	35.74 / 7.22	
I-B	3	–4.12 / 235.8	20.2 / 945.6	34.5 / 3.52	
I-B	4	–6.03 / 391.5	46.0 / 2279	34.5 / 3.52	
I-B	5	–7.43 / 505.4	67.0 / 3375	37.0 / 11.2	
I-V	1	–1.02 / –16.87	1.38 / –28.6	31.27 / –6.185	
I-V	2	–1.722 / 40.34	2.86 / 48.23	33.36 / 0.0694	
I-V	3	–2.53 / 106.3	8.33 / 331	28.6 / –14.2	
I-V	4	–3.65 / 197.2	15.0 / 720	28.6 / –14.23	
I-V	5	–4.85 / 295.5	27.0 / 1336	29.4 / –11.7	

**%AVFM = percentage of absolute variance from model; "–" entries indicate that a value is less than the model value.*

Notes:

U1 = UPSET: CIT current injected during a CPM's sense window caused the inhibition of 1 CPM output pulse immediately following the CIT current.

U2 = UPSET: CIT current during CPM's sense window caused inhibition and the resynchronization of the CPM's timing cycle. That is, rather than continuing through the sense cycle, the CPM started a new refractory period coincident with the CIT current pulse.

Table 3. Phase I CIT test results for bipolar pacemakers

CPM	CIT level	Peak (A) /%AVFM*	Normalized energy/%AVFM*	Frequency (MHz) /%AVFM*	Observation
D	1	–1.42 /–17.14	4.13 / –26.7	35.74 / 0.0697	
D	2	–2.5 / 45.8	13.8 / 322	35.7 / 0.0693	
D	3	–3.62 /111.7	27.9 / 755.8	37.06 / 3.776	
D	4	–4.98 /191	46.2 /1317	35.74 / 0.0697	
D	5	–5.94 /247	49.7 /1426	33.36 / –6.602	U2
H	1	–1.42 /–17.14	4.47 / 37.13	35.74 / 0.0697	
H	2	–2.54 / 48.28	14.5 / 344.6	35.74 / 0.0697	
H	3	–3.475 /103	30.1 / 824.8	35.74 / 0.0697	
H	4	–5.119 /199.1	57.7 /1670	35.74 / 0.0697	
H	5	–6.54 /282	99.7 /2961	34.5 / –3.381	U1
J	1	–1.468 /–14.23	4.36 / 33.82	35.74 / 0.0697	
J	2	–2.6 / 51.95	15.0 / 359	35.74 / 0.0697	
J	3	–3.773 /120.44	29.0 / 788.7	35.74 / 0.0697	
J	4	–5.19 /203.18	56.1 /1623	35.74 / 0.0697	
J	5	–5.75 /235.66	52.1 /1500	34.5 / –3.381	
K	1	–1.393 /–18.6	4.63 / 42.13	35.74 / 0.0697	U2
K	2	–2.601 / 51.95	16.3 / 401.3	35.74 / 0.0697	U2
K	3	–3.723 /117.54	32.1 / 885.3	35.74 / 0.0697	U2
K	4	–5.189 /203.18	70.9 /2079	34.51 / –3.381	U2
K	5	–6.934 /305.11	116 /3448	34.51 / –3.381	U2
C-A	1	–1.393 /–18.6	1.97 / –39.4	35.74 / 0.0697	
C-A	2	–2.39 / 39.63	7.17 / 120.2	35.74 / 0.0697	
C-A	3	–3.62 /111.5	15.3 / 368	34.51 / –3.381	
C-A	4	–5.15 /200.94	32.3 / 892.7	33.36 / –6.602	
C-A	5	–6.74 /293.5	59.6 /1730	33.36 / –6.602	
C-B	1	–2.015 / 17.75	7.06 / 116.7	38.49 / 7.77	
C-B	2	–3.62 /111.5	25.3 / 676.6	33.36 / –6.602	
C-B	3	–4.915 /187.15	41.0 /1160	38.49 / 7.77	
C-B	4	–6.94 /305.61	90.6 /2681	35.74 / 0.0697	
C-B	5	–9.31 /444	161 /4844	35.74 / 0.0697	
C-V	1	–1.27 /–25.86	1.65 / –49.5	34.51 / –3.381	
C-V	2	–2.144 / 25.26	5.25 / 61.26	34.51 / –3.381	
C-V	3	–3.093 / 80.7	10.8 / 230.6	32.28 / –9.615	
C-V	4	–4.278 /150	20.9 / 540.2	33.36 / –6.602	
C-V	5	–5.84 /241	41.2 /1163	32.28 / –9.615	

**%AVFM = percentage of absolute variance from model; "–" entries indicate that a value is less than the model value.*

Notes:

U1 = UPSET: CIT current injected during a CPM's sense window caused the inhibition of 1 CPM output pulse immediately following the CIT current.

U2 = UPSET: CIT current during CPM's sense window caused inhibition and the resynchronization of the CPM's timing cycle. That is, rather than continuing through the sense cycle, the CPM started a new refractory period coincident with the CIT current pulse.

Table 4. Phase II CIT test results for unipolar pacemakers

CPM	CIT level	Peak (A) /%AVFM*	Normalized energy/%AVFM*	Frequency (MHz) /%AVFM*	Observation
B	1	–1.24 / 1.38	2.29 / 18.3	34.51 / 3.52	
B	2	–2.17 / 76.4	7.4 / 283	34.51 / 3.52	
B	3	–3.06 / 149.2	14.4 / 644.9	34.51 / 3.52	U1
B	4	–4.52 / 268.2	32.4 / 1577	33.36 / 0.0694	U1
B	5	–5.89 / 380.03	50.3 / 2505	33.36 / 0.0694	U1
E	1	— / —	— / —	— / —	
E	2	— / —	— / —	— / —	
E	3	— / —	— / —	— / —	
E	4	— / —	— / —	— / —	
E	5	— / —	— / —	— / —	
F	1	— / —	— / —	— / —	
F	2	— / —	— / —	— / —	
F	3	— / —	— / —	— / —	
F	4	— / —	— / —	— / —	
F	5	— / —	— / —	— / —	
G	1	— / —	— / —	— / —	
G	2	— / —	— / —	— / —	
G	3	— / —	— / —	— / —	
G	4	— / —	— / —	— / —	
G	5	–6.934 / 465	90.1 / 4564	34.51 / 3.52	
I-A	1	— / —	— / —	— / —	
I-A	2	— / —	— / —	— / —	
I-A	3	— / —	— / —	— / —	
I-A	4	— / —	— / —	— / —	
I-A	5	–5.745 / 368.2	40.5 / 1996	30.33 / –9.03	
I-B	1	— / —	— / —	— / —	
I-B	2	— / —	— / —	— / —	
I-B	3	— / —	— / —	— / —	
I-B	4	— / —	— / —	— / —	
I-B	5	–8.32 / 578	85.3 / 4312	37.1 / 11.189	
I-V	1	— / —	— / —	— / —	
I-V	2	— / —	— / —	— / —	
I-V	3	— / —	— / —	— / —	
I-V	4	— / —	— / —	— / —	
I-V	5	–5.35 / 336	33.6 / 1640	29.4 / –11.7	

**%AVFM = percentage of absolute variance from model; "–" entries indicate that a value is less than the model value.*

Notes:

U1 = UPSET: CIT current injected during a CPM's sense window caused the inhibition of 1 CPM output pulse immediately following the CIT current.

U2 = UPSET: CIT current during CPM's sense window caused inhibition and the resynchronization of the CPM's timing cycle. That is, rather than continuing through the sense cycle, the CPM started a new refractory period coincident with the CIT current pulse.

Table 5. Phase II CIT test results for bipolar pacemakers

CPM	CIT level	Peak (A) /%AVFM*	Normalized energy/%AVFM*	Frequency (MHz) /%AVFM *	Observation
D	1	— / —	— / —	— / —	
D	2	— / —	— / —	— / —	
D	3	— / —	— / —	— / —	
D	4	— / —	— / —	— / —	
D	5	— / —	— / —	— / —	
H	1	— / —	— / —	— / —	
H	2	— / —	— / —	— / —	
H	3	–3.38 / 97.23	29.4 / 802.5	34.51 / –3.381	
H	4	–5.05 /195	65.8 /1920	35.74 / 0.0697	U1
H	5	–6.835 /299.3	114 /3385	34.51 / –3.381	U1
J	1	— / —	— / —	— / —	
J	2	— / —	— / —	— / —	
J	3	— / —	— / —	— / —	
J	4	— / —	— / —	— / —	
J	5	–7.033 /311	110 /3277	35.74 / 0.0697	
K	1	— / —	— / —	— / —	
K	2	— / —	— / —	— / —	
K	3	— / —	— / —	— / —	
K	4	— / —	— / —	— / —	
K	5	— / —	— / —	— / —	
C-A	1	— / —	— / —	— / —	
C-A	2	— / —	— / —	— / —	
C-A	3	— / —	— / —	— / —	
C-A	4	— / —	— / —	— / —	
C-A	5	–7.033 /311	78.4 /2307	33.36 / –6.602	
C-B	1	— / —	— / —	— / —	
C-B	2	— / —	— / —	— / —	
C-B	3	— / —	— / —	— / —	
C-B	4	— / —	— / —	— / —	
C-B	5	–9.51 /456	168 /5057	35.74 / 0.0697	
C-V	1	— / —	— / —	— / —	
C-V	2	— / —	— / —	— / —	
C-V	3	— / —	— / —	— / —	
C-V	4	— / —	— / —	— / —	
C-V	5	–6.14 /259	51.5 /1482	35.74 / 0.0697	

**%AVFM = percentage of absolute variance from model; "–" entries indicate that a value is less than the model value.*

Notes:

U1 = UPSET: CIT current injected during a CPM's sense window caused the inhibition of 1 CPM output pulse immediately following the CIT current.

U2 = UPSET: CIT current during CPM's sense window caused inhibition and the resynchronization of the CPM's timing cycle. That is, rather than continuing through the sense cycle, the CPM started a new refractory period coincident with the CIT current pulse.

3.4 Other Efforts

Two independent theoretical efforts were undertaken in parallel with the testing described here. The results of these efforts were used to reinforce test data and aid in the quantification of the upper bound current values. The first effort consisted of a combination of purely analytic treatments (low frequency) and computer-implemented finite-difference time-domain solutions to Maxwell's equations (high frequency) to predict the response of pacemakers to EMP. The second effort used a computer code, in which the implanted pacemaker was treated as a transmission line, to calculate EMP-induced currents on pacemaker leads.

3.4.1 Finite-Difference Time-Domain Calculations

The computer code "FMD" [8] was used to predict the response of a unipolar pacemaker to EMP for the frequency range of 20 to 200 MHz. The FMD is a 3-D code for treating electromagnetic problems via finite-difference solutions of Maxwell's equations in the time domain. In order to determine the frequency response of the pacemaker, successive runs were made using pure sinusoids, of various frequencies, as the sources. For the frequencies of 10 kHz to 20 MHz, a purely analytic treatment of the problem was used [9]. This analysis, as mentioned earlier, is referred to as the "Goldstein analysis." The Goldstein analysis was used to determine the frequency-domain pacemaker transfer functions analogous to the measured transfer functions discussed in section 2.3. The transfer functions were then convolved with the same computer-generated AESOP fields that were used with the experimental data and transformed to the time domain.

Three calculations were made corresponding directly to the following AESOP locations: A at 1.5 m high, A at 10 m high, and B at 1.5 m high. The calculations were performed with the vertically standing man and unipolar pacemaker only and were driven by only vertical E-fields, at the appropriate location. Although these scenarios do not produce the upper bound current results (as determined from test results), they do serve as comparison points for corresponding experimental data. The pacemaker configuration within the body was modelled in a more realistic manner than the worst-case straight lead run used throughout the cw tests. Figure 24 depicts the implanted pacemaker orientation used in the Goldstein analysis versus the pacemaker configuration used in the cw tests. Although the 90-deg bends in the pacemaker lead are exaggerated, this configuration is essentially a more realistic CPM lead route than the straight lead run.

Figure 25 compares the measured transfer function with the Goldstein or theoretical transfer function for a unipolar pacemaker in a grounded man (a man standing vertically on the ground). The theoretical transfer function magnitude is approximately 20 dB (a factor of 10) less than the experimental transfer function magnitude throughout the frequency spectrum of interest.

Figure 24. Pacemaker configurations within the body.

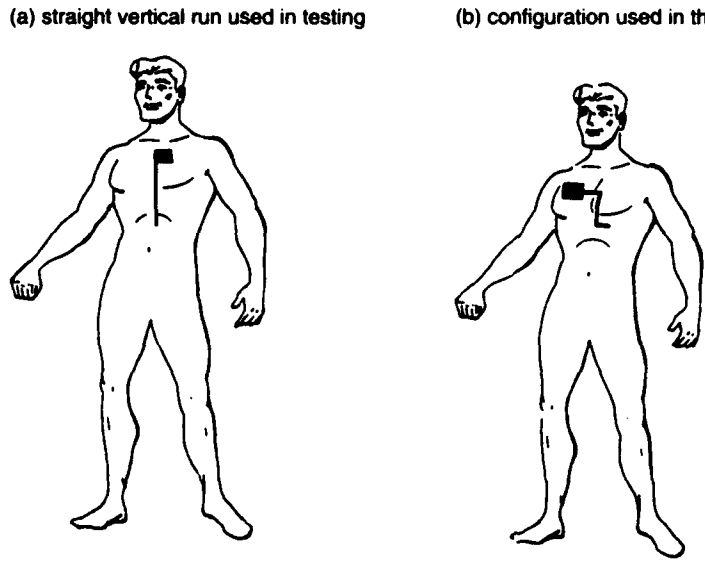

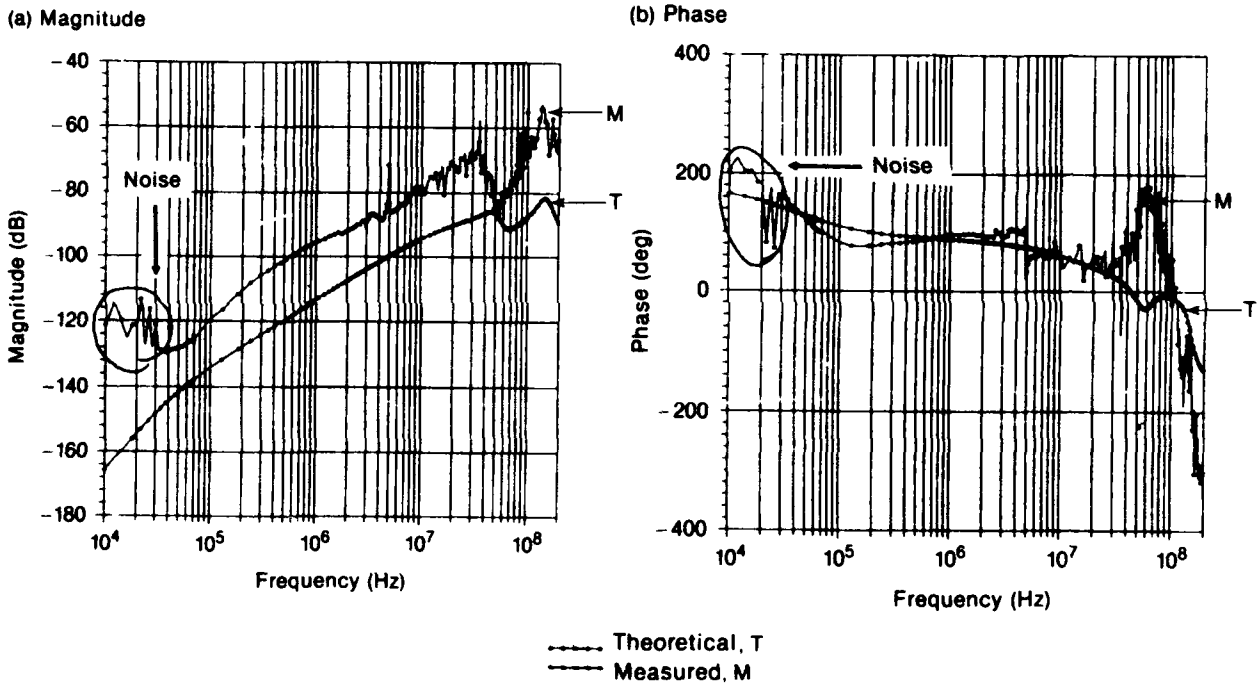

Figure 25. Comparison of empirical and theoretical unipolar pacemaker transfer functions for a pacemaker in vertical phantom on ground.

The phase comparisons are in reasonable agreement, with the exception of the resonances. In fact, both the magnitude and phase responses resonate at slightly higher frequencies in the theoretical data plots. The differences in the resonances are attributed to the computer code's use of varying tissue parameters as a function of tissue type as well as frequency (the testing efforts used whole body averages for a specific frequency). The 20-dB difference in magnitudes is attributed to the difference in the pacemaker lead orientations. The cw tests were performed with the CPM leads totally straight to promote

maximum coupling, whereas the computer model pacemaker configuration was only partially vertical, effectively reducing the vertical lead length and the vertical E-field coupling.

Figure 26 compares the theoretical and measured transfer functions for a unipolar pacemaker in the elevated man (isolated from ground contact). Overall, the isolated man results are in closer agreement than the grounded man transfer function comparisons; however, the theoretical results again have slightly higher resonances. The greater difference in the grounded man results may be attributed to the "perfect" ground achievable in the computer code used by Goldstein, whereas perfect grounding is not realistic in the testing. Figures 27 to 29 compare the time-domain CPM lead currents for three AESOP locations. In each case the experimental currents are approximately five to six times greater in peak amplitude, and ring at a slightly lower frequency than the theoretical results. However, the wave-shape structures are very similar. Accounting for configurational and parametrical differences, the theoretical results are in excellent agreement with the experimental results.

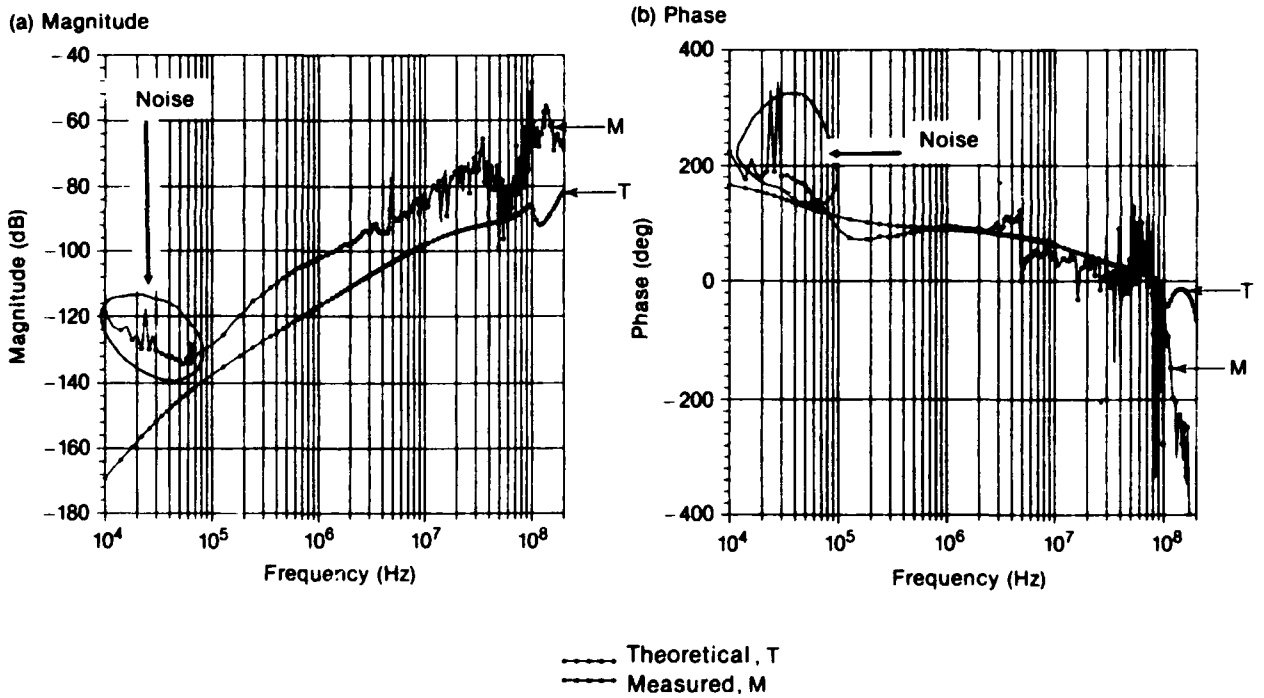

Figure 26. Comparison of empirical and theoretical unipolar pacemaker transfer functions for a pacemaker in vertical phantom elevated above ground.

Figure 27. Comparison of empirically generated and theoretical unipolar pacemaker responses, in vertical phantom on ground, to AESOP at location A, 1.5-m height.

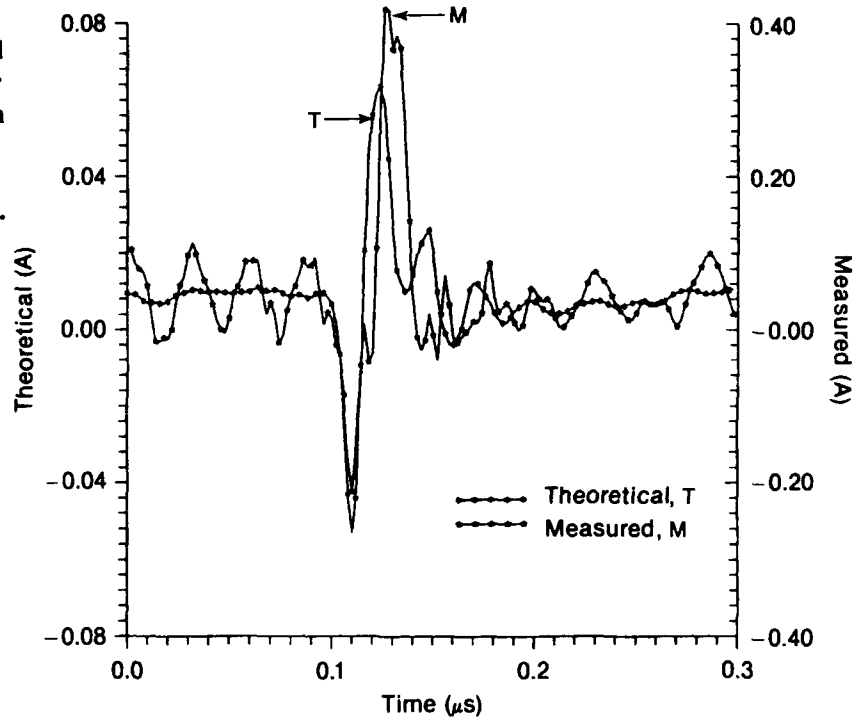

Figure 28. Comparison of empirically generated and theoretical unipolar pacemaker responses in vertical phantom on ground, to AESOP at location B, 1.5-m height.

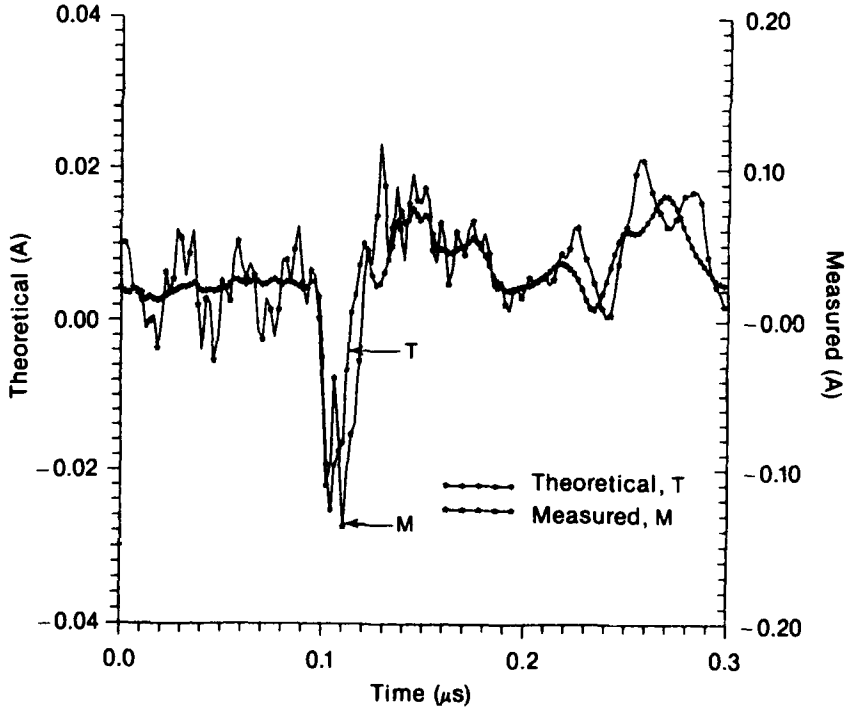

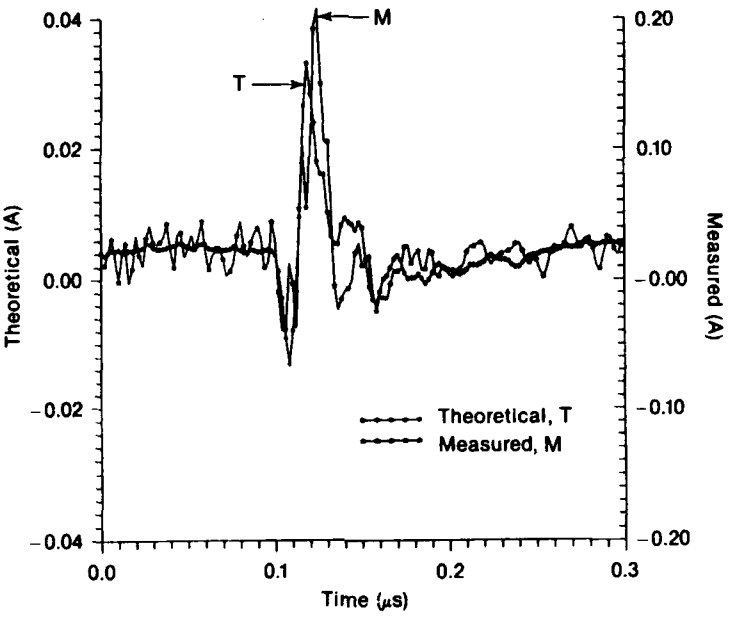

Figure 29. Comparison of empirically generated and theoretical unipolar pacemaker responses, in elevated vertical phantom, to AESOP at location A, 10-m height.

3.4.2 Transmission Line Model Calculations

In addition to the Goldstein analysis, a transmission line computer model (QV7TB) was used to analytically predict the response of an implanted unipolar pacemaker to EMP [1]. To implement QV7TB, a unipolar pacemaker was modeled as a transmission line (T-line). The E-fields inside the body, due to an EMP incident on the body, were calculated and then applied to the transmission line pacemaker model. The current flowing on the pacemaker lead into the pacemaker was determined. The T-line model calculation was performed in an absolute worst-case manner to obtain a "quick-look" analysis of the greatest currents an EMP could theoretically induce on a pacemaker lead.

The incident EMP waveform used in this effort was not an AESOP field as used in the other efforts, but a standard double-exponential free-field EMP waveform given by

$$E(t) = E_{peak} \times 1.05 \times (e^{-bt} - e^{-at}) ,$$

where

$$a = 4.76 \times 10^8 \text{ s}^{-1} ,$$

$$b = 4.00 \times 10^6 \text{ s}^{-1} .$$

Figure 30 depicts the double-exponential EMP waveform with a peak field of 10 kV/m. This 10-kV/m double exponential is an approximation of the largest field that AESOP would produce outside WRF if the field did not interact with the ground, i.e., free-field. To facilitate a comparison of analytic and empirical data, this 10-kV/m E-field was convolved with all the measured unipolar transfer functions in elevated phantoms and transformed to time-domain CPM lead currents. Only elevated phantom transfer functions were included

because both the T-line model and the free-field double exponential used are ignorant of ground plane interaction. Likewise, the orientation of the phantom has no interpretation in the T-line model; therefore, both horizontal and vertical elevated transfer functions were used.

The upper bound* CPM lead current, resulting from the double-exponential convolution with the transfer functions, occurs for the elevated horizontal phantom. Figure 31 depicts the upper bound empirical results and the T-line model results for a 10-kV/m incident double-exponential EMP. The T-line model results are approximately 12 times greater (22 dB) in peak current than the empirical results.

Figure 30. Standard double-exponential EMP waveform with 10-kV/m peak.

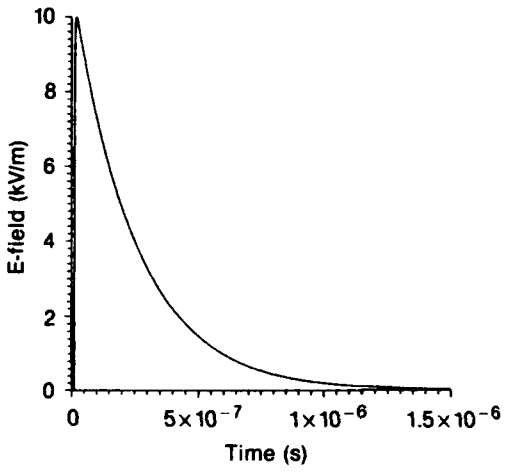

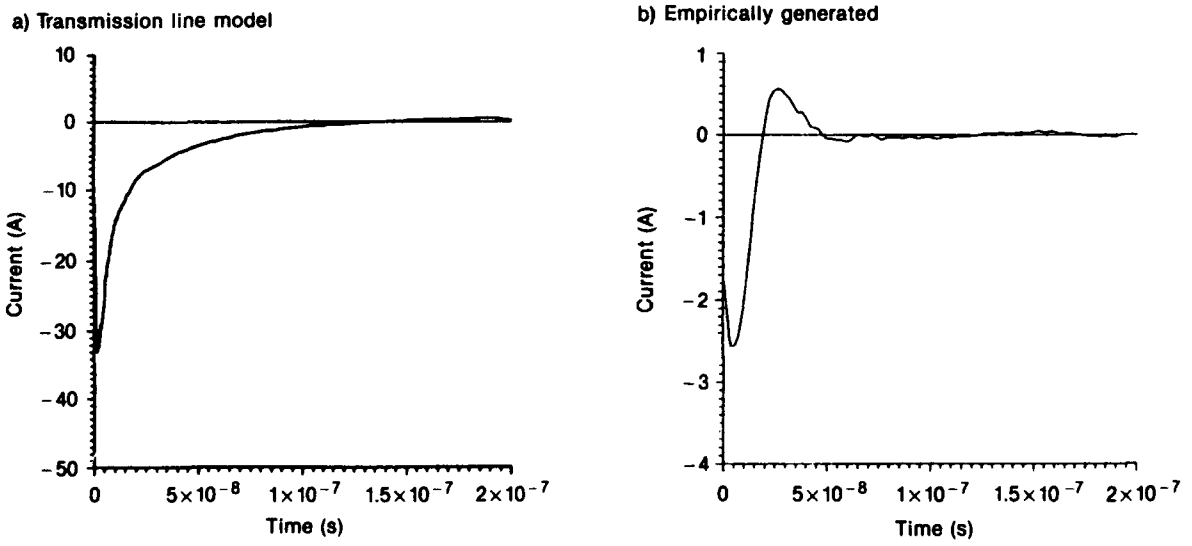

Figure 31. Comparison of transmission line model analysis and empirically generated equivalent due to double-exponential EMP excitation of a unipolar pacemaker.

** Again, upper bound determination is based on the scalar waveform characteristics of peak, normalized energy, and peak derivative.*

4. Discussion and Conclusions

The testing in this effort was performed in a manner which promoted upper bound results. Pacemaker leads were oriented to maximize coupling of EM energy, and the electrical parameters of the human body were chosen to emphasize the EM absorption resonances of the body. Locations at the WRF border were identified where AESOP fields are greatest for various polarizations. While the test efforts were performed to promote upper bound results, care was taken not to impose totally unrealistic conditions.*

The frequency-domain transfer functions of pacemakers in phantoms were empirically determined and analytically convolved with AESOP fields to produce the pacemaker lead current responses to AESOP excitation. The upper bound results (greatest CPM lead currents) occur for a horizontal man elevated 10 m above ground and on the centerline of AESOP. The 10-m height is an upper bound for the realistic elevated height of a man. A man in a cherry-picker (i.e., a telephone repairman) is represented by this height. All pacemakers were then tested, via current injection, to this upper bound lead current.

Phase I of the current injection testing was performed on all 10 pacemaker samples, with all pacemakers set to their individual nominal or factory-shipped settings. During the phase I test, five pacemakers experienced upset. Three of the pacemakers upset at currents with a peak amplitude 247 percent greater than the upper bound current and with energies on the order of 1400 percent greater than the upper bound current. The other two pacemakers, units F and K, experienced upset at currents roughly equivalent to the upper bound currents.

Phase II involved only the six pacemakers that could be reprogrammed. Two units (B and H) experienced upset, but at levels greater than upper bound current (150 percent greater in peak current and 640 percent greater in energy). These same two pacemakers had experienced phase I upset, but the phase II upsets occurred at lower current levels than the phase I currents, which is understandable, if not expected, since the CPMs were programmed to be more sensitive. No failure or damage to any unit was noted at any time during the testing.

The results of the CIT testing suggest that modern sophisticated pacemakers that might be just outside the confines of WRF will not experience any discernible effect from AESOP operation. Conclusions regarding the two older units (F and K) that experienced upset at current levels near the upper bound current levels are not as clearly defined. Because of limitations in the CIT pulser, F and K were not tested at levels where no upset occurred (i.e., below CIT level 1); therefore, a threshold for effects is not determinable for

**The CIT testing at high levels above the upper bound levels was unrealistic for a CPM wearer outside the WRF but was performed to obtain effects thresholds.*

these units. The CPM upsets near upper bound current levels during testing do not dictate their upset due to AESOP. Although these units upset near the upper bound current levels, the upper bound conditions are not physically probable. Under the conditions in which the upper bound currents were determined, a cardiac pacemaker wearer would have to be wearing an older model CPM and be lying horizontal at a 10-m height on the centerline of AESOP. Additionally, the wearer would have to be subjected to an AESOP output pulse at the same time his or her pacemaker is in its sense mode and at a time at which his or her heart is failing and requiring a pacemaker output pulse. Even if these conditions were coincident, the effect of one AESOP pulse would be to inhibit only one CPM output pulse. Taking it a step further, if all these conditions could occur every time AESOP fired and AESOP was operated at its maximum rate, the CPM wearer could lose one CPM output pulse every 5 min (approximately 1 out of 250 CPM output pulses) during AESOP operation.

For those pacemakers tested and the test conditions imposed, older CPMs experienced upsets when subjected to AESOP EMP fields on the order of 8 kV/m (peak E-field). The modern technology pacemakers were insensitive to upset up to EMP levels of approximately 20 kV/m (the equivalent peak E-field level required to induce the lowest level phase II upsets). No damage to any of the pacemakers was noted during the CIT testing, which attained equivalent EMP E-field levels of at least 25 kV/m.* Even the upsets noted are temporary upsets normally without risk.† These peak E-field thresholds are for upper bound conditions. The actual thresholds for effects are in all probability higher than those stated. A direct comparison to the Goldstein results suggests that the upper bound condition thresholds may be 15 dB higher than the actual thresholds. Therefore if a 15-dB safety margin is assumed with the peak E-field thresholds, the upsets experienced by the older CPMs may not be probable.‡ Even if a 15-dB threshold is not justified, the straight CPM lead orientation used in the testing produces results on the order of 9.5 dB higher (factor of 3) than the Goldstein results that used a more realistic lead orientation.

Comparing the empirical results to the Goldstein analysis leads to a quantification of the upper bound conditions imposed in the test efforts. The Goldstein analysis was performed in a more physically realistic manner than the actual testing in that the frequency dependence of the electrical parameters of the body are accounted for, and the pacemaker lead was configured in a "winding" run rather than a straight run. Direct comparison of the results of the two efforts shows that the empirical results are approximately a factor of 6, or 15.5 dB, greater than the Goldstein results. A primary factor affecting the

**The peak fields cited are associated with typical AESOP E-field wave-shapes only.*

†According to the "Pacemaker Standard" (see app A), the upsets noted are class II rate responses defined as temporary upsets normally without risk.

‡An actual effects threshold would have to be established for the two older CPMs before a more affirmative statement could be made.

difference between the theoretical and experimental results is the difference in the pacemaker lead configurations. The Goldstein analysis used a lead configuration that resulted in approximately one-third of the lead being vertically oriented. Since the case used for comparison is for the vertical man in vertical E-fields, the amount of energy coupled to the CPM lead is directly proportional to the vertical lead length. The difference in vertical lead lengths between the theoretical and experimental results accounts for roughly a factor of three (9.5 dB) in the results between the two methods.

Other factors affecting the difference between the Goldstein results and the empirical results could be discussed; however, the quantification of the effect of these factors on the CPM lead currents is not obvious. The Goldstein analysis accounts for the frequency dependence of human tissue spatially and by tissue type, whereas the cw test used constant electrical parameters. The conductivity used in the cw tests was specifically chosen to produce upper bound results. Additionally, the E-fields at the cw test site are not purely vertical and although cross-coupling of minor fields is subordinate to the major field, cross-coupled fields could increase the experimental results. Another source of differences between the Goldstein results and the empirical data is the theory's imposition of perfect conditions, such as grounding, which are not always realistic under test conditions.

The T-line model was used to obtain a quick-look, absolutely worst-case evaluation of the EMP effects on pacemakers and was primarily focussed on determining energy-related damage to pacemakers. The difference between the test results and the transmission line model results is much greater than the Goldstein/test comparison. The T-line results were 12 times (22 dB) greater than the equivalent experimental results. There are many possible sources for the discrepancies in the results.

The T-line model used is not actually designed to handle the application for which it was used. Therefore in order to implement it, assumptions were made and worst-case conditions were imposed to validate its use by assuring that the results produced would be greater than actual. The body was treated as an infinite slab of muscle tissue, and the E-fields at several depths within the slab were calculated. The E-fields within the slab were then applied to the T-line model with perfect coupling, and reflections were disallowed by terminating the line in its characteristic impedance. The use of perfect coupling and perfect termination alone is guaranteed to produce results that are greater than the actual currents that would be produced.

Although the T-line model was compounded with totally unrealistic worst-case conditions, the conclusion by the authors of the T-line calculation was that damage (energy-related) to pacemakers was unlikely, with the EMP field used. This conclusion is a particularly significant assertion because under the methodology used, the pacemaker currents determined could not theoretically be any greater, yet damage is not considered likely.

5. Recommendations

Although the application of the methods used in this effort are specific to the EMP produced by AESOP, these methods may be applied to any EMP simulator operation as well as myriad other EMI sources, such as lightning, automobile ignitions, electrical switching, or static discharges. Furthermore, these methods may be modified, simplified in many cases, and applied to any EM field to determine effects on CPMs.

There has been a longstanding need to develop a material that will accurately simulate the electrical characteristics of human tissue over a broad frequency range. An effort was made in this program to duplicate tissue parameters at the CPM transfer function resonances; however, these resonances are not particularly pronounced. The effects on other portions of the frequency spectrum have not been investigated, although comparisons of the experimental data and the "Goldstein" results, which accounted for the frequency dependence of tissue, substantiates the test results as being upper bound using this approach. The development of a wide-band material for simulating human tissue would greatly increase the exactness of future test data.

As an independent effort, conclusions regarding the robustness of cardiac pacemakers to EMP in general cannot be drawn from the data compiled here. A more significant sample base is required before the author would attempt to make generalizations of this type. However, the results do support past findings regarding the increased resistance of modern pacemakers to EMI and furnish the expected effects of AESOP, specifically on CPMs.

Present operations of EMP facilities, equivalent to that of AESOP, do not appear to pose an immediate threat to the well-being of CPM wearers. Nevertheless, a need exists for firmly establishing acceptable EMP exposure levels for CPM wearers employed at EMP facilities, as well as CPM wearers in the general public.

Acknowledgments

The author would like to express his gratitude to the following individuals or groups for their contributions to this effort: Dr. Lawrence Weston of the Walter Reed Medical Center for providing pacemaker test samples and support equipment, and Thomas J. Bock (HDL), Eugene Patrick (HDL), the members of the Army Working Group for the Susceptibility of Medical Electronics to EMP, and the WRF EIS Technical Review Panel for their technical critique and input throughout the program.

References

1. J. W. Erler, D. G. Edelman, and W. B. Byers, *Simulator EMP Effects On Medical Equipment,* Draft Final Report, Volumes 1 and 2, Science Applications International Corporation, SAIC-102-89-004, prepared under HDL contract DAAL02-86-D-0041 DO53 (February 1990).

2. Thomas J. Bock, *EMP Tests of Implantable Cardiac Pacemakers,* Harry Diamond Laboratories, preliminary report, HDL-PRL-88-3 (March 1988).

3. J. Martz and G. Brunhart, *Potential Hazards of High Altitude Electromagnetic Pulse to Implanted Cardiac Pacemakers*, Annual Research Report, AFRRI (July 1972–June 1973).

4. Pacemaker Standards Subcommittee of AAMI, *Pacemaker Standard, Labeling Requirements, Performance Requirements, and Terminology for Implantable Artificial Cardiac Pacemakers*, Final Report, Association for the Advancement of Medical Instrumentation (AAMI), FDA/HFK-76/38, under FDA contract 223-74-5083 (August 1975).

5. Carl H. Durney, Habib Massoudi, and Magdy F. Iskander, *Radiofrequency Radiation Dosimetry Handbook (Fourth Edition)*, Final Report, USAF School of Aerospace Medicine (RZP), USAFSAM-TR-85-73 (October 1986).

6. K. R. Holstine, J. J. Connery, L. M. Rose, and W. J. Stark, *Data Analysis Report for CW Calibration Test for Horizontal Polarization (Volume I): Field Mapping Experiment, Technical Report,* Mission Research Corporation, MRC/COS-R-801, prepared under HDL contract DAAL02-86-D-0043 DO50 (August 1988).

7. R. A. Dalke, P. McKenna, and P. Ng, *Field Calculations for the AESOP EMP Simulator—Volume I*, Electro Magnetic Applications, Inc., EMA-89-R-57 (July 1989).

8. Dennis M. Sullivan, Om P. Gandhi, and Alan Taflore, *Use of the Finite-Difference Time-Domain Method for Calculating EM Absorption in Man Models*, IEEE Trans. Biomed. Eng., 35, No. 3 (March 1988).

9. Bart Goldstein and Ed Kalasky, *The Effects of an EMP Simulator on Cardiac Pacemakers*, Draft Technical Report, Mission Research Corporation, MRC-R-1253-R, prepared under HDL contract DAAL02-86-D-0043 DO82 (30 October 1989).

Appendix A.—Extracts from "Pacemaker Standard"*

Appendix A is an extract of all relevant information in the "Pacemaker Standard" applicable to the effort described in the main body of this report and to testing pacemakers to electromagnetic fields. The extract describes test equipment and procedures for testing the electromagnetic compatibility to cardiac pacemakers.

*Taken from Pacemaker Standard, Association for the Advancement of Medical Instrumentation (AAMI), August 1975.

4.1.8 Test Method for Electromagnetic Compatibility (EMC)

4.1.8.1 Radiated Method

4.1.8.1.1 Energy Source. The energy source is described as follows:

(1) Frequency: 450 MHz +/- 50 MHz.

(2) Modulation: 100 percent, using

$$^{+0.2}_{1\ \text{msec}}{}_{-0.0}$$

rectangular pulses 200 V/m peak pulse amplitude at pulse repetition frequencies of 125% +/- 10% of basic rate of pulse generator.

4.1.8.1.2 Polarization. Polarization of the radiated field shall be with the E field in the direction of the lead or circular.

4.1.8.1.3 Test Cell Specifications. The following specifications shall be used:

(1) Medium: Saline - 375 ohm cm resistivity (approximately 0.03 molar NaCl).

(2) Container Material. Material with an attenuation such that incident radiation shall not be attenuated at the test frequency more than 1 dB by any of the walls.

(3) Size and Shape: rectangular shape; minimum inside dimensions - 20 cm x 40 cm x 80 cm (Figure 21).

4.1.8.1.4 Procedure. The following procedure shall be used:

(1) Test Sample Orientation. The pacemaker shall be placed in the test cell as shown in figure 1. Each pulse generator shall be tested with each side (the two with the largest surface area) in a plane perpendicular and proximal to the incident field.

(2) Coupling Method. Monitoring electrodes shall be immersed in the saline. The monitoring electrodes shall not touch the pacemaker system nor interfere with the incident field.

(3) Pacemaker Operating Mode. Signals shall not be applied to simulate cardiac activity.

(4) Modulation. When a pulse generator output pulse synchronizes with the incident electromagnetic signal, the modulation shall be gradually increased to 3.00 pps +/- 10%.

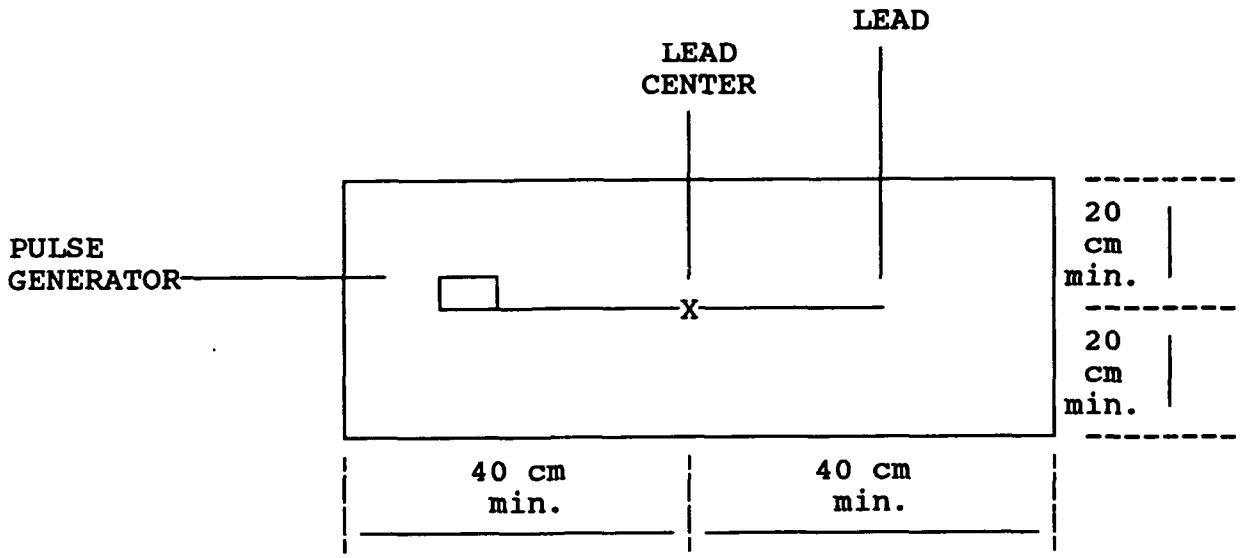

(a) Top View

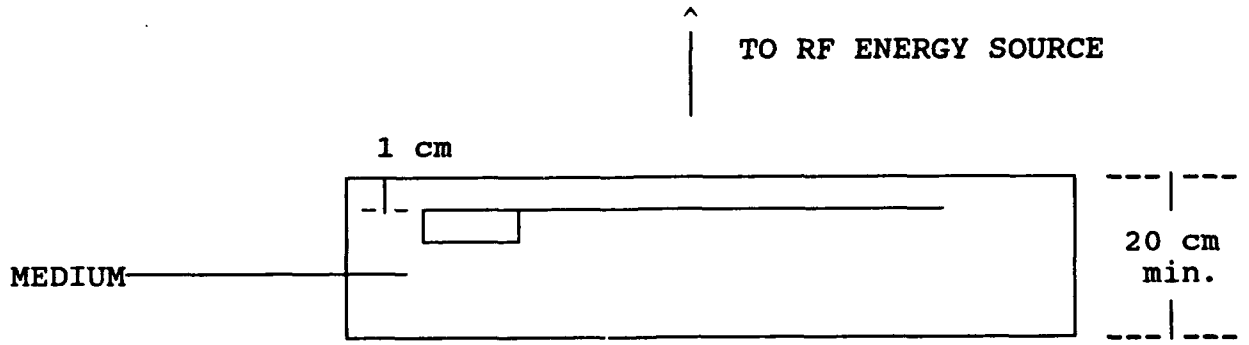

(b) Side View

Figure 21.

Test Cell and Sample Placement

(5) Monitoring of Characteristics. The following pulse generator characteristics shall be monitored before, during and after the test:

(A) Rate
(B) Pulse Duration
(C) Pulse Amplitude

4.1.8.2 Conducted Method

4.1.8.2.1 Energy Sources. The following describes energy sources which shall be used:

(1) Frequencies. 50 Hz, 60 Hz and 400 Hz

(2) Modulation. None

(3) Amplitude. 100 mV RMS

4.1.8.2.2 Test Medium. The test medium shall be the same as Paragraph 4.1.8.1.3 (1).

4.1.8.2.3 Procedure. The following procedure shall be used:

(1) Test Sample Orientation. The pacemaker shall be immersed in the test medium with its lead straight.

(2) Coupling Method. Monitoring electrodes shall be immersed in the saline. The monitoring electrodes shall not touch the pacemaker.

(3) Voltage. The low frequency signal shall be injected directly into the medium so that 100 mV RMS is present at the pulse generator terminals.

(4) Pacemaker Operating Mode. Signals shall not be applied to simulate cardiac activity.

(5) Performance. The following pacemaker parameters shall be monitored during the test:

(A) Rate

(B) Pulse Duration

(C) Pulse Amplitude

COPY

5.3 Classification. The following are classes of pacemaker rate[1] response to environmental interference (other than response to specific diagnostic tests).

CLASS	PACEMAKER RESPONSE TO INTERFERENCE
I	NO RESPONSE TO INTERFERENCE
II	TEMPORARY EFFECTS[2] - NORMALLY WITHOUT RISK A. Episodes of change in rate at least 10 seconds apart, not exceeding 2 seconds in duration B. Pacemaker goes to interference rate C. Pacemaker goes up in rate but stays below 150 ppm or below its upper specified design limit D. Pacemaker goes down in rate but stays above 50 ppm or its lower specified design limit
III	PERMANENT OR PROLONGED EFFECTS[3] - NORMALLY WITHOUT RISK A. Episodes of change in rate at least 10 seconds apart, not exceeding 2 seconds in duration B. Pacemaker goes to interference rate C. Pacemaker goes up in rate but stays below 120 ppm or below its upper specified design limit D. Pacemaker goes down in rate but stays above 50 ppm or its lower specified design limit
IV	TEMPORARY EFFECTS[2] - POTENTIALLY WITH RISK A. Pacemaker goes above 150 ppm or its upper specified design limit B. Pacemaker goes below 50 ppm but above 25 ppm C. Pacemaker goes below 25 ppm or stops
V	PERMANENT OR PROLONGED EFFECTS - POTENTIALLY WITH RISK A. Pacemaker goes above 120 ppm or its upper specified design limit B. Pacemaker goes below 50 ppm but above 25 ppm C. Pacemaker goes below 25 ppm or stops

[1]Other parameter changes are being considered. However, rate is the one of primary interest.

[2]Returns to normal operation within 2 beats or 2 seconds after termination of interference.

[3]Rate doesn't return to normal operation within 2 beats or 2 seconds after exposure.

Appendix A

Rationale for the Development of This Pacemaker Standard

This Pacemaker Standard was developed by six working groups under the auspices of the AAMI Pacemaker Standard Subcommittee. Each working group developed requirements for certain aspects of this standard, according to rationale set forth below.

A15. EMC Pacemaker Performance Requirement

The electromagnetic compatibility requirements were generated due to some reports of patient problems as well as concern by the FDA and the DOD for pacemaker susceptibility. Some laboratory tests (Brooks AFB) have indicated potential problems although most data are from older design pulse generators. Many physicians believe that, in spite of laboratory tests, interface of pulse generators by electromagnetic signals has not been observed to be a significant clinical problem.

The 450 MHz frequency was selected as a compromise frequency that represents good body penetration and has been used by expert personnel in the field in previous testing. The modulation, polarization and repetition rates were chosen with regard to worst-case simulations and current generation capability. Mitchell et al. has shown that repetition rates approaching those of heart rate are appropriate.

The 200 V/m level was adopted based upon recommendations by the U.S. Air Force to the FDA as representing a reasonable choice based upon maximum expected electromagnetic environments. The maximum electromagnetic environment to which continuous exposure is permissible is accepted in the U.S. as 10 mW/cm^2. This value should represent the upper limit of power density which a person may encounter in normal circumstances. In a uniform field without amplitude modulation, the E-field required to produce a power density of 10 mW/cm^2 is approximately 200 V/m.

The test cell was specified as a representation of the human chest cavity. The saline solution resistivity requirements and container material are approximations of the human body.

The orientation of the pacemaker in the test cell, with respect to the incident field, was chosen as a representation of orientation in the body. The orientation specified, however, tends toward a worst-case situation.

Simulation of cardiac activity during the test is not permitted because any effects on pulse rate due to external interference may be masked by such simulation.

Appendix A

The parameters selected for monitoring and performance criteria (rate, pulse width and pulse amplitude) are those that are the primary determinant of acceptable pacing. The pacemaker performance limits prescribed were selected as being clinically acceptable limits in the judgment of the physicians participating on this effort. These are based on classifications of pacemaker response to EMI developed by a working group of the AAMI Pacemaker Standard Subcommittee in 1972.

The low frequencies specified are power frequencies. These are most likely to be encountered by a patient in daily living. The voltage level was selected based on the human threshold of perception. Voltages below the threshold of perception were believed to be the most dangerous to the patient if his pacemaker were affected. Patient contact with power frequency potentials above the threshold of perception are less hazardous from the point of view of affecting the pacemaker due to the patient's awareness of the contact. A perception threshold of 2 ma[4] and total body impedance of approximately 1000 ohms would require a 2-volt potential at the skin. It is known that the total resistance incurred is primarily at the skin interfaces. Within the body only a small portion of the voltage drop will appear across the pulse generator terminals. Assuming the impedance of the body represents no more than 10% of the total impedance path, 100 mV is considered to be the maximum voltage difference which would occur in that region of the body in which the pacemaker is placed.

When a pulse generator synchronizes with the radiated signal, 1.5 pps is not an effective test since the unit will be operating between 50 and 150 ppm. Thus, it is required that modulation frequency be doubled to determine if the pulse generator performance will stay within the required range of 50 to 150 ppm.

---

[4]Dalziel, "Electric Shock Hazard," IEEE Spectrum, Feb. 1972.

Appendix B.—Computer-Generated AESOP Fields*

*R. A. Dalke, P. McKenna, and P. Ng, ***Field Calculations for the AESOP EMP Simulator—Volume I***, Electro Magnetic Applications, Inc., EMA-89-R-57 (July 1989).*

Figure B-1. E-fields at location A, 0.2-m height.

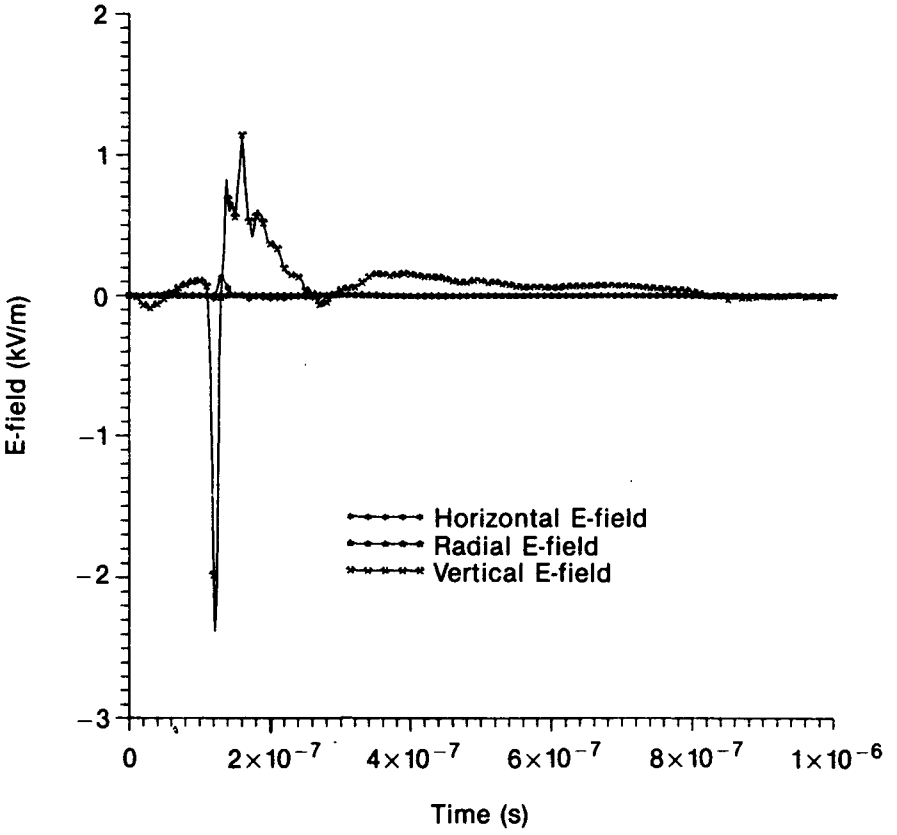

Figure B-2. E-fields at location A, 1.5-m height.

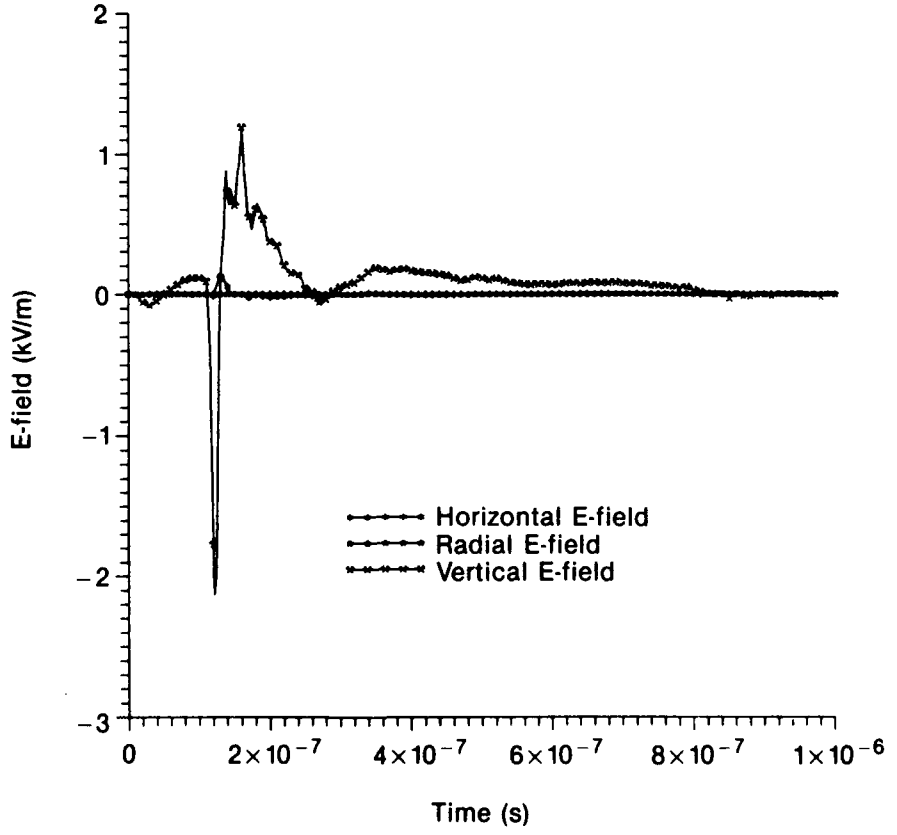

Figure B-3. E-fields at location A, 10-m height.

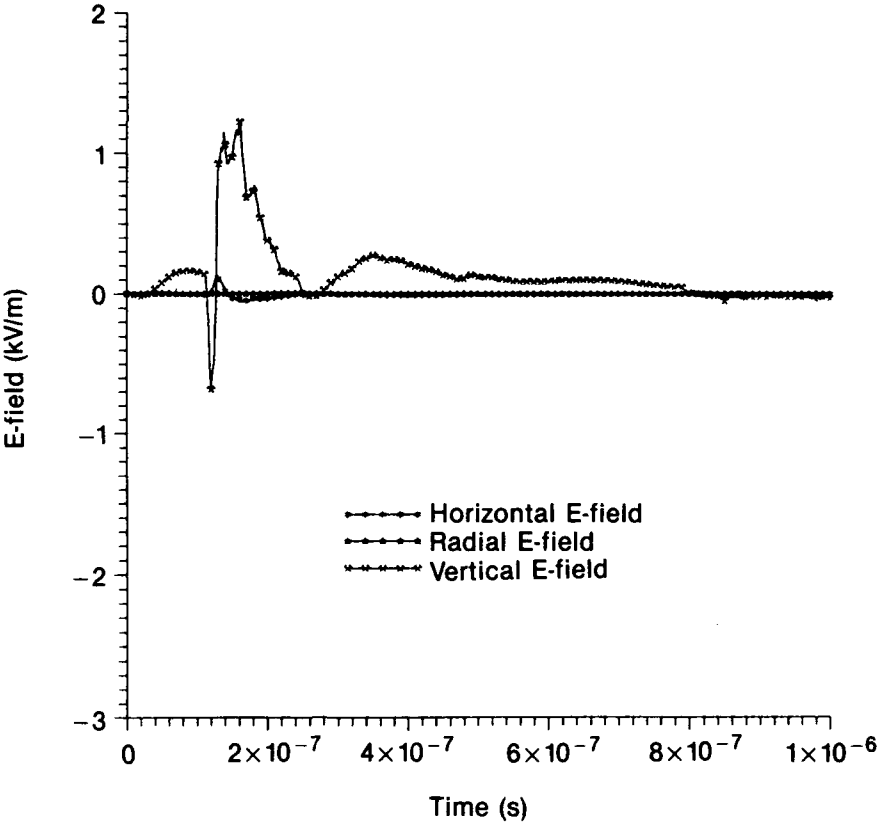

Figure B-4. Vertical E-fields at location A.

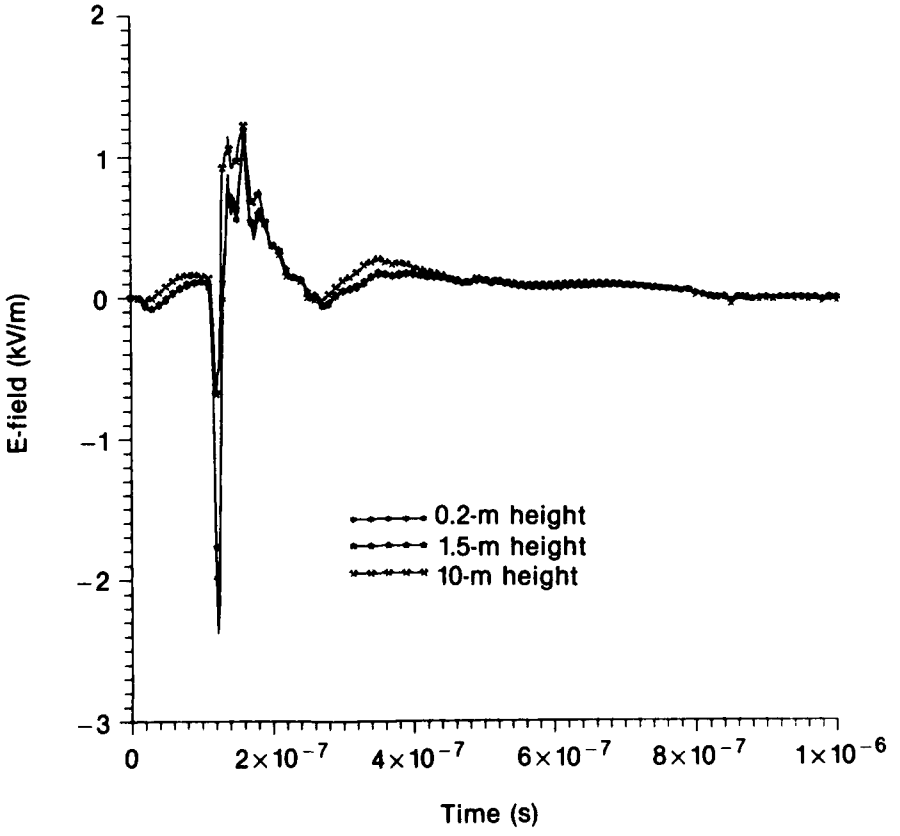

Figure B-5. H-fields at location A, 0.2-m height.

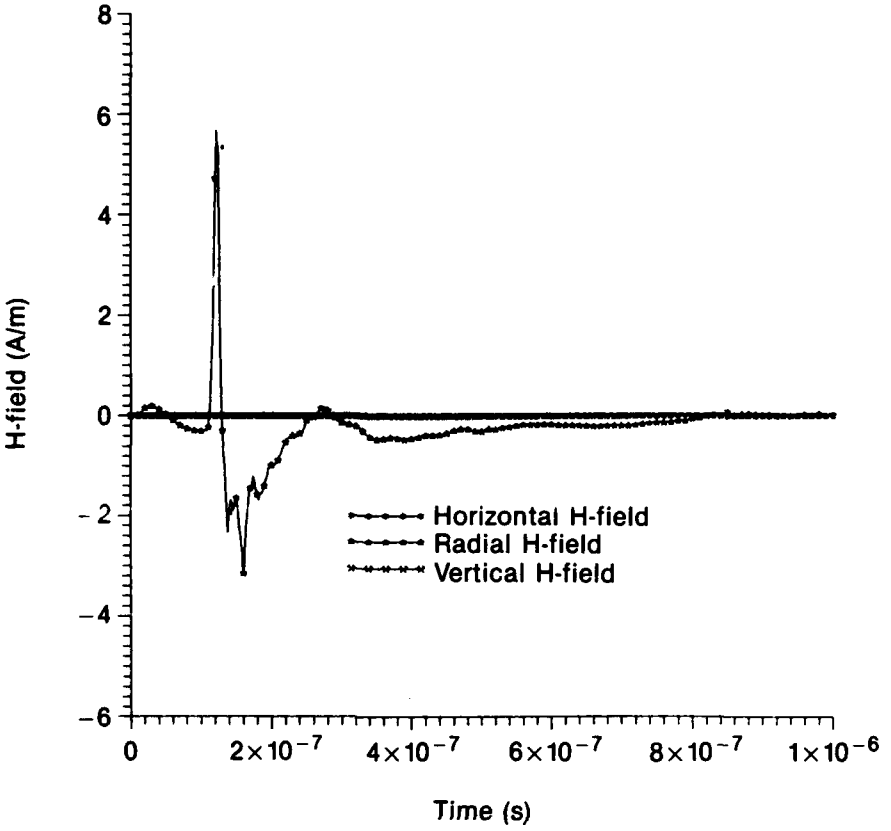

Figure B-6. H-fields at location A, 1.5-m height.

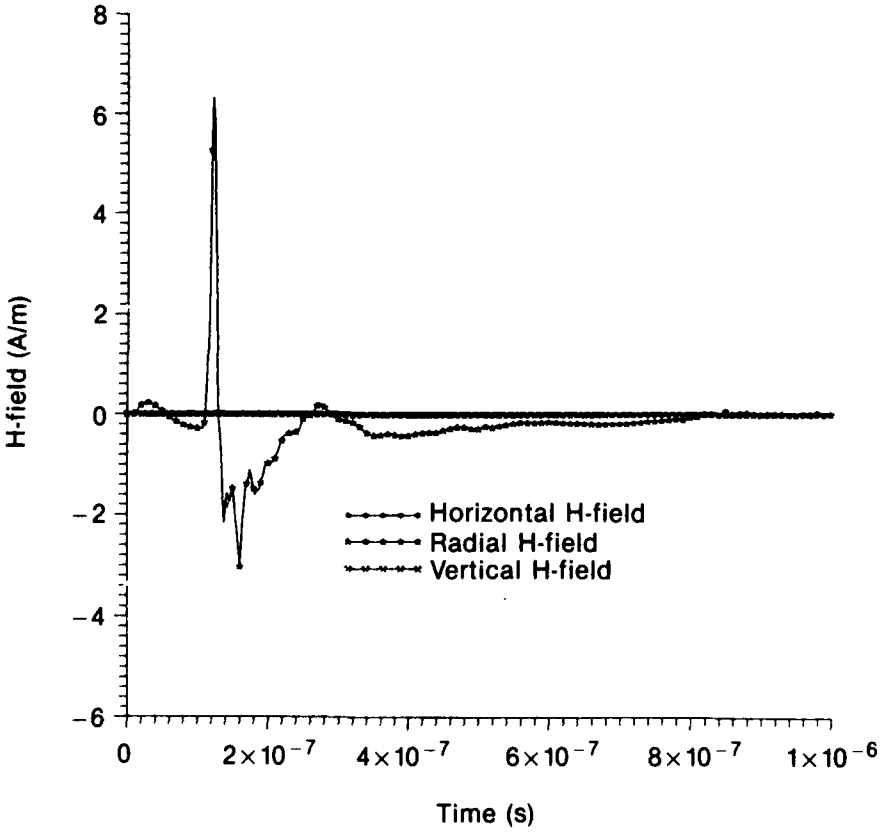

Appendix B

Figure B-7. H-fields at location A, 10-m height.

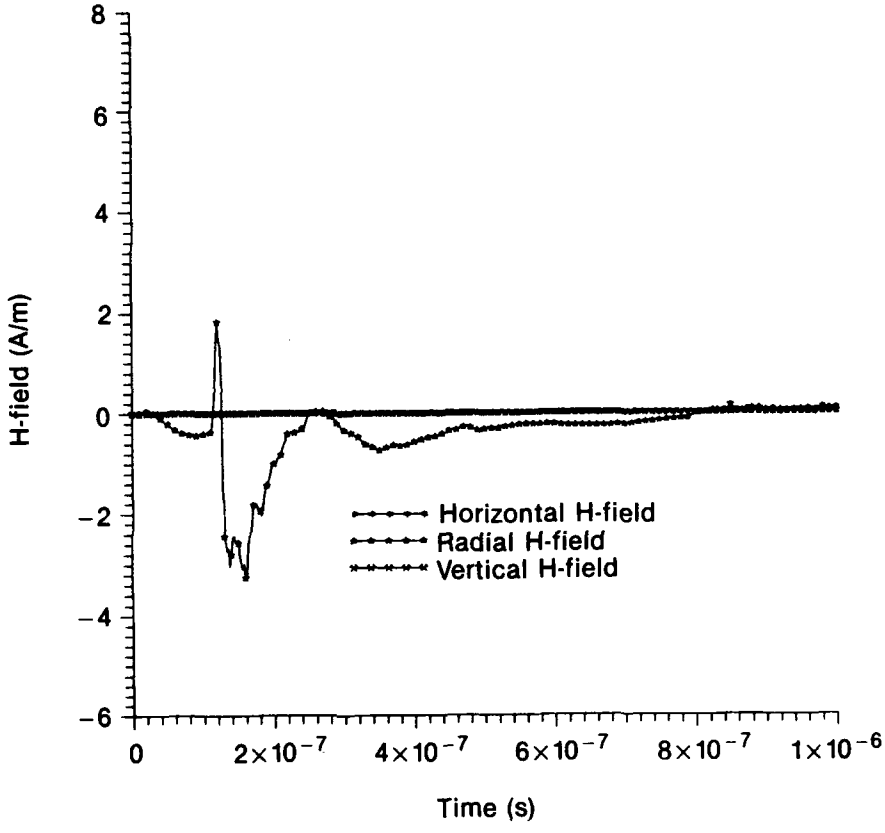

Figure B-8. Radial H-fields at location A.

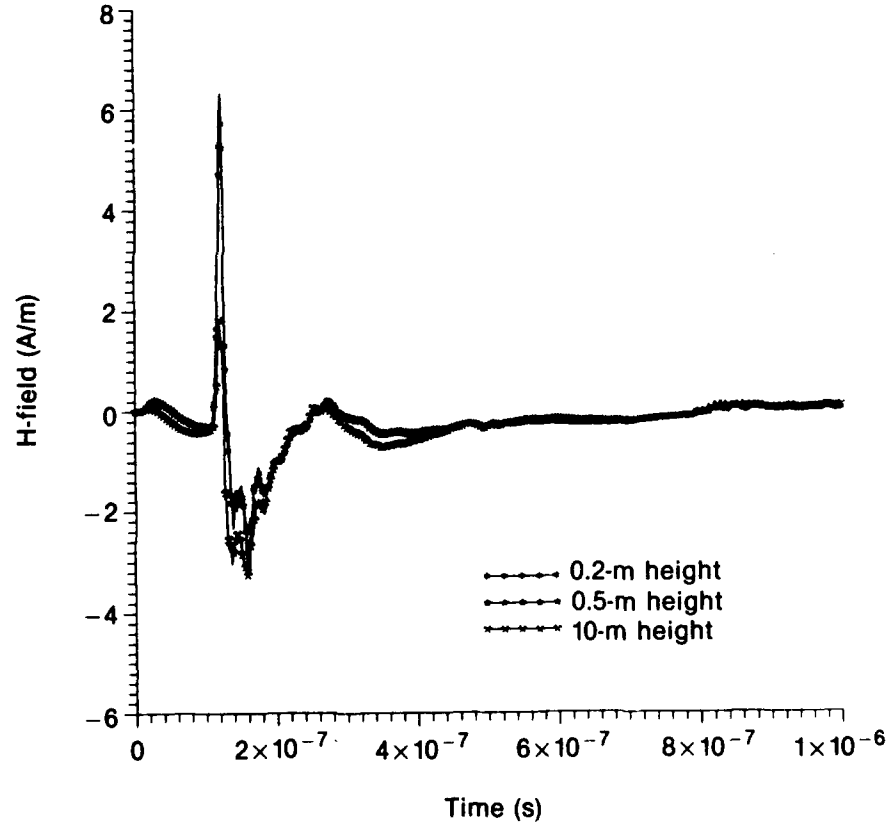

Figure B-9. E-fields at location B, 0.2-m height.

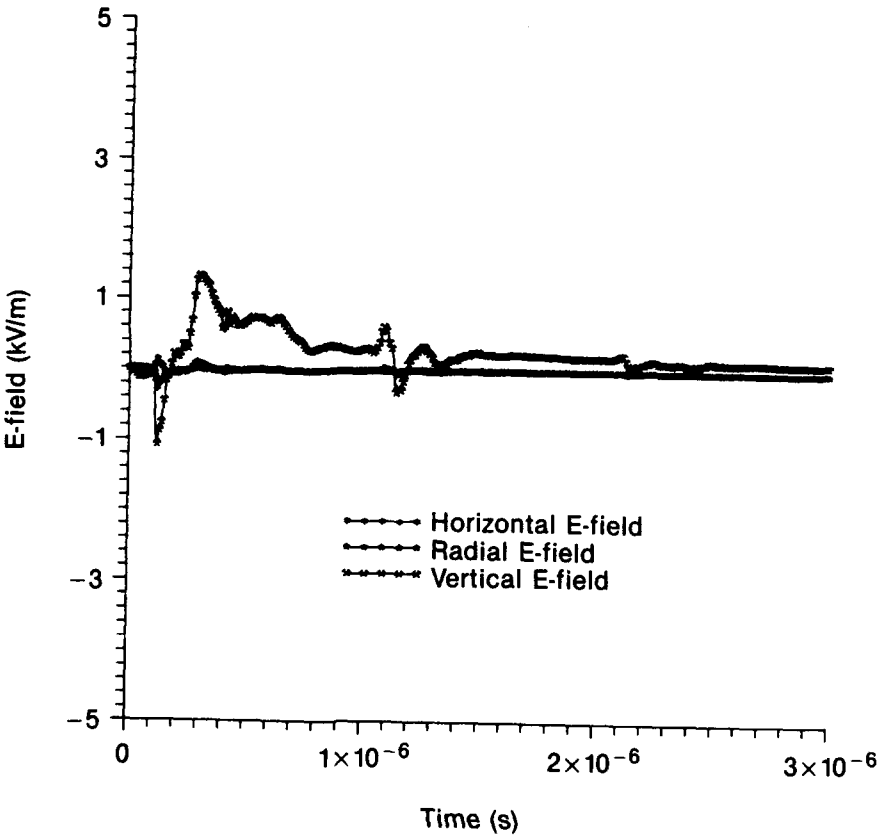

Figure B-10. E-fields at location B, 1.5-m height.

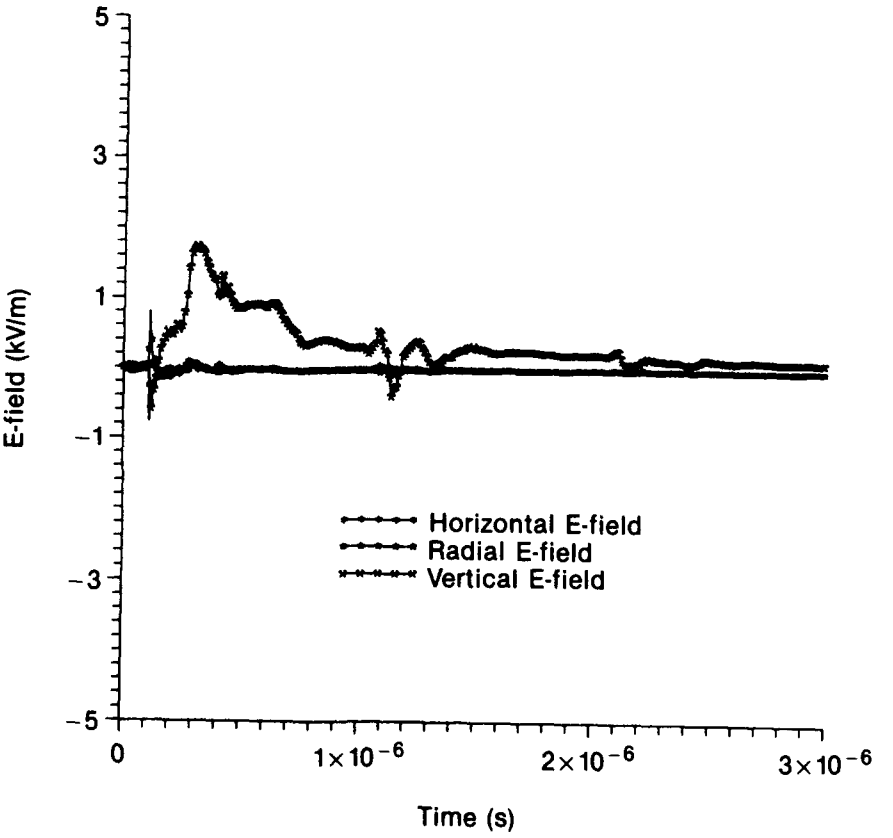

Figure B-11. E-fields at location B, 10-m height.

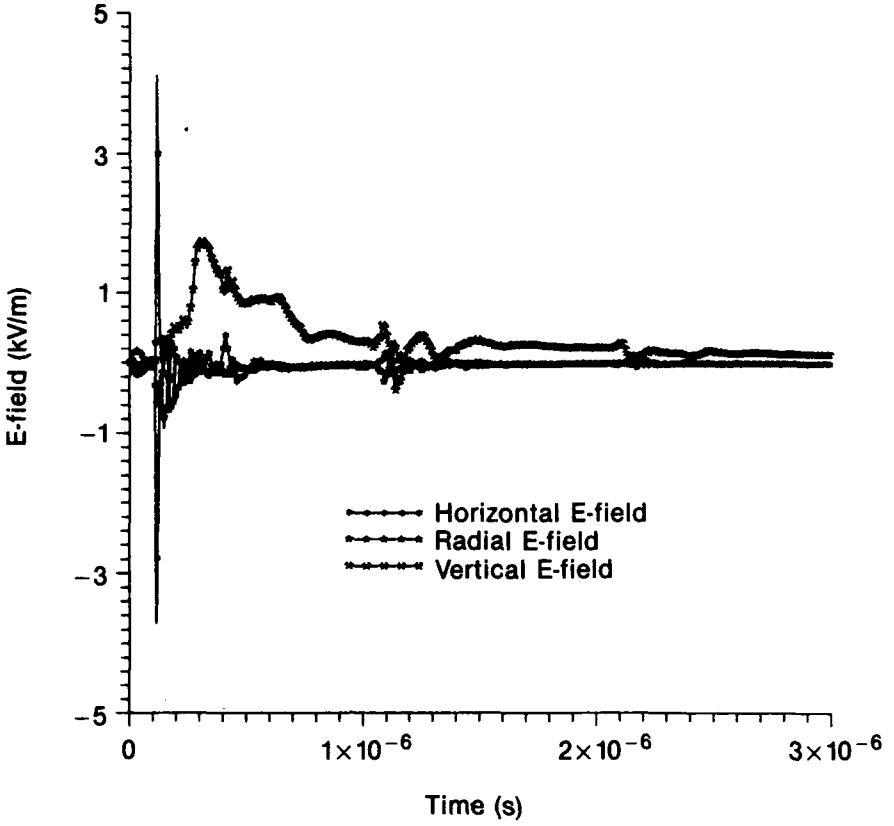

Figure B-12. Vertical E-fields at location B.

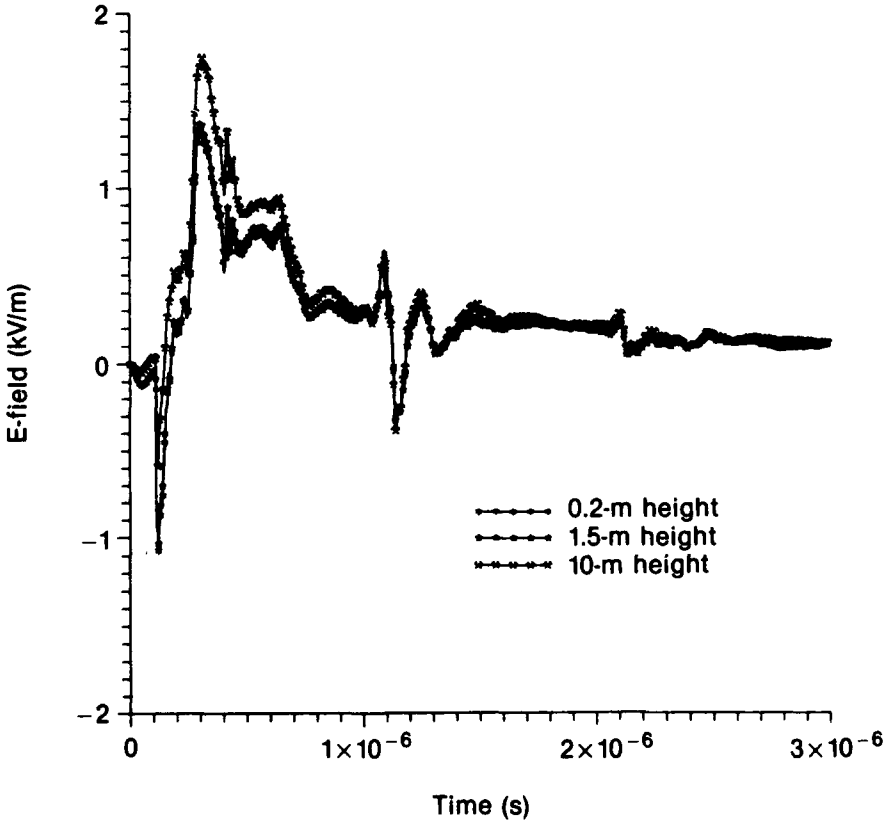

Figure B-13. H-fields at location B, 0.2-m height.

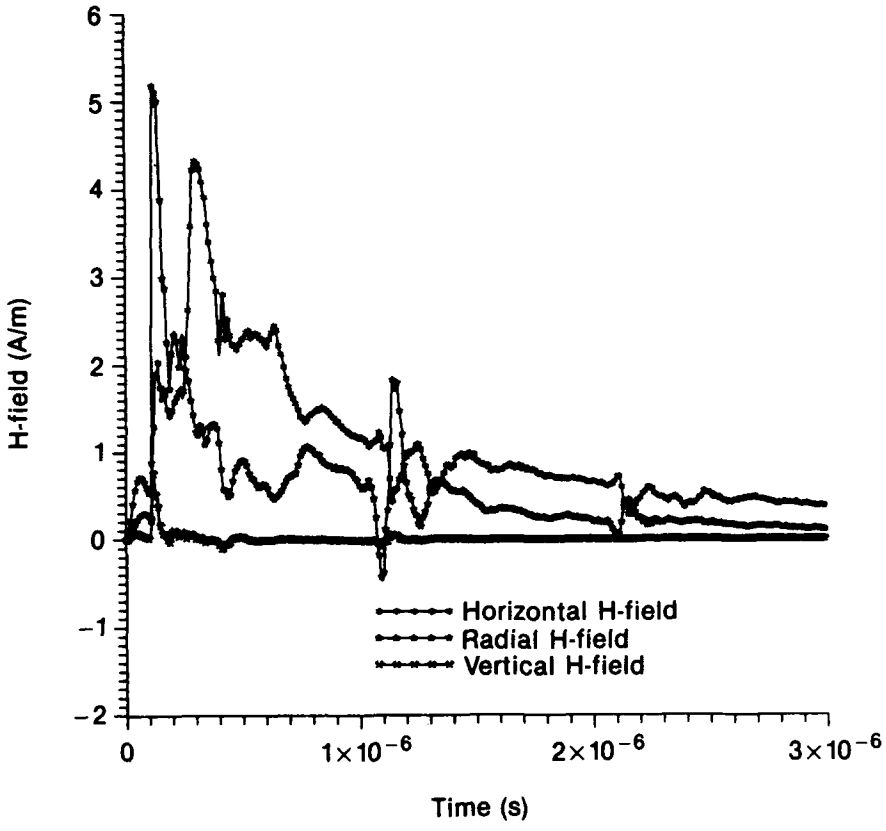

Figure B-14. H-fields at location B, 1.5-m height.

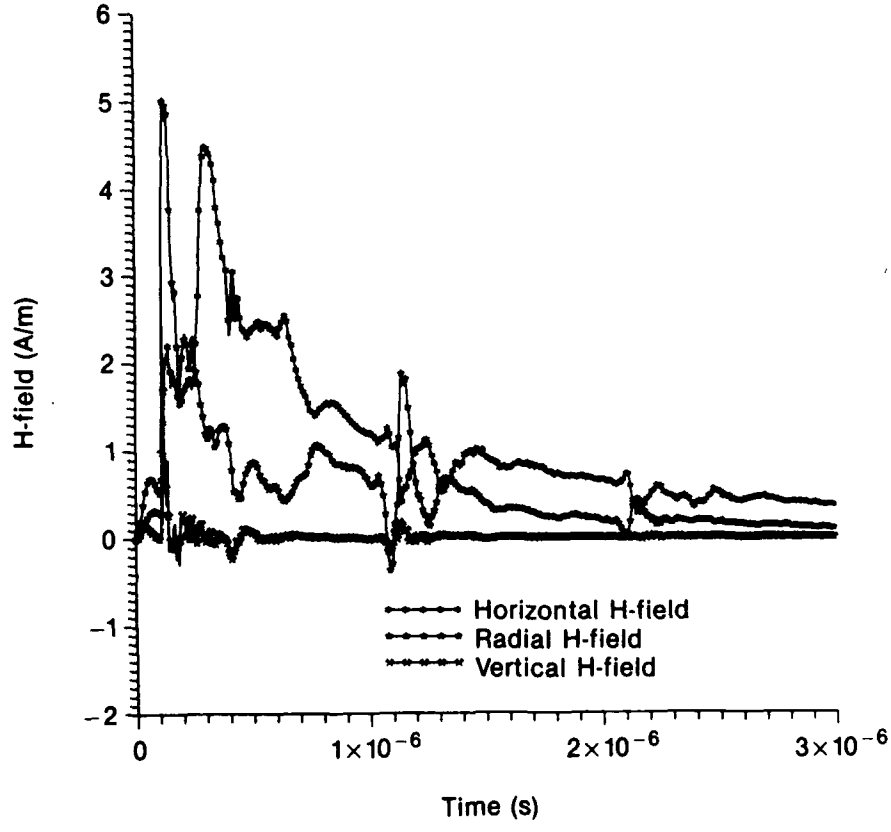

Figure B-15. H-fields at location B, 10-m height.

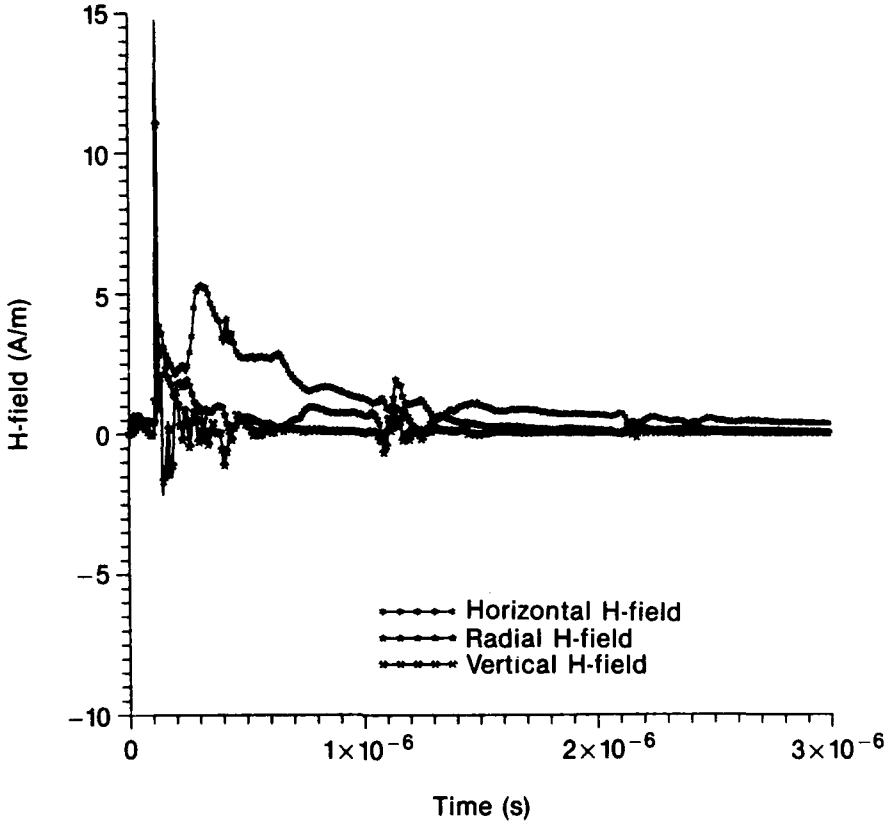

Figure B-16. Horizontal H-fields at location B.

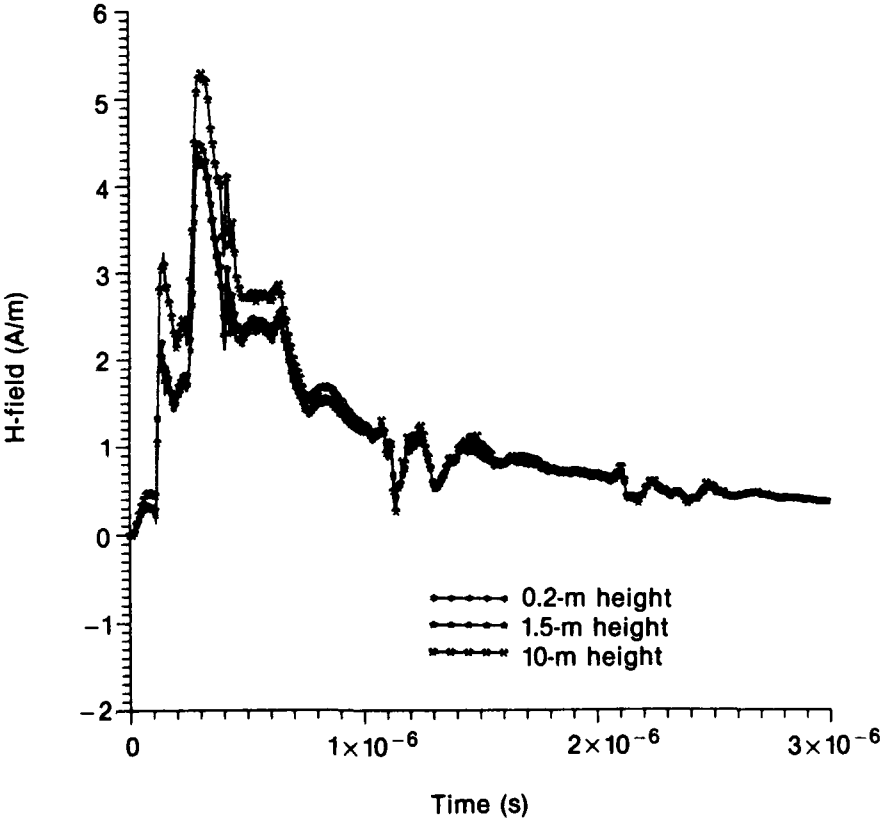

Figure B-17. Radial H-fields at location B.

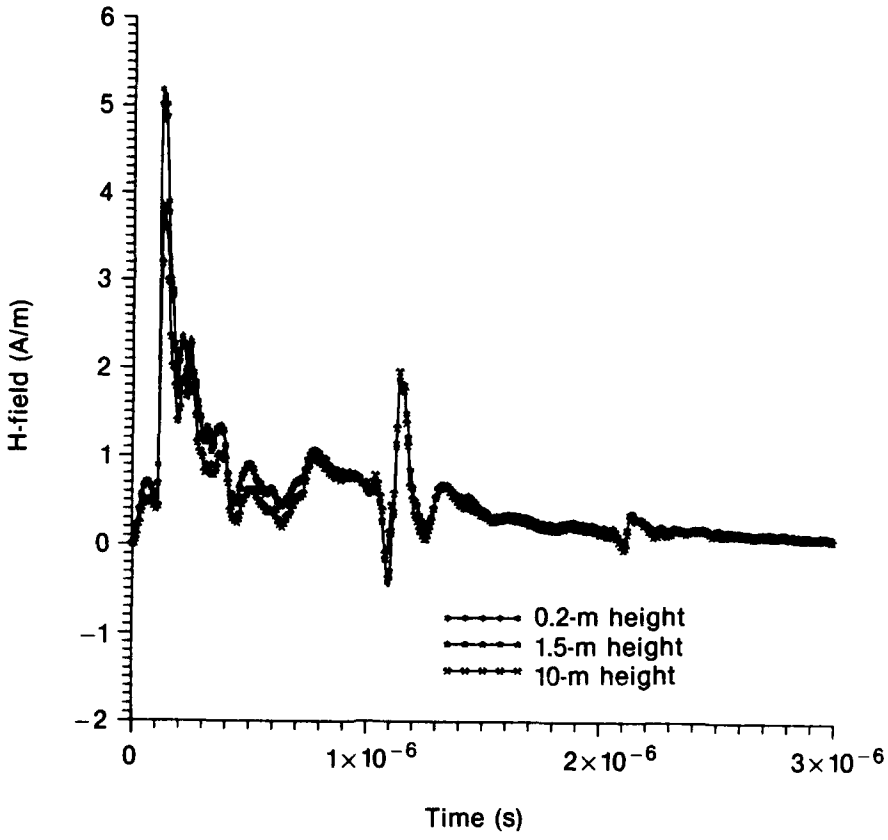

Figure B-18. E-fields at location C, 0.2-m height.

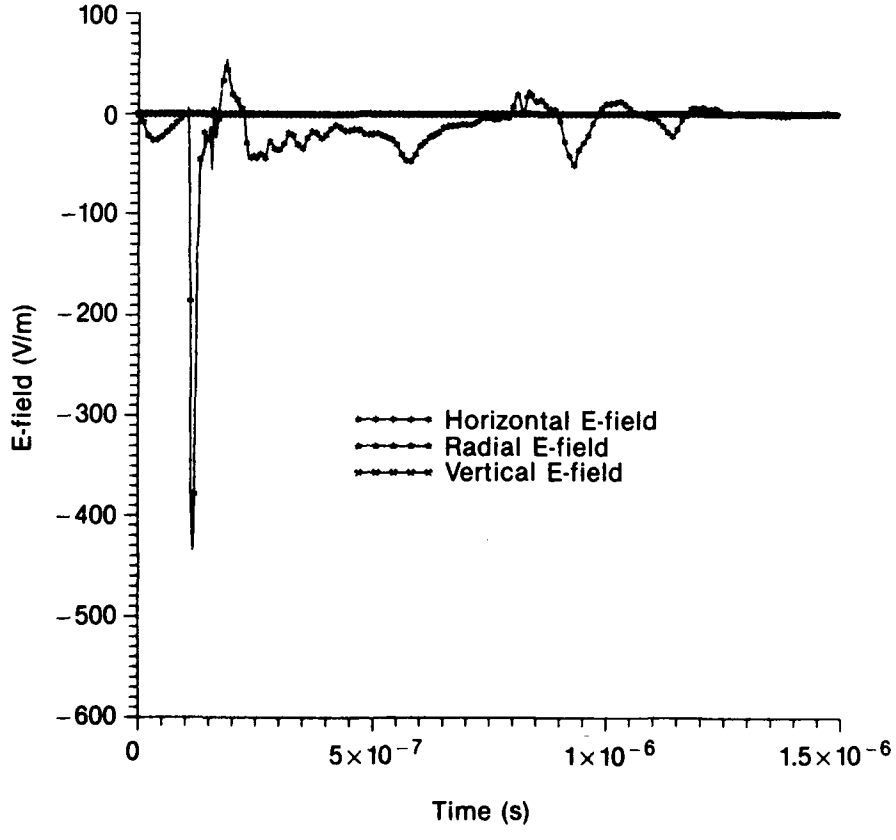

Figure B-19. E-fields at location C, 1.5-m height.

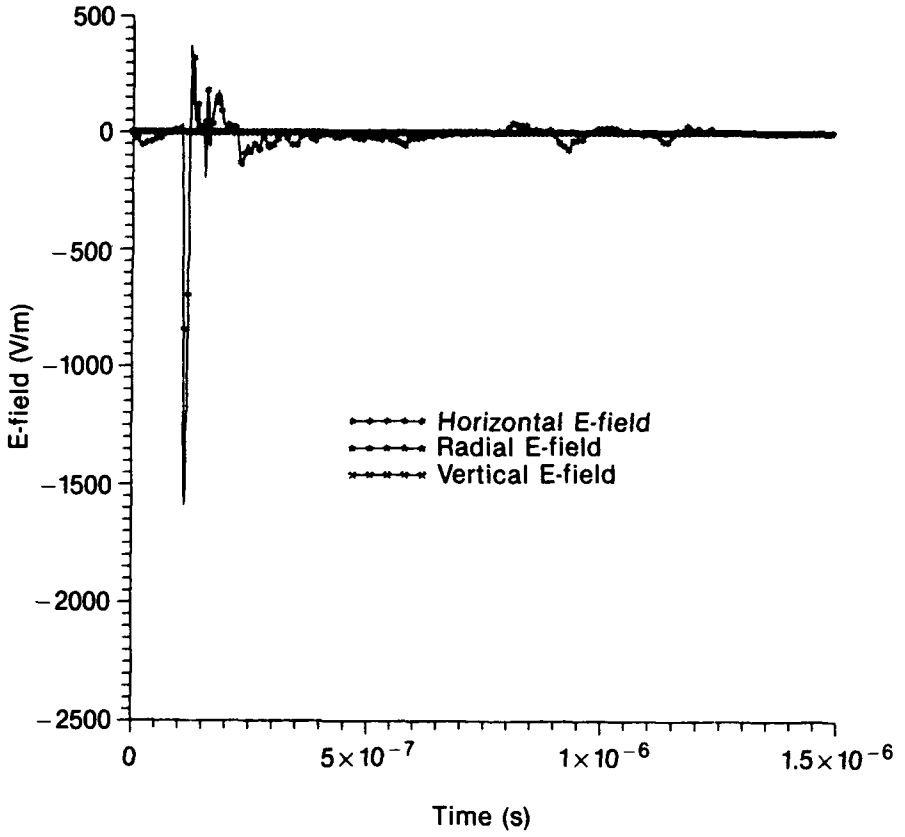

Figure B-20. E-fields at location C, 10-m height.

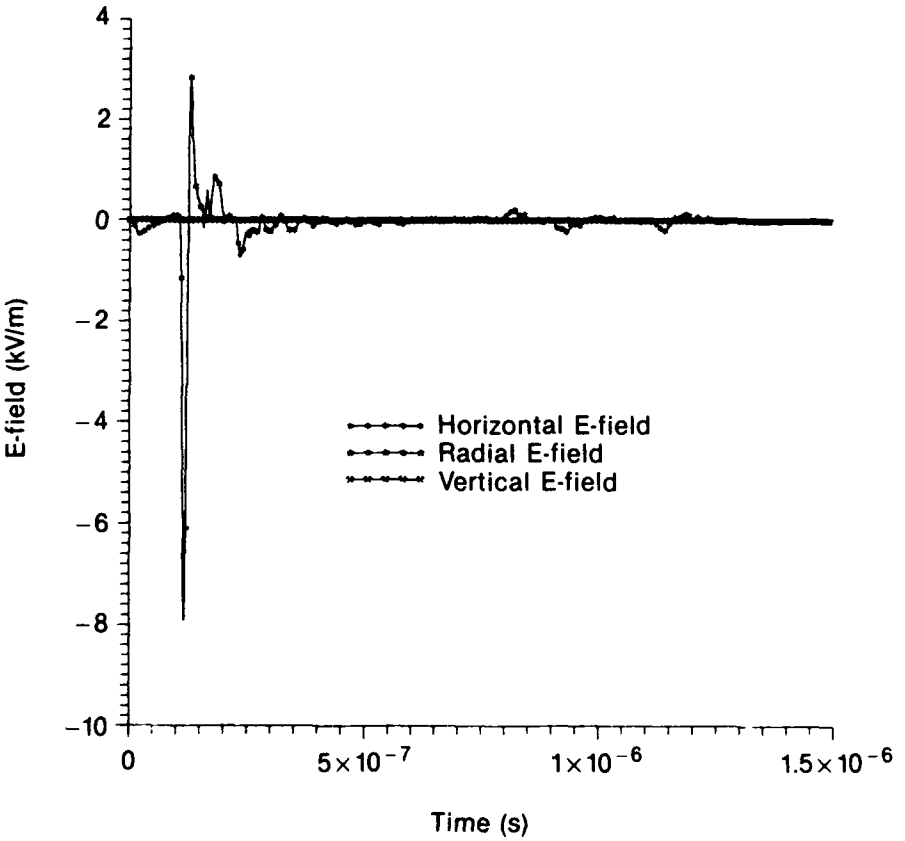

Figure B-21. Horizontal E-fields at location C.

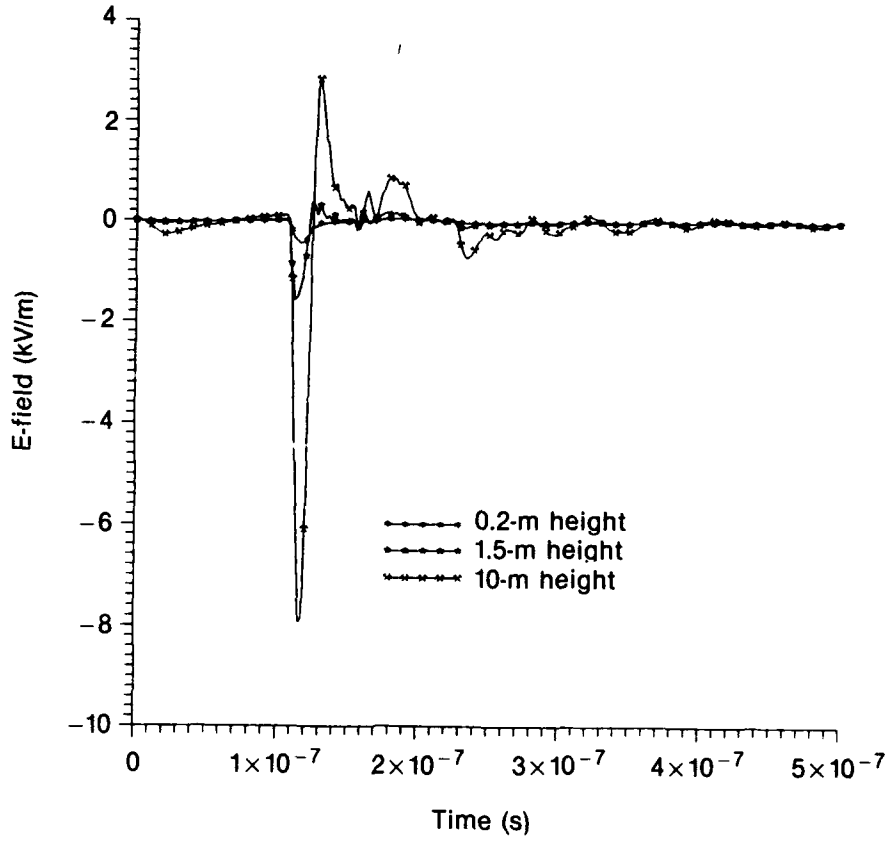

Figure B-22. H-fields at location C, 0.2-m height.

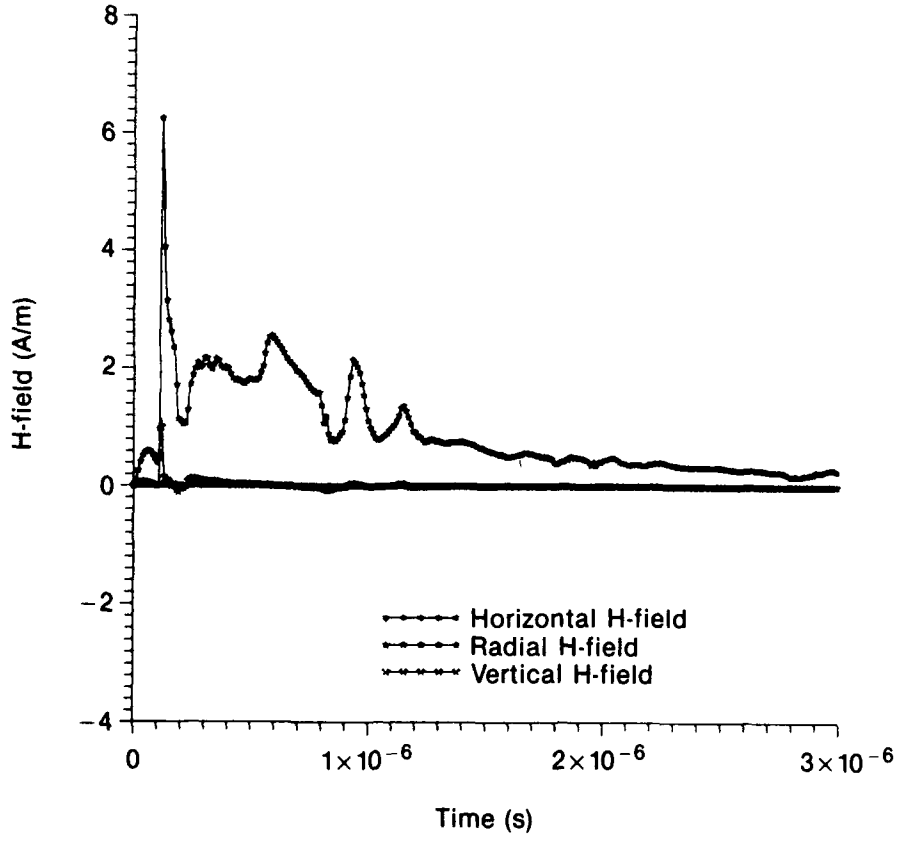

Figure B-23. H-fields at location C, 1.5-m height.

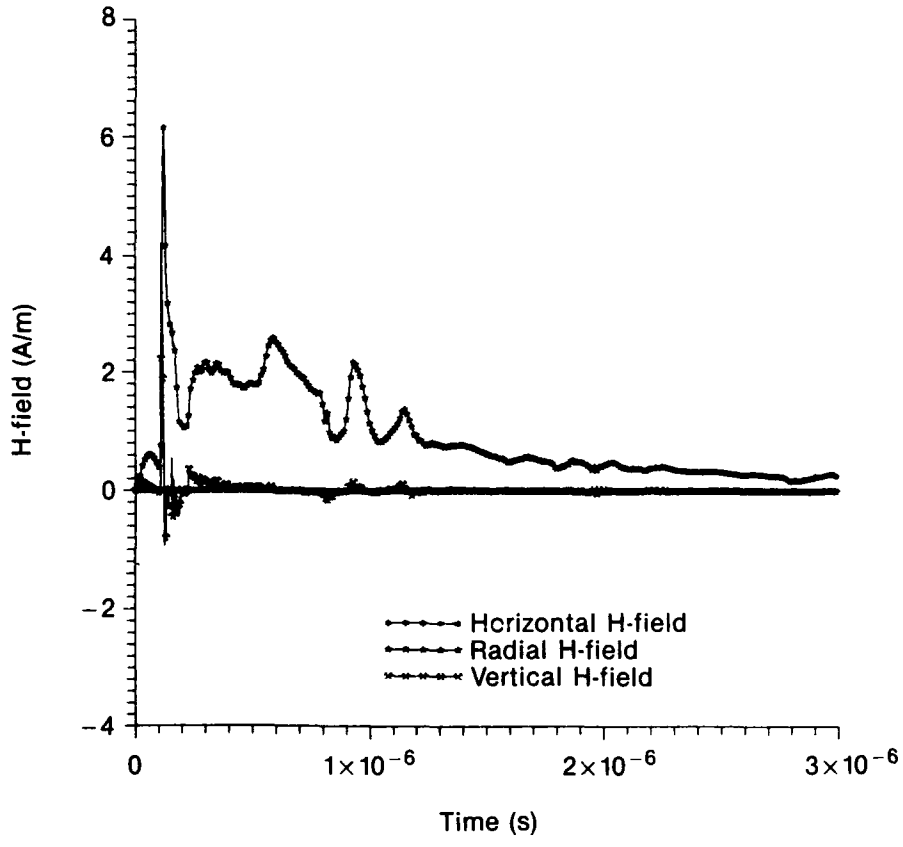

Figure B-24. H-fields at location C, 10-m height.

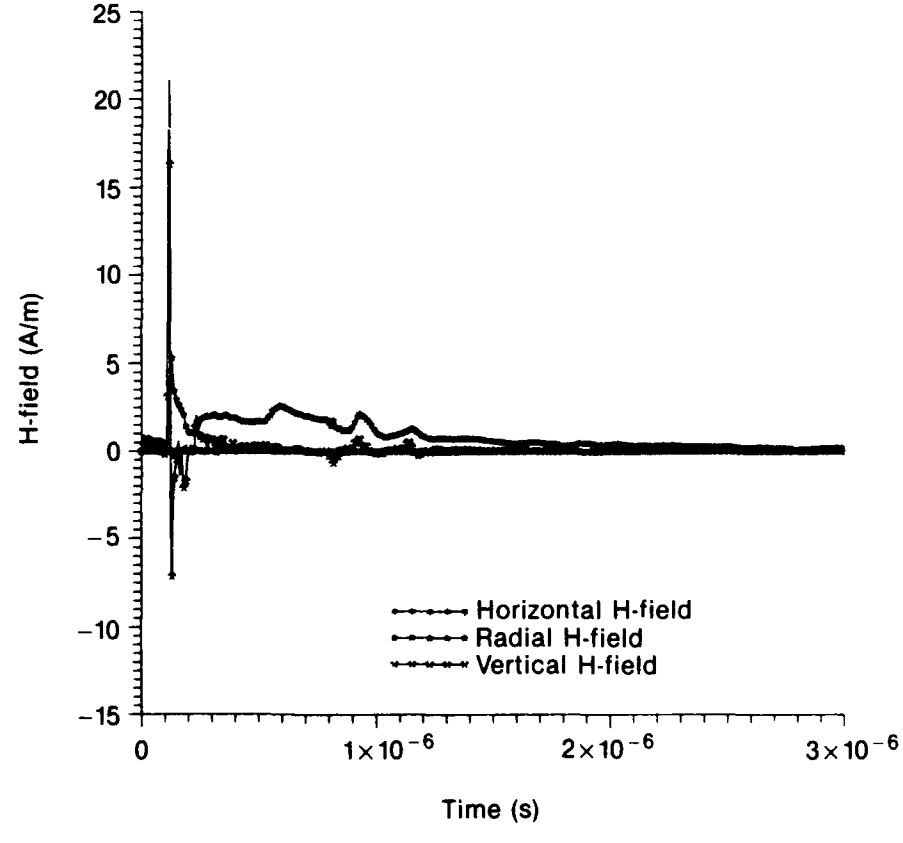

Figure B-25. Radial H-fields at location C.

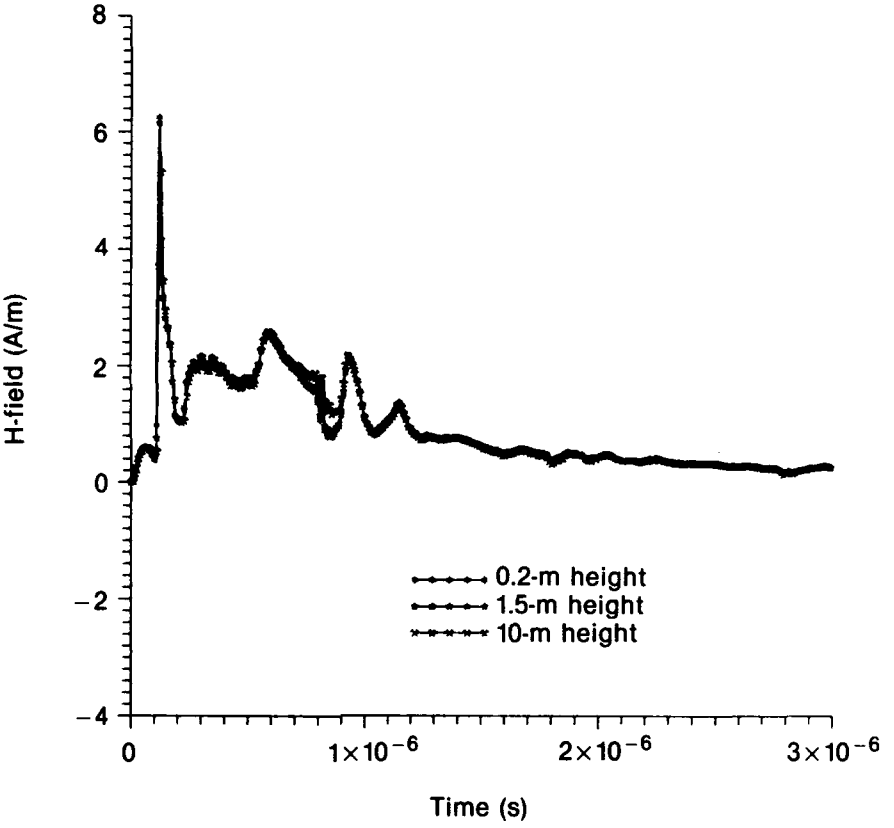

Figure B-26. Maximum horizontal E-fields.

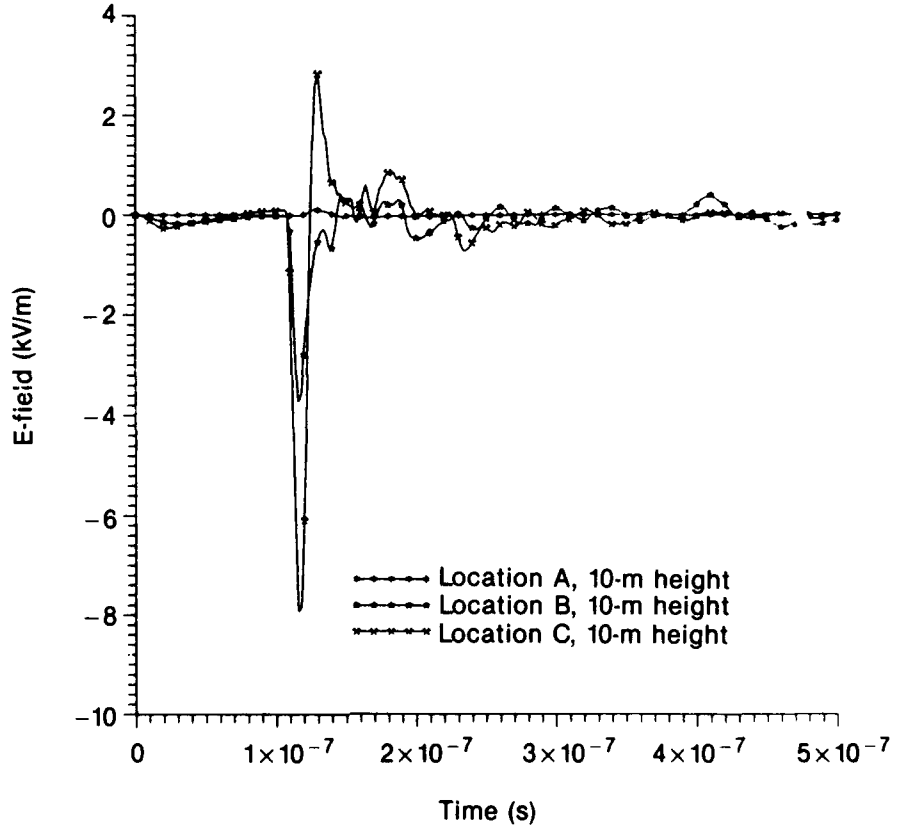

Figure B-27. Maximum vertical E-fields.

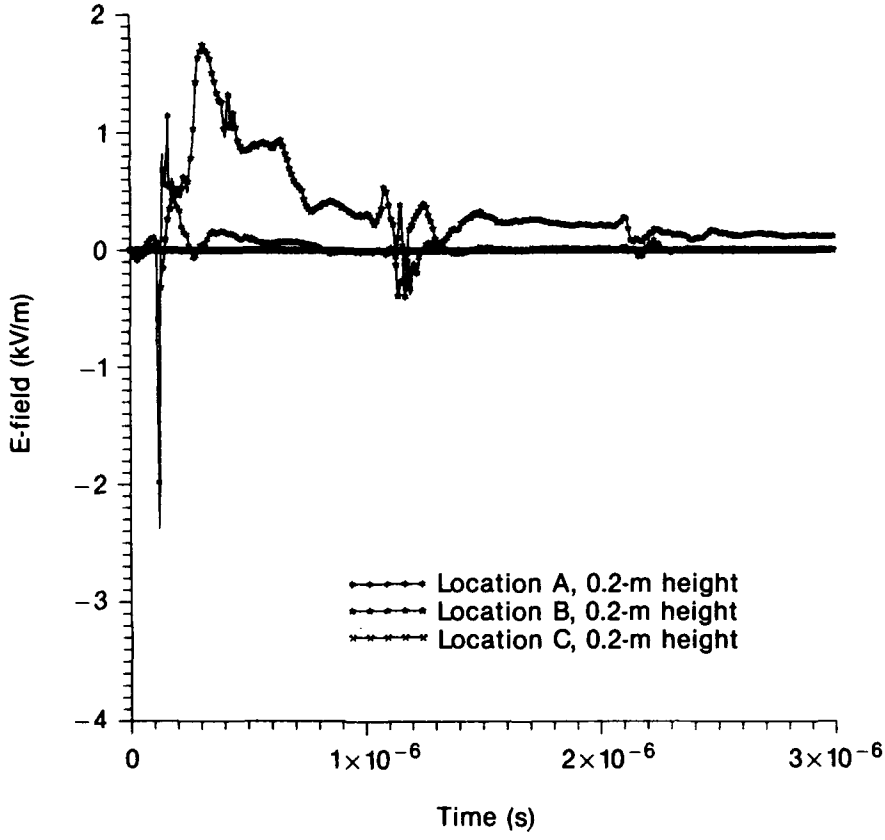

Figure B-28. Maximum radial H-fields.

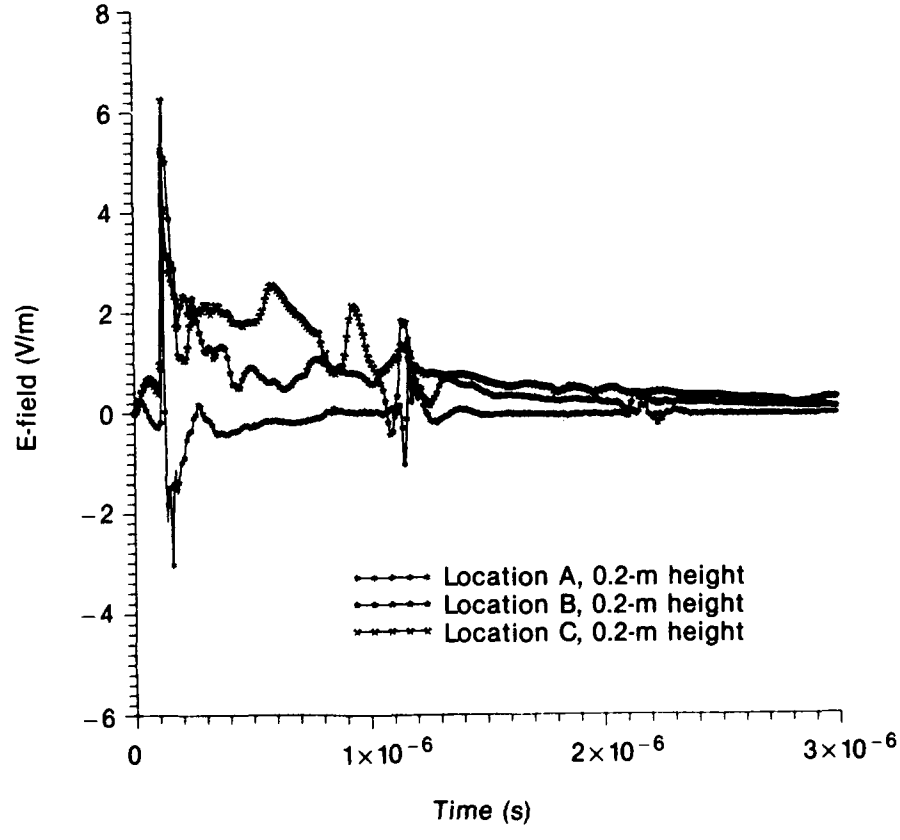

Distribution

Administrator
Defense Technical Information Center
Attn DTIC-DDA (2 copies)
Cameron Station, Building 5
Alexandria, VA 22304-6145

Director
Defense Communications Agency
Attn Code B410
Attn Code B430
Attn Code C313
Attn Code 312
Washington, DC 30405

Director
Defense Intelligence Agency
Attn DB-4C2
Attn RTS-2A, Technical Library
Washington, DC 20301

Director
Defense Nuclear Agency
Attn RAAE, Atmospheric Effects Div
Attn RAEE
Attn TISI-Scientific Information Div
6801 Telegraph Road
Alexandria, VA 22310-3398

Dept of the Army, Surgeon General
Attn SGPS-PSP-E, LTC C. Day
5109 Leesburg Pike
Falls Church, VA 22041-3258

Director
US Army Ballistic Research Laboratory
Attn SLCBR-DD-H, Safety & Health
Aberdeen Proving Ground, MD 21005

US Army Environmental Hygiene Agency
Attn HSHB-MR-LM,C. Hicks
Aberdeen Proving Ground, MD
21010-6422

Commander
US Army Materiel Command
Attn AMCCN-N
Attn AMCPM
Attn AMCSG-R, MAJ Connock
5001 Eisenhower Ave
Alexandria, VA 22333-0001

Director
US Army Signals Warfare Center
Attn AMSEL-RD-SW-CE,
Communications/SW Div
Attn AMSEL-RD-SW-DT, Tactical Data
Systems Div
Attn AMSEL-RD-SW-EE, Electronics/
EW Div
Attn AMSEL-RD-SW-OS, Office of the
Scientific Advisor
Attn AMSEL-RD-SW-RA, Analysis
&Applications Div
Attn AMSEL-SS, Signal Security Office
Vint Hill Farms Station
Warrenton, VA 22186-5000

Commander
USACECOM
Attn AMCPM-IEW-NV
FT Belvoir, VA 22060-5677

Commander
USACECOM
Attn AMCPM-IEW-FA
Attn AMCPM-IEW-QF
Attn AMCPM-IEW-SW
Attn AMCPM-IEW-TB
Attn AMC-PEO-IEW
Vint Hill Farms Station
Warrenton, VA 22186-5115

Distribution (cont'd)

Commander
USAMCCOM
Attn AMC-PEO-AR
Picatinny Arsenal, NJ 07806-5000

Commander
USAMCCOM
Attn AMC-PEO-CN
Aberdeen Proving Ground, MD
21010-5401

Commander
USAMCCOM
Attn AMC-PEO-CN
Attn AMC-PEO-CNB
Attn AMC-PEO-CNN
Attn AMC-PEO-CNS
Attn AMSMA-CG
Rock Island, IL 61299-6000

Commander
USAMCCOM
Attn AMC-PEO-CA
4300 Goodfellow Blvd
St Louis, MO 63120-1798

Commander
USATACOM
Attn AMCPM-AMBS
Attn AMCPM-BFVS
Attn AMCPM-IRV
Attn AMCPM-M113
Attn AMCPM-M60
Attn AMCPM-M9
Attn AMCPM-SS
Attn USATACOM
Attn AMSTA-CG
Warren, MI 48397-5000

Commander
USATROSCOM, Belvoir R&D Center
Attn STRBE-FG
Attn STRBE-Z
FT Belvoir, VA 22060-5606

Commander
USAVSCOM
Attn AMCPM-AAH
Attn AMCPM-ALSE
Attn AMCPM-ASE
Attn AMCPM-BH
Attn AMCPM-CH47M
Attn AMCPM-CO
Attn AMCPM-TP
4300 Goodfellow Blvd
St Louis, MO 63120-1798

Commander
Belvoir Research Development &
Engineering Center
Attn STRBE-FG
Ft Belvoir, VA 22060-5606

Walter Reed Army Institute of Research
Attn SGRD-UWI-D, H. Bassen
Washington, DC 20307-5100

Walter Reed Army Medical Center
Cardiology Services
Attn Dr. L. Weston
Washington, DC 20307-5001

US Navy
Naval Research Laboratory
Attn 2600, Technical Info Div
Attn 6000, Matl & Rad Sci & TE
Attn Code 2620, Tech Library Br
Attn Code 4720
4555 Overlook Ave, SW
Washington DC 20375

Commander
Naval Surface Warfare Center
Attn Code F30
Attn Code F32
Attn E-43, Technical Library
Attn R-40, Radiation Div
White Oak, MD 20910

Distribution (cont'd)

Commander
Naval Surface Warfare Center
Attn DX-21 Library Div
Dahlgren, VA 22448

NASA
Attn Tech Library
600 Independence Avenue, SW
Washington, DC 20456

Director
NASA
Attn Code 2620, Tech Library Br
Langley Research Center
Hampton, VA 23665

Director
NASA, Goddard Space Flight Center
Attn Space Power Applications Branch
Greenbelt, MD 20771

NASA
Sci & Tech Info Facility
Attn Tech Library
6571 Elkridge Landing Rd
Linthicum Hgts, MD 21090

Director
NASA
Attn Technical Library
John F. Kennedy Space Center
Kennedy Space Center, FL 32899

Director
NASA
Attn Technical Library
Lewis Research Center
Cleveland, OH 44135

Director
National Institute of Standards & Technology
Attn Library
Washington, DC 20234

US Department of Commerce
NIST
Attn Library
Washington, DC 20234

Lawrence Livermore National Laboratory
Attn Technical Info Dept Library
PO Box 808
Livermore, CA 94550

Sandia National Laboratories
Attn Technical Library
PO Box 5800
Albuquerque, NM 87185

Asea Brown Boveri Ltd
ABB EMI-Control Center
Attn Dr. D. Hansen
CH-5405 Baden-Dattwil/Switzerland

Goodyear Aerospace Corp,
Arizona Division
Attn Tech Lib
Litchfield Park, AZ 85340

Honeywell, Inc
Aerospace & Defense Group
Attn Tech Lib
13350 US Highway 19 South
Clearwater, FL 33516

Hughes Aircraft Company, S&CG
Attn Technical Lib
PO Box 92919, Airport Station
Los Angeles, CA 90009

Intermedics, Inc
Reliability Dept
Attn J. Lin
PO Box 617
Freeport, TX 77541

Distribution (cont'd)

Mission Research Corporation
Attn B. Goldstein
735 State Street, PO Drawer 719
Santa Barbara, CA 93102

Rockwell International Corp
Attn Technical Library
3370 Miraloma Avenue
Anaheim, CA 92803

SRI International
Attn Tech. Library
333 Ravenswood Ave
Menlo Park, CA 94025

US Army Laboratory Command
Attn AMSLC-DL, R. Vitali

Installation Support Activity
Attn SLCIS-CC-IP, Legal Office

USAISC
Attn AMSLC-IM-VA, Admin Ser Br
Attn AMSLC-IM-VP, Tech Pub Br
(2 copies)

Harry Diamond Laboratories
Attn Laboratory Directors
Attn SLCHD-TL, Library (3 copies)
Attn SLCHD-TL, Library (WRF)
Attn SLCHD-NW, W. Vault
Attn SLCHD-NW-E, Chief
Attn SLCHD-NW-EH, Chief
Attn SLCHD-NW-EP, Chief
Attn SLCHD-NW-ES, Chief
Attn SLCHD-NW-P, Chief
Attn SLCHD-NW-R, Chief
Attn SLCHD-NW-RF, Chief
Attn SLCHD-NW-RP, Chief
Attn SLCHD-NW-RS, Chief
Attn SLCHD-NW-TN, Chief
Attn SLCHD-NW-TS, Chief
Attn SLCHD-NW-E, E. Patrick (5 copies)
Attn SLCHD-NW-ES, T. Bock
Attn SLCHD-NW-ES, V. Ellis (50 copies)